NASA CONTRACTOR REPORT

NASA CR-1516

EVALUATION OF REFRACTORY/AUSTENITIC BIMETAL COMBINATIONS

by R. W. Buckman, Jr., and R. C. Goodspeed

Prepared by
WESTINGHOUSE ASTRONUCLEAR LABORATORY
Pittsburgh, Pa.
for Lewis Research Center

NATIONAL AERONAUTICS AND SPACE ADMINISTRATION • WASHINGTON, D. C. • APRIL 1970

1. Report No. NASA CR-1516	2. Government Accession No.	3. Recipient's Catalog No.
4. Title and Subtitle EVALUATION OF REFRACTORY/AUSTENITIC BIMETAL COMBINATIONS		5. Report Date April 1970 6. Performing Organization Code
7. Author(s) R.W. Buckman, Jr., and R. C. Goodspeed		8. Performing Organization Report No. WANL-PR-(EE)-004
9. Performing Organization Name and Address Westinghouse Astronuclear Laboratory P.O. Box 10864 Pittsburgh, Pa. 15236		10. Work Unit No. 11. Contract or Grant No. NAS 3-7634
12. Sponsoring Agency Name and Address National Aeronautics and Space Administration Washington, D.C. 20546		13. Type of Report and Period Covered Contractor Report 14. Sponsoring Agency Code

15. Supplementary Notes

16. Abstract

The interdiffusion behavior between 16 refractory/austenitic bimetal sheet combinations was investigated at 1400°, 1500°, and 1600° F for times up to 2700 hours. The bimetal composites, produced by explosive bonding, were made up of columbium, tantalum, Cb-1Zr, FS-85, and T-222 in combination with types 321 and 347 stainless steel and the nickel base alloys Inconel 600 and Hastelloy N. Detailed evaluation, which consisted of room temperature tensile strength, 1350° F creep rupture strength, and cyclic and isothermal testing, was conducted on nine selected combinations. It was concluded that the optimum refractory/austenitic bimetal combination evaluated was tantalum/321 stainless steel.

17. Key Words *(Suggested by Author(s))* Bimetallic combinations Explosive bonding Refractory/austenitic bimetals Refractory metal	18. Distribution Statement Unclassified - unlimited		
19. Security Classif. (of this report) Unclassified	20. Security Classif. (of this page) Unclassified	21. No. of Pages 116	22. Price* $3.00

*For sale by the Clearinghouse for Federal Scientific and Technical Information
Springfield, Virginia 22151

FOREWORD

This report was prepared by personnel of the Astronuclear Laboratory of the Westinghouse Electric Corporation under NASA Contract NAS 3-7634 and was originally issued as Westinghouse Report WANL-PR-(EE)-004, August 1969. The work was done under the direction of the Space Power Systems Division, NASA Lewis Research Center, with Mr. P. L. Stone as Technical Manager. This work was administered at the Astronuclear Laboratory under the direction of R. T. Begley.

TABLE OF CONTENTS

LIST OF FIGURES

LIST OF FIGURES (Continued)

LIST OF FIGURES (Continued)

LIST OF TABLES

LIST OF TABLES (Continued)

SUMMARY

The interdiffusion behavior between sixteen refractory/austenitic bimetal sheet combinations was investigated at 1400, 1500, and 1600°F for times of 1600 and 2700 hours. The bimetal composites, formed by explosive bonding, were made up of columbium, tantalum, Cb-1Zr, Cb-27Ta-10W-1Zr (FS-85), Ta-10W-2.5Hf-0.01C (T-222) in combination with types 321 and 347 stainless steel, and the nickel base alloys Inconel 600 and Hastelloy N. Each of the bimetal combinations could be conveniently grouped according to the rate of interdiffusion zone growth at 1600°F. The group with the lowest rate of interdiffusion at 1600°F exhibited a parabolic rate constant (K) of 6.9×10^{-6} in-hr$^{-1/2}$ and consisted of tantalum and T-222 in combination with the stabilized stainless steels 321 and 347. The second group exhibited a $K = 2.6 \times 10^{-5}$ in-hr$^{-1/2}$ and consisted of columbium, FS-85, Cb-1Zr with the stabilized 321 and 347 stainless steels and the T-222/Inconel 600 combination. The highest rate of interdiffusion at 1600°F ($K = 4.1 \times 10^{-5}$ in-hr$^{-1/2}$) consisted of combinations having the nickel base alloys Inconel 600 or Hastelloy N as the austenitic component.

Detailed evaluation which consisted of room temperature tensile strength, 1350°F creep rupture strength, and cyclic and isothermal testing was conducted on nine selected combinations. Isothermal exposure for 1600 hours at 1500°F and subsequent cyclic thermal exposure between 600°F and 1350°F resulted in severe bond degradation for combinations having an interdiffusion zone thickness of greater than 7.5×10^{-4} inch. Combinations having an interdiffusion zone thickness of less than 5×10^{-4} inch withstood 20 thermal cycles between 600°F and 1350°F without degradation of the interface bond. Electron beam microprobe analyses of the interdiffusion zones were made on selected isothermally exposed specimens, and concentration profiles were established.

The room temperature tensile yield strengths of the as-explosively bonded composites ranged from 75,000 to 98,000 psi with tensile elongation values of 55-70%. Fractures were extremely ductile and there was no evidence of delamination of the interfaces at fracture.

The isothermal exposure at 1500°F essentially recovered the work hardening increment induced during explosive bonding. The room temperature yield strength values of 30,000 to 45,000 psi for thermally exposed material corresponded closely to the reported yield strength values of the annealed components. If the interdiffusion zone thickness was less than 5×10^{-4} inch, the fractures were ductile with no evidence of delamination of the interfaces at fracture.

The stress for 1000 hour rupture life for the Ta-321 and Ta-347 composites at 1350°F was in the range of 18-20 ksi. The stress value for the 1350°F, 1000 hour rupture life of cold worked tantalum is 21 ksi and 8 and 11 ksi for annealed types 321 and 347 stainless steel respectively.

The mode of fracture during creep rupture testing was similar for all the refractory/austenitic composites and can be described by:

(a) A highly ductile shear type failure in the refractory metal component with 100% reduction in area.

(b) Intergranular separation in the austenitic component with negligible reduction in area except for a 0.015 inch wide zone adjacent to the refractory metal interface where no intergranular separation occurred.

There was no evidence of delamination along the interfaces during creep rupture testing or at fracture of as-explosively bonded and thermally cycled bimetal specimens.

I. INTRODUCTION

The objective of this work was to evaluate the compatibility of various refractory/austenitic bimetal combinations under cyclic and isothermal exposures. Much impetus was given to this investigation when it became apparent that a refractory metal would be required as the mercury containment material in the SNAP-8 boiler, the details of which are described elsewhere[1].

The use of austenitic/refractory bimetal composites in some applications would be highly desirable so that one could take advantage of properties unique to each of these classes of materials. However, there are some formidable compatibility problems between iron and nickel base alloys and columbium and tantalum refractory metal alloys. Joining of these two classes of metals using conventional fusion welding techniques is impractical since the melting point of the refractory metals is near or above the boiling temperature of the austenitic materials. In addition, brittle intermetallic compounds and low melting eutectics are formed between the iron or nickel base austenitic alloys and the refractory metal alloys which would result in metallurgically unsound joints. Another complicating factor is the difference in thermal expansion coefficients. The coefficient of expansion for the austenitic materials is about 2-1/2 times greater than that of the refractory metal alloys. However, this problem may be minimized by proper design. The use of explosive cladding techniques does permit a sound metallurgical bond to be made between these two classes of material without the formation of a metallographically observable brittle interface in the as-bonded condition. At elevated temperatures, however, there will be interdiffusion and the growth of a brittle intermetallic zone. The rate of growth of this brittle intermetallic during service will be a function of the operating temperature and time which in the case of the SNAP-8 boiler is approximately 1350°F for over 10,000 hours.

The bimetal combinations studied were the refractory metals columbium and tantalum and the refractory metal alloys Cb-1Zr, Cb-27Ta-10W-1Zr (FS-85) and Ta-10W-2.5Hf-0.01C (T-222) clad by explosive bonding with Inconel 600 (Ni-16Cr-7Fe), type 347 stainless steel

(Fe-18Cr-10Ni-Cb stabilized), type 321 stainless steel (Fe-18Cr-10Ni-Ti stabilized), and Hastelloy N (Ni-16Mo-7Cr-5Fe). Both destructive and non-destructive tests were used to evaluate bond integrity of the various refractory/austenitic bimetal combinations in the as-bonded condition and after subjecting the composites to various cyclic and isothermal exposures.

Refractory/austenitic bimetal composites were evaluated according to the schedule outlined in Figure 1. Sixteen bimetal combinations, formed by explosive bonding by the DuPont Explosives Department, were inspected for bond integrity by dye penetrant, ultrasonic resonance, and reverse bend testing of as-received and liquid nitrogen thermally cycled material.

Specimens from all sixteen composites were annealed for 1600 and 2700 hours at 1400, 1500, and 1600°F for the purpose of determining interdiffusion rates between the austenitic and refractory materials.

Specimens from nine selected combinations were further evaluated by means of room temperature tensile tests and creep rupture tests at 1350°F to determine the effects of isothermal and cyclic thermal exposure on mechanical properties. Isothermal exposure consisted of 1600 hours at 1500°F and cyclic thermal exposure consisted of twenty cycles between 1350°F and 600°F.

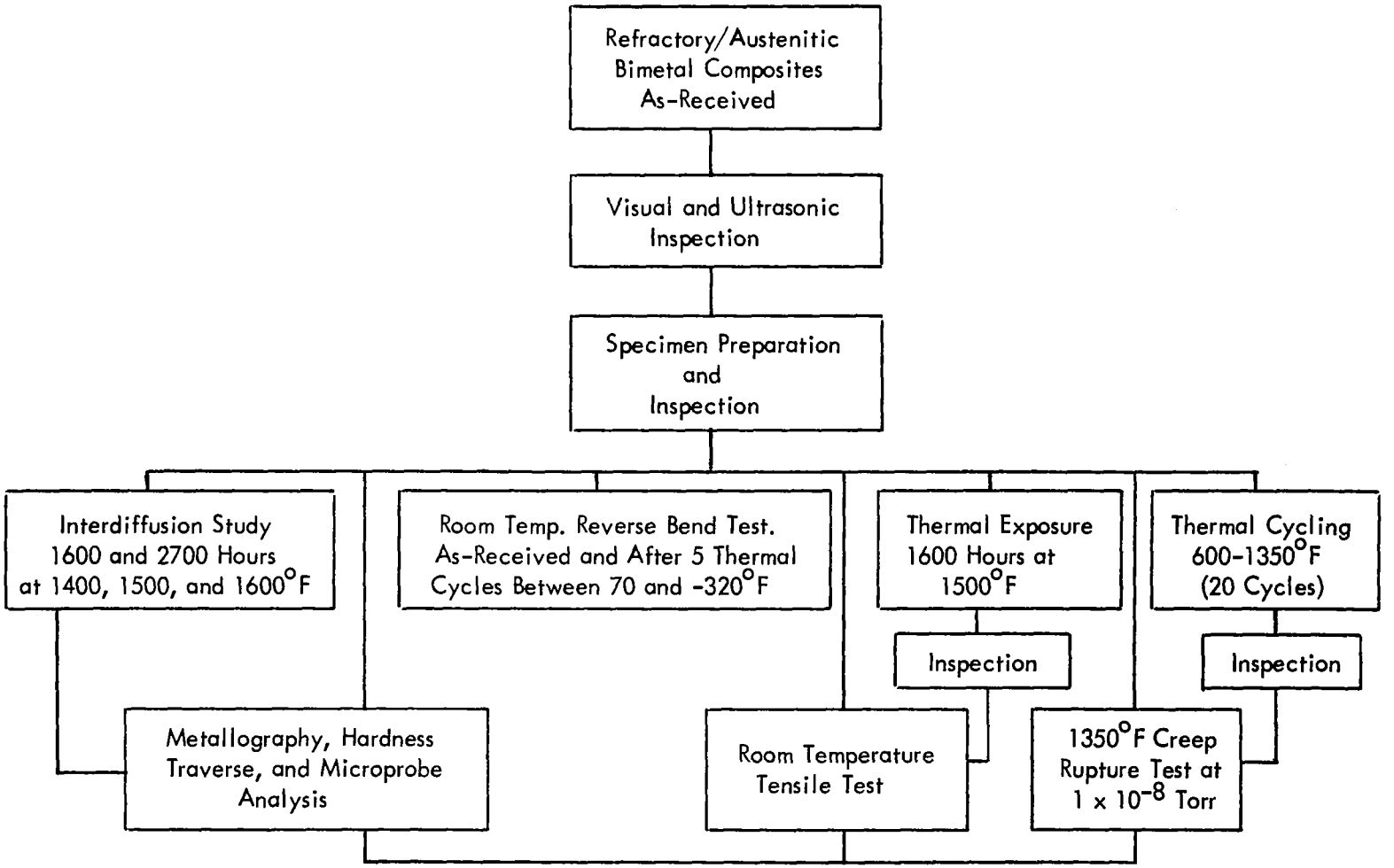

FIGURE 1 - Testing and Inspection Schedule for Refractory/Austenitic Bimetal Combinations

II. EXPERIMENTAL RESULTS AND DISCUSSION

A. STARTING MATERIAL

The sixteen (16) refractory/austenitic bimetal combinations, listed in Table 1 were supplied by NASA for evaluation. The bimetal composites were prepared by explosive bonding by the E. I. DuPont de Nemours & Co., Gibbstown, New Jersey. Bonding parameters were not made available since they are considered proprietary to DuPont.

The bimetal combinations were fabricated from 0.06 inch thick austenitic material and a 0.03 inch thick refractory metal or alloy sheet. All materials used in the preparation of the composites were in the fully recrystallized condition with the exception of the unalloyed tantalum sheet which was in the wrought condition. Mechanical property and chemical analysis data for the austenitic and refractory metal components are listed in Tables 2, 3, 4, and 5. Microstructures of the tantalum, columbium, T-222, and FS-85 sheet material prior to explosive bonding are shown in Figure 2. None of the starting Cb-1Zr sheet was available for characterization.

Explosive bonding, by which the bimetal combinations were formed, is a unique method for effecting a metallurgical bond between dissimilar metals. The physics of the process are involved[2] and hence will not be discussed in detail. However, certain features of the process are summarized in the following discussion taken from the paper of Holtzman and Cowan[3].

Bonding is accomplished by the collision between explosively propelled sheet or plate. For optimum bonding, the collision must occur at a rate in excess of a critical velocity which is a function of the physical properties of the materials being bonded. Two sheets of material, one or both of which has a layer of explosive affixed to it are positioned

TABLE 1 - Refractory/Austenitic Explosively Bonded Bimetal Composites

Composition (Refractory Metal/Austenitic Metal)
Cb/321
Cb/347
Cb/Inconel 600
Cb-1Zr/347
Cb-1Zr/Inconel 600
Ta/321
Ta/347
Ta/Inconel 600
Ta/Hastelloy N
FS-85/321
FS-85/347
FS-85/Inconel 600
FS-85/Hastelloy N
T-222/321
T-222/347
T-222/Inconel 600

Remarks (Nominal Composition in weight percent)

AISI 321 (Fe-18Cr-10Ni-0.08C Max - Ti stabilized)
AISI 347 (Fe-18Cr-10Ni-0.08C Max - Cb stabilized)
Inconel 600 (Ni-16Cr-7Fe)
Hastelloy N (Ni-16Mo-7Cr-5Fe)
FS-85 (Cb-27Ta-10W-1Zr)
T-222 (Ta-10W-2.4Hf-0.01C)

TABLE 2 - Vendor* Analysis of Austenitic Starting Materials

Element (w/o)	Inconel 600	321(1)	321(2)	347	Hastelloy N**
C	0.026	0.061	0.055	0.046	0.06
Mn	0.10	1.56	1.67	1.36	0.51
P	0.014	0.023	0.025	0.020	0.001
S	0.006	0.016	0.010	0.011	0.007
Si	0.39	0.56	0.72	0.58	0.39
Cr	15.74	17.10	17.94	18.47	6.44
Ni	Bal.	10.57	10.44	10.64	Bal.
Cu	0.01	0.15	0.22	0.17	0.01
Ti	0.22	0.46	0.58		0.01
Co	0.06	0.03		0.04	0.17
Al	0.13				0.01
Fe	6.80	Bal.	Bal.	Bal.	4.05
Mo		0.29	0.27	0.17	16.42
Cb				0.68	
Ta				0.01	
V					0.24
B					0.004

* Austenitic Metals purchased from Industrial Standard Steel Inc.
** Vendor - Stellite Division, Union Carbide
(1) Heat 31094
(2) Heat 60171

TABLE 3 - Mechanical Properties(a) of Austenitic Materials Used for Fabrication of Composites

Alloy	0.2% Y.S. (psi)	U.T.S. (psi)	% Elongation	Hardness R_B	Hardness DPH
AISI 321	33,600	84,200	51	78	149
AISI 347	41,900	86,200	46	80	153
Inco 600	31,100	87,900	45	71	130
Hastelloy N	52,750	114,350	52	--	--

(a) Vendor furnished certified test results, all materials in the annealed condition.

TABLE 4 - Vendor* Analysis of Refractory Starting Materials

Alloying Additions (w/o)	Cb-1Zr Ingot	Cb-1Zr Sheet(1)	Cb-1Zr Ingot	Cb-1Zr Sheet(2)	T-222 Ingot	T-222 Sheet	Ta Ingot	Ta Sheet	Cb Ingot	Cb Sheet	FS-85 Ingot	FS-85 Sheet
Cb	Bal.	---	Bal.	---	---	---	---	---	Bal.	---	Bal	---
Zr	1.04	---	1.0	---	---	---	---	---	---	---	.93	.92
Ta	---	---	---	---	Bal	---	Bal.	---	---	---	27.8	27.8
W	---	---	---	---	9.2	---	---	---	---	---	10.6	10.7
Hf	---	---	---	---	2.6	---	---	---	---	---	---	---
Impurities ppm												
Al	---	---	---	---	---	---	<10	---	<20	---	<20	---
C	<30	60	35	40	115	170	35	70	35	<30	45	80
H	4.4	2.5	4.2	27	3.1	2	2.7	1.4	4.2	2.7	3.7	1.7
N	65	65	87	55	20	16	23	70	37	35	35	25
O	145	190	180	240	<50	220	75	80	50	140	75	120
B	<1	---	<1	---	---	---	<1	---	<1	---	<5	---
Cb	---	---	---	---	485	---	<50	---	---	---	---	---
Cd	<5	---	<5	---	---	---	<1	---	<5	---	<5	---
Co	<20	---	<20	---	---	---	<5	---	<10	---	<10	---
Hf	<80	---	<80	---	---	---	---	---	<80	---	80	---
Fc	<100	---	<100	---	40	---	<15	---	<50	---	<50	---
Pb	<20	---	<20	---	---	---	<5	---	<20	---	<20	---
Mn	<20	---	<20	---	---	---	<10	---	<20	---	<20	---
Mo	<20	---	<20	---	30	---	<10	---	27	---	< 10	---
Ni	<20	---	<20	---	<20	---	<10	---	<20	---	<20	---
Si	<100	---	<100	---	---	---	<10	---	<50	---	<50	---
Ta	520	---	<500	---	---	---	---	---	705	---	---	---
Ti	<150	---	<150	---	---	---	<10	---	<40	---	<40	---
V	<20	---	<20	---	---	---	<10	---	<20	---	<20	---
W	<300	---	<300	---	---	---	<10	---	37	---	---	---
Zr	---	---	---	---	---	---	<50	---	<100	---	---	---
Sn	---	---	---	---	---	---	<10	---	<10	---	<10	---

*All refractory metals purchased from Wah Chang Corp. (1) Heat 912-1211-Cb-1Zr. (2) Heat 912-1189-Cb-1Zr
(Only interstitial elements were determined on final sheet product)

TABLE 5 - Mechanical Properties of 0.03 Inch Thick Refractory Metal Alloy Sheet Used for Fabrication of Bimetal Composites

Alloy	Heat Treatment	0.2% Offset Yield Strength (psi)	Ultimate Tensile Strength (psi)	Elongation (%)	Hardness DPH
Cb	1 hr. at 2200°F	13,100	24,900	44.5	73
FS-85	4 hrs. at 2400°F	73,400[(a)]	83,300	30.5	194
Ta	Wrought	64,900	73,900	14.0	159
T-222	4 hrs. at 2400°F	81,600	106,400	28.5	238

(a) Upper yield point, lower yield point 68,300 psi

(a) Unalloyed Columbium 73 DPH

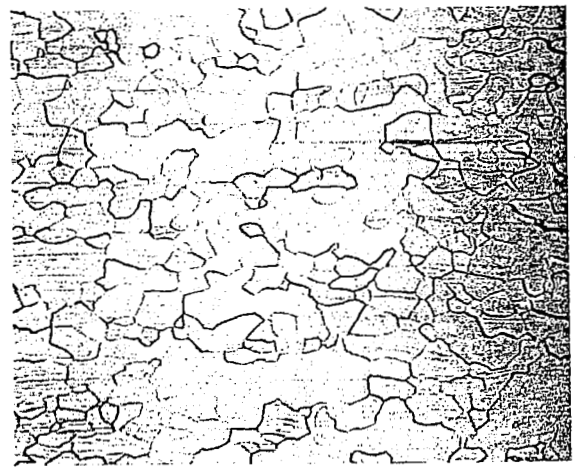

(b) FS-85 (Cb-27Ta-10W-1Zr) 194 DPH

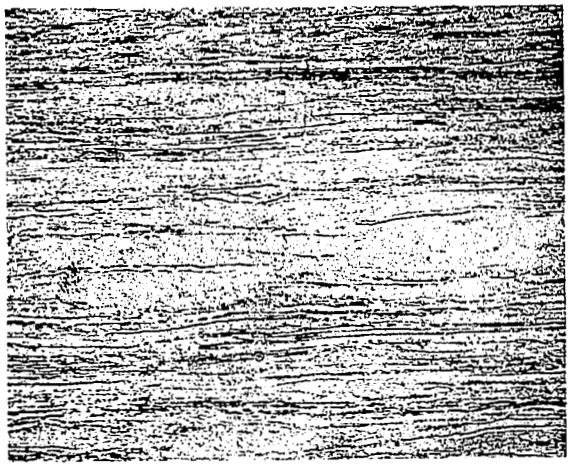

(c) Unalloyed Tantalum 159 DPH

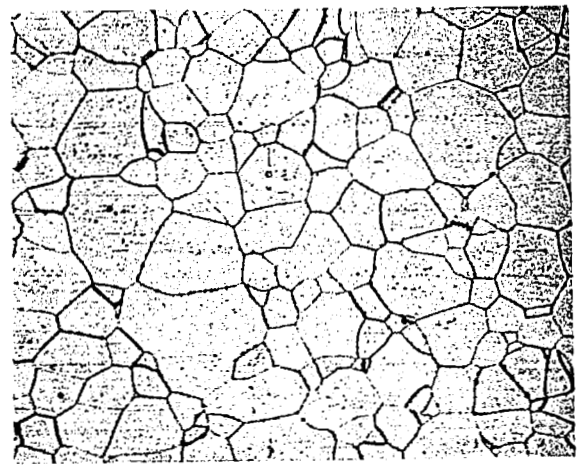

(d) T-222 (Ta-10W-2.5Hf-0.01C) 238 DPH

FIGURE 2 - Microstructure and Hardness of Refractory Metal Alloys Used to Manufacture the Bimetal Composites Mag. 250X

in any one of the frequently used arrangements shown below.

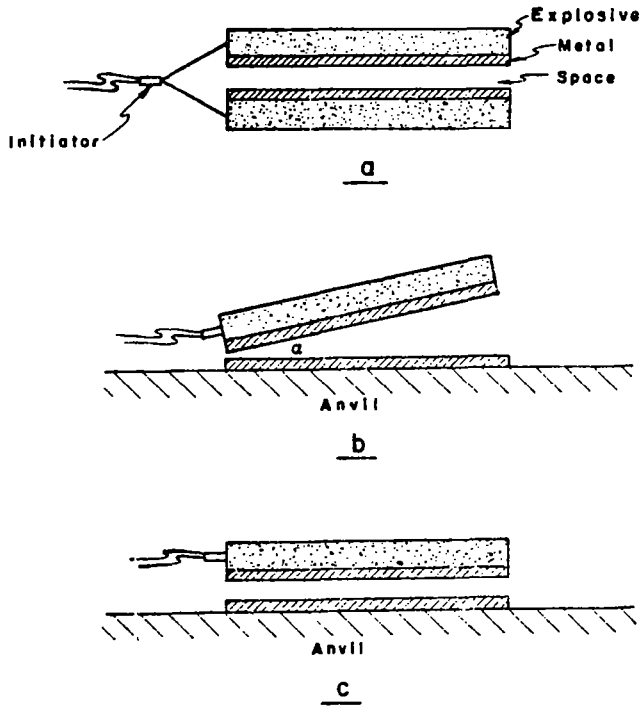

The explosive charge is detonated and the explosively propelled sheet collides. A sufficiently large pressure is generated ahead of the point of collision which causes the free surfaces of the metal just ahead of the collision point to flow into the space between the plates. It is the characteristics of this jet flow which determine the characteristics of the bond. When the jet flow becomes trapped, a sufficient portion of the kinetic energy is converted into heat as frictional forces bring part of the jet to rest, and a layer of molten material is formed. The exact mechanisms are, however, uncertain. When the collision region becomes unstable, oscillations occur and the result is the formation of an interface which has a sinusoidal wave form. Most of the energy is expended in the formation of the waves and melting, but a continuous layer of molten material is not formed. This type of interface is considered optimum. The wave propagation is very directional and the sinusoidal

wave form will be observed only when viewing the interface transverse to the direction of wave propagation. A planar interface would then be observed when viewing the interface parallel to the direction of wave propagation.

The bimetal combinations prepared for this investigation were made by bonding 12 inch wide x 20 inch long x 0.03 inch thick refractory metal sheet to 0.06 inch thick austenitic material of the same dimensions. As noted earlier, the details of the bonding were not made available since DuPont considers this proprietary information. Thus details such as position, amount, and type of explosive, set up geometry, stand-off distance, included angle, and whether both sheets were propelled or one was stationary cannot be described. The only information supplied was the direction of the explosive shock wave which propagated along the 20 inch dimension. This was readily discernible from metallographic examination of the as-received composites. The as-bonded composite sheets were severely distorted and required flattening. To facilitate flattening, the composites were cut into two sections 6 inches wide x 20 inches long and flattened by either stretcher straightening or roller leveling. The as-bonded and straightened composite sheets were visually and ultrasonically inspected and the results are summarized in Table 6. Two types of defects observed visually on the surfaces of the as fabricated components were "bubbles" or "blisters" and "ripples". The bubble or blister type defect when observed occurred only on the refractory metal side and may have been caused by air entrapment between the sheets during the bonding process. The ripple type defect also occurred on the refractory metal side and is shown in Figure 3. This type of defect may have resulted from an uncontrolled instability during the collision of the thinner refractory metal sheet with the heavier austenitic material.

Ultrasonic inspection for bond integrity was made using a Vidigage thickness measuring device. Using a 3/8 inch diameter quartz crystal transducer and an induced frequency of 9 MHz., determinations were made from the austenitic side at the intersections of a 1 inch grid spacing. A 0.090 inch thick piece of 300 series stainless steel was used for the reference standard. Thus unbonded areas would indicate a thickness of 0.06 inch. Determinations

TABLE 6 - Summary of Visual and Ultrasonic Resonance Inspection Results of As-Bonded Refractory/Austenitic Bimetal Composite Specimens

Composition	Ultrasonic Indications	Visual Indications
Cb/321	None	None
Cb/347	None	None
Cb/Inc 600	Two defects, ~1" square	None
Cb-1Zr/Inc 600	None	None
Cb-1Zr/347	None	Two defects, 1" x 5", 2-1/2" x 1"
Ta/321	None	None
Ta/347	One defect 3" x 10"	1/2" x 2" within area of ultrasonic indication
Ta/Inc 600	Two defects, 3-1/2" x 2", 1" x 3"	Two defects, 1" x 3-1/2", 2" x 4"
Ta/Hastelloy N	One defect 2" x 2"	One defect ~2" x 2"
FS-85/321	Two defects, 1" x 6", 1" x 12"	None
FS-85/347	1/4 the area of the sheet unbonded	None
FS-85/Inc 600	Two defects, 1" x 6", 2" x 16"	One area 2" x 17"
FS-85/Hastelloy N	Two defects, 1" x 9", 1" x 6"	One area 2" x 2"
T-222/321	None	None
T-222/347	None	None
T-222/Inc 600	None	None

FIGURE 3 - "Rippled" Surface Defect in Ta/Inconel 600. Mag. 1X
Defect in Ta Side of Composite.

were not made in areas containing visually observed defects. The defects uncovered by the ultrasonic test were verified by metallographic examination. All the bimetal composites exhibited good bonding based on the results of the ultrasonic inspection with the exception of the composites containing the columbium alloy FS-85 as the refractory metal component. The FS-85/austenitic composites exhibited unbonded areas of from 10-25% of the total. A typical unbonded area contour revealed by the ultrasonic inspection of a FS-85/347 bimetal is shown in Figure 4. Since there is no reason to believe that FS-85 would be intrinsically more difficult to bond to the austenitic material, it would appear that improper parameters and/or explosives were used for the preparation of these particular composites.

The ultrasonic inspection readily discriminated between areas where a metallurgical bond existed between the dissimilar metal components and where there was only mechanical contact. Areas where no bond ultrasonic indications were observed would separate freely when cut from the surrounding bonded areas. Ultrasonic inspection is a very useful tool for identifying the areas of gross unbound. However, investigation of the feasibility of using ultrasonic techniques for determining the degree of bond was beyond the scope of this investigation.

Metallography* samples were taken from the ends and center section of each of the 6 x 20 x 0.09 inch thick composites. The samples were taken such that the surface examined was parallel to the 20 inch dimension and thus transverse to the direction of shock wave propagation. Since no bonding details were made available it was not possible to orient the sheets with respect to the point of explosion initiation. The microstructural examination revealed a wide variation in the geometry of the interfaces between the austenitic and refractory metal which are illustrated in the photomicrographs of Figure 5. Typically,

---

*Metallographic procedures used for preparing the bimetal composites for examination are described in Appendix I.

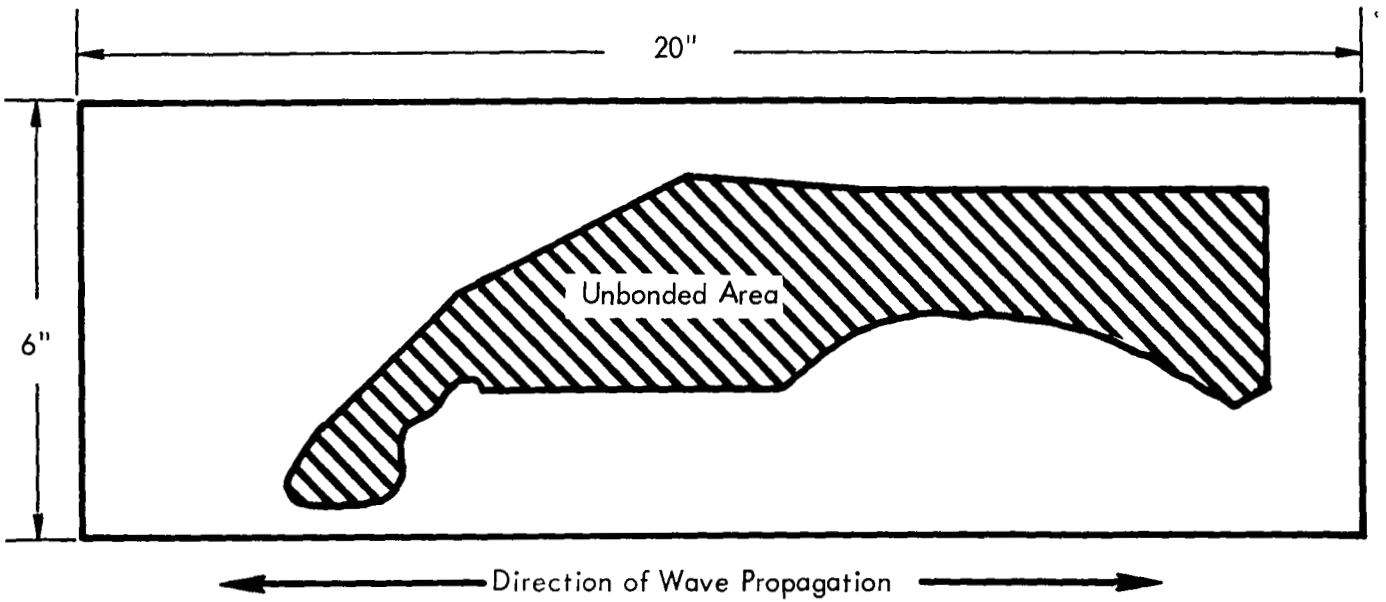

FIGURE 4 - Typical Defect Area in FS-85/347 Revealed by Ultrasonic Inspection
Scale 3/8" = 1"

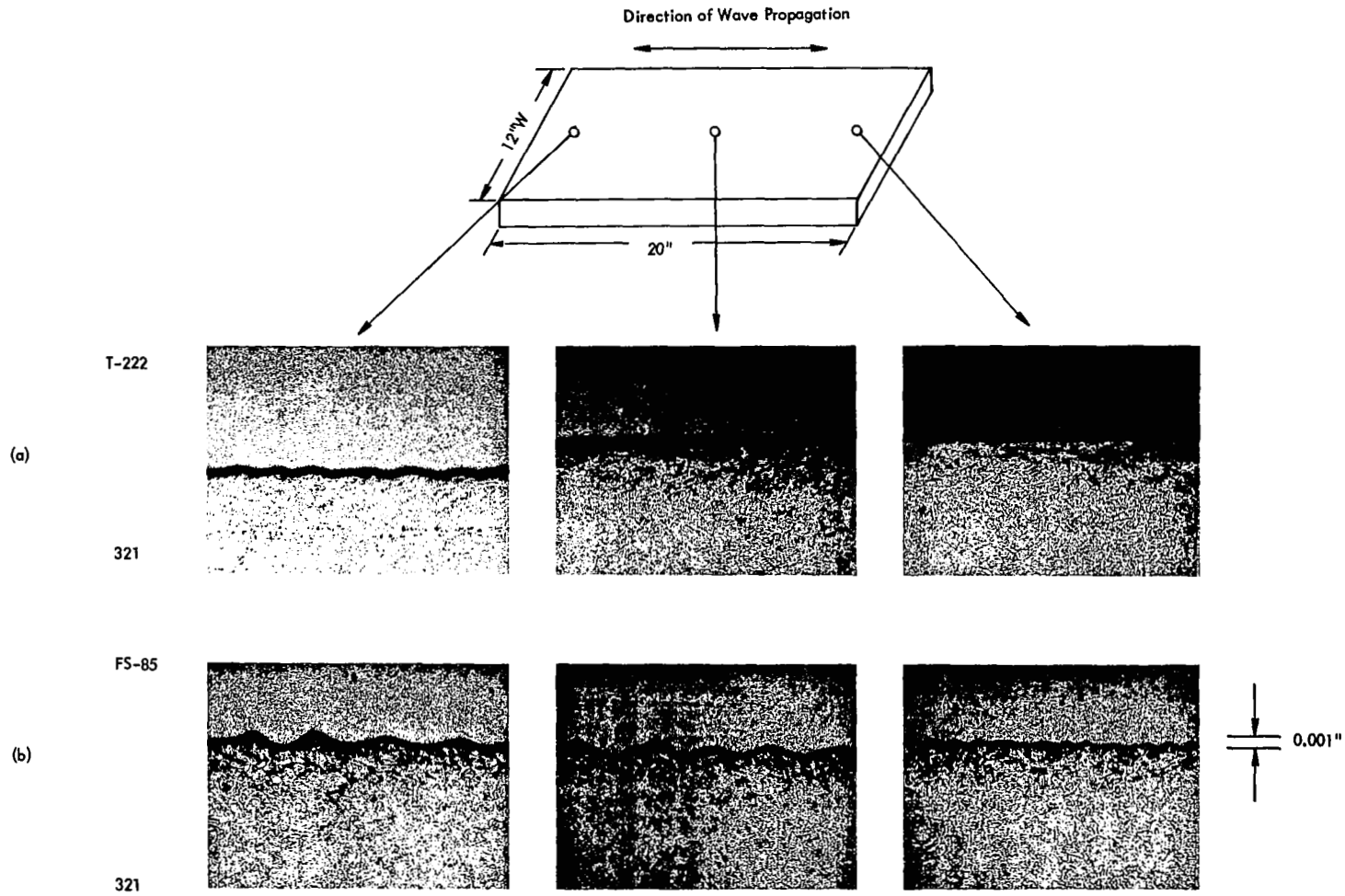

FIGURE 5 - Photomicrographs of Explosively Bonded Refractory/Austenitic Bimetal Composites Showing Geometry of Interface (Note: Shadows at Interface Caused by Relief Between Austenitic and Refractory Metal Components are not Separations)

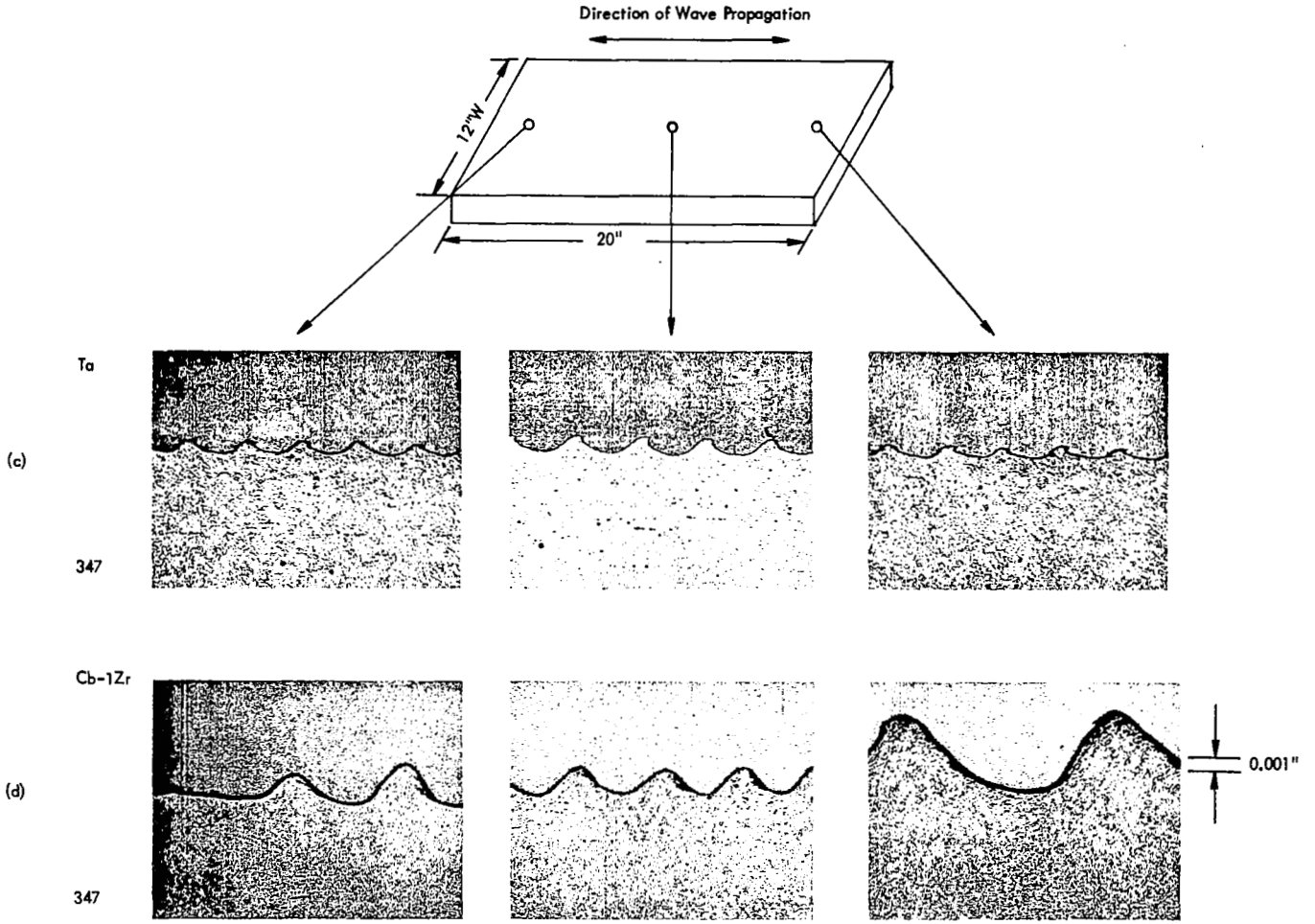

FIGURE 5 (Continued) - Photomicrographs of Explosively Bonded Refractory/Austenitic Bimetal Composites Showing Geometry of Interface (Note: Shadows at Interface Caused by Relief Between Austenitic and Refractory Metal Components are not Separations)

they can be described as:

1. Little or no wave form, tending toward planar interface (Figure 5a).

2. Combination planar and wave form, with variation in amplitude of wave (Figure 5b).

3. Crested wave peak exhibiting a "hooked" effect, and uniform amplitude (Figure 5c).

4. Wave form of varying frequency (Figure 5d).

All of the metallographic specimens were taken from areas of sheet which were metallurgically bonded as determined ultrasonically. Thus there does not appear to be any correlation between interface geometry and bond integrity. In none of the sixteen composite combinations was there a metallographically observable interdiffusion zone of measurable thickness even when examined at a magnification of 10,000X. There were of course some discrete areas observed metallographically where mechanical mixing of the two components occurred and were usually found near the crests of the wave at the interface. These metallographic observations were later verified during subsequent electron beam microprobe analysis which is discussed in a latter section.

Microhardness traverses were made on each of the bimetal composites. Hardness impressions were made at 1, 2, 3, 5, 10 and 20 mils from the interface into each of the metal components. The DPH values for each of the metal components were measured at a distance halfway between the interface and surface of the sheet. The hardness traverse data show that at this distance the hardness has reached essentially a constant value. Comparison of the hardness data in Table 7 for the as-explosively bonded composites with that of the starting material (See Table 2 and 5) reveal that two changes have occurred during the explosive bonding process. (1) There was a significant increase in the hardness level of each component as well as (2) a hardness gradient near the bimetal interface. For example,

TABLE 7 - Hardness of As-Bonded Refractory/Austenitic Bimetal Composites

Composition	Knoop Hardness Distance from Interface (mils)												Base Metal Hardness DPH[a]	
	Refractory Material						Austenitic Material							
	20	10	5	3	2	1	1	2	3	5	10	20	Ref.	Austenitic
Cb/347	107	119	127	121	120	118	434	458	430	394	336	315	97	277
Cb/321	108	125	116	128	133	138	421	398	381	409	305	293	82	263
Cb/Inc. 600	112	118	112	119	129	126	374	300	295	313	295	236	105	226
Cb-1Zr/347	150	171	167	171	174	168	463	409	409	425	364	313	120	247
Cb-1Zr/Inc. 600	142	152	148	153	164	154	398	390	381	364	295	292	118	243
FS-85[b]/347	231	282	263	295	298	261	332	326	318	241	278	219	232	231
FS-85/Inc. 600	278	336	269	289	310	298	413	409	451	355	358	267	251	258
FS-85/347	298	293	305	271	308	326	413	390	329	329	271	271	232	234
FS-85/321	254	278	293	292	303	298	488	477	405	409	425	342	226	297
FS-85/Hast. N	241	271	280	293	313	323	451	390	390	390	326	287	224	227
Ta/321	171	189	207	207	207	201	473	473	443	405	368	326	172	259
Ta/Inc. 600	188	183	180	191	193	216	378	351	358	351	318	247	172	240
Ta/Hast. N	183	176	178	160	186	186	584	654	552	413	361	329	146	264
T-222/Inc. 600	295	313	374	358	398	358	430	409	374	342	321	278	290	228
T-222/321	310	351	351	385	381	390	468	447	387	409	324	274	291	234
T-222/347	335	355	394	413	385	378	488	417	447	458	355	303	282	285

(a) Base hardness level, measurement made equidistant between interface and surface.
(b) Traverse taken at area of "no-bond".

the hardness value reported for the annealed 321 and 347 stainless steel starting material was 150 DPH. The hardness level of the 321 and 347 after explosive bonding was 230 to 297 DPH. This represents a 53 to 98% increase over the starting hardness level.

During the explosive bonding, a shock wave passes through the metal and plastic deformation is reported to occur on a very localized scale[3]. Thus although no gross change in macroscopic dimensions are observed, appreciable hardening of the metal does occur. Dieter[4] discusses this phenomena in some detail. In addition to the intrinsic work hardening characteristics of the metal, the degree of hardening during explosive bonding depends on the peak pressure of the shock wave with the highest pressure shocks causing the highest degree of hardening[3]. As noted earlier, the greatest increase in hardness (53-98%) as a result of the shock loading was measured on the high rate of work hardening austenitic materials. The low rate of work hardening refractory metals exhibited only a 20-30% increase in hardness level. The unalloyed tantalum exhibited only a minor increase in hardness as a result of the shock loading. However, the unalloyed tantalum material was used in the as-rolled condition and therefore had a significant increment of cold work already present.

Since interdiffusion between the as-explosively bonded austenitic and refractory metal components could not be detected, the hardness increase of each of the bimetal components near the interface must result from the highly localized plastic flow which occurred in this region during explosive bonding. This change in hardness near the interface for austenitic components Inconel 600, Type 321 S. S. and Type 347 S. S. is illustrated in Figure 6a, b, and c respectively. Similar data for the refractory metal alloy component is plotted in Figure 6d. Since there were a number of individual combinations, none of which were duplicated, the data presentation in Figure 6 was selected as being most illustrative. It is evident that there is a significant range of hardness values for each of the austenitic components. However, it appears that the change in hardness of the austenitic component is similar irrespective of the refractory metal to which it was bonded. Also, the austenitic component exhibits the highest hardness values when bonded to the high strength refractory

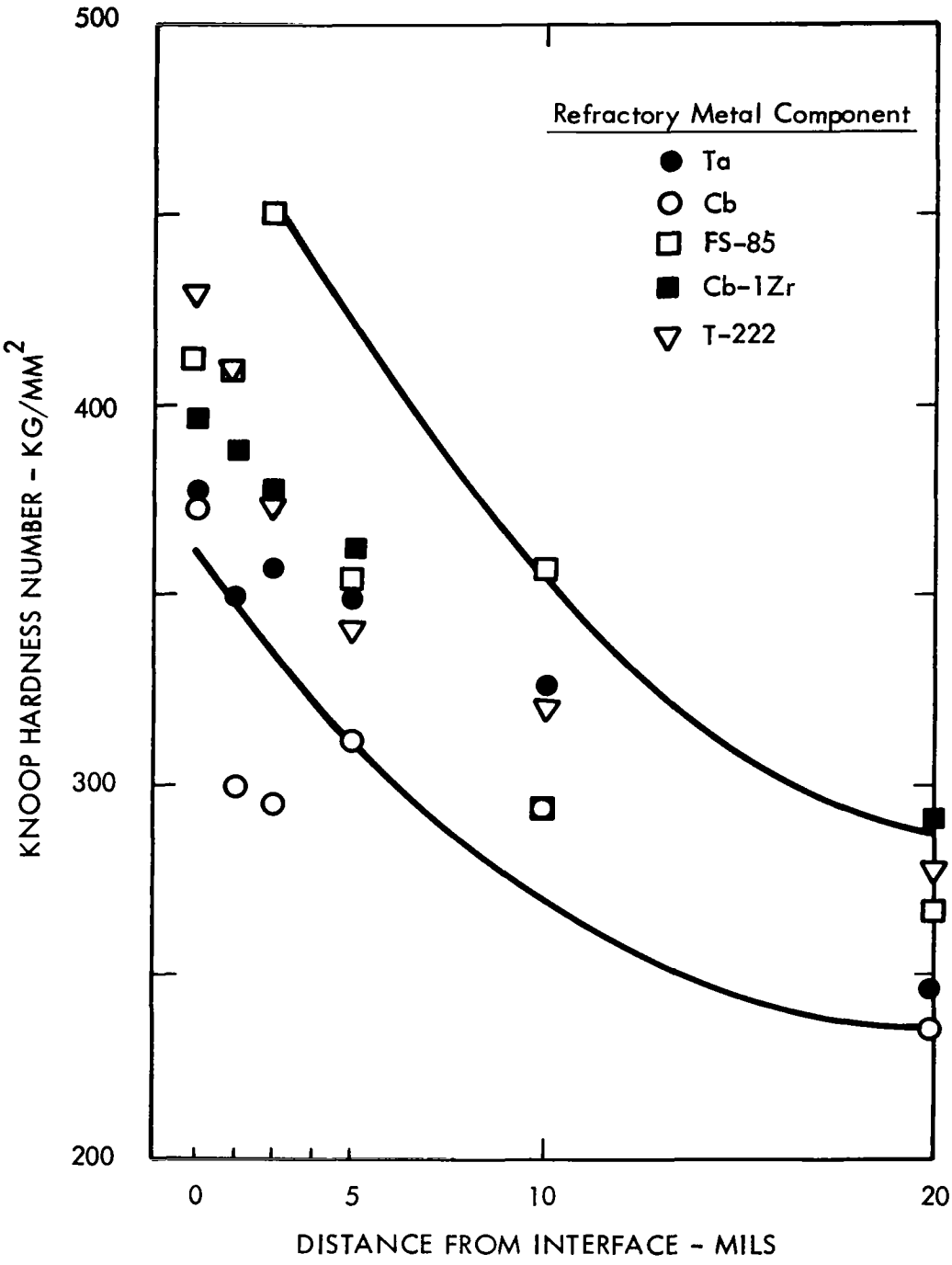

FIGURE 6a - Hardness Traverses of Selected Components of As-Bonded Refractory/Austenitic Bimetal Composites (a) Inconel 600 Bonded to Refractory Metal Alloys

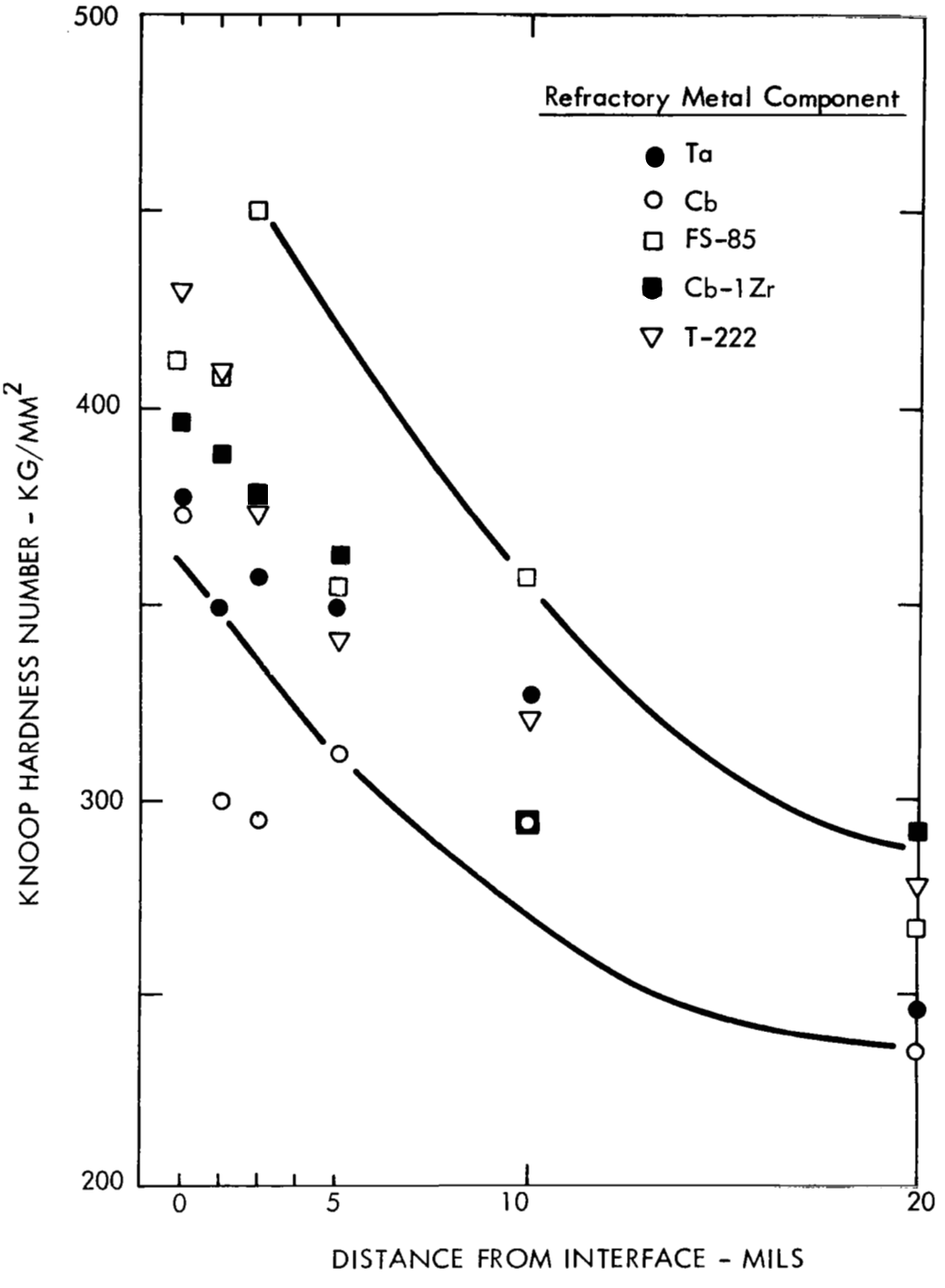

FIGURE 6b - Hardness Traverses of Selected Components of As-Bonded Refractory/Austenitic Bimetal Composites (b) Type 321 Stainless Steel Bonded to Refractory Metal Alloys

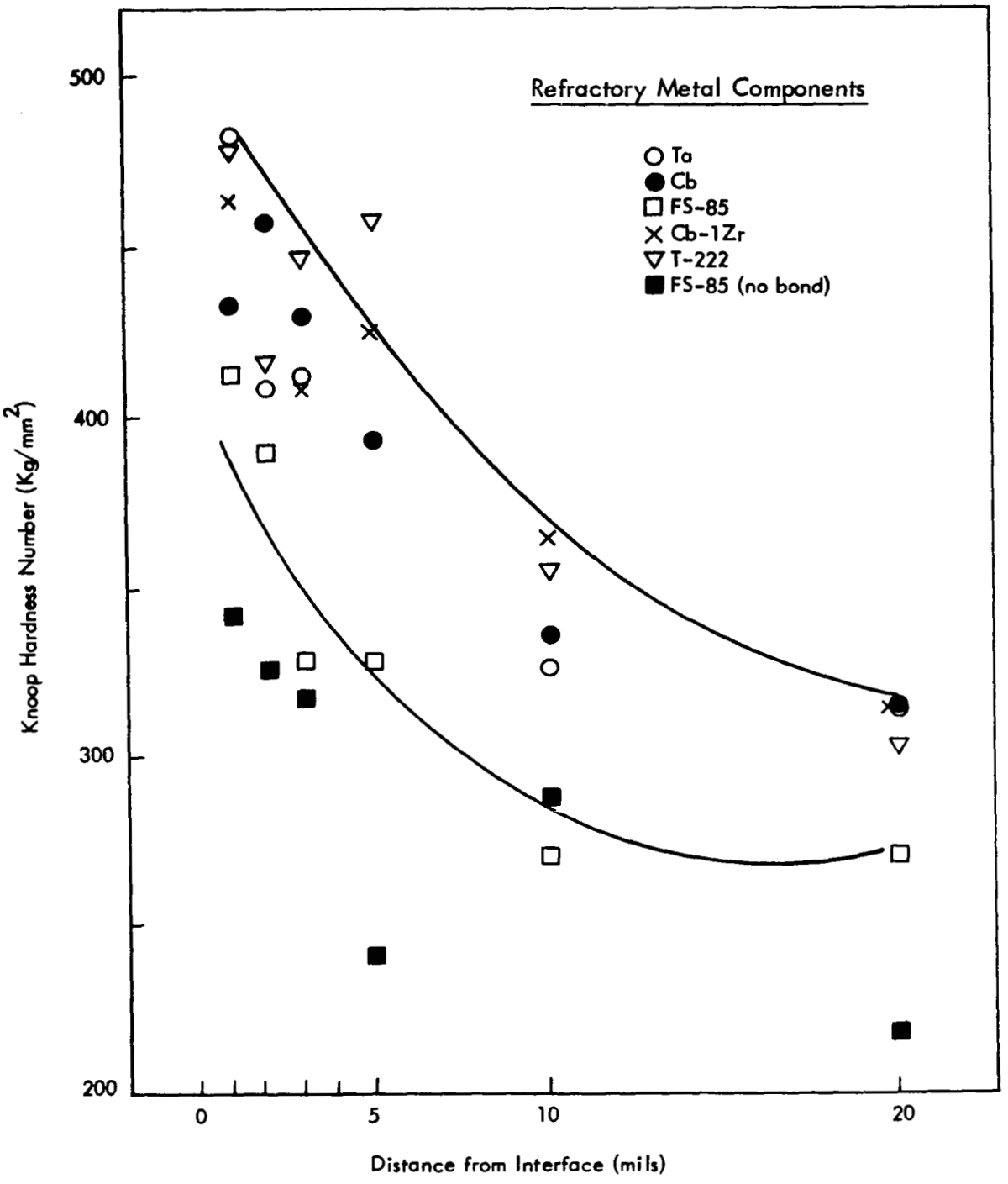

FIGURE 6c - Hardness Traverses of Selected Components of As-Bonded Refractory/ Austenitic Bimetal Composites (c) Type 347 Stainless Steel Bonded to Refractory Metal Alloys

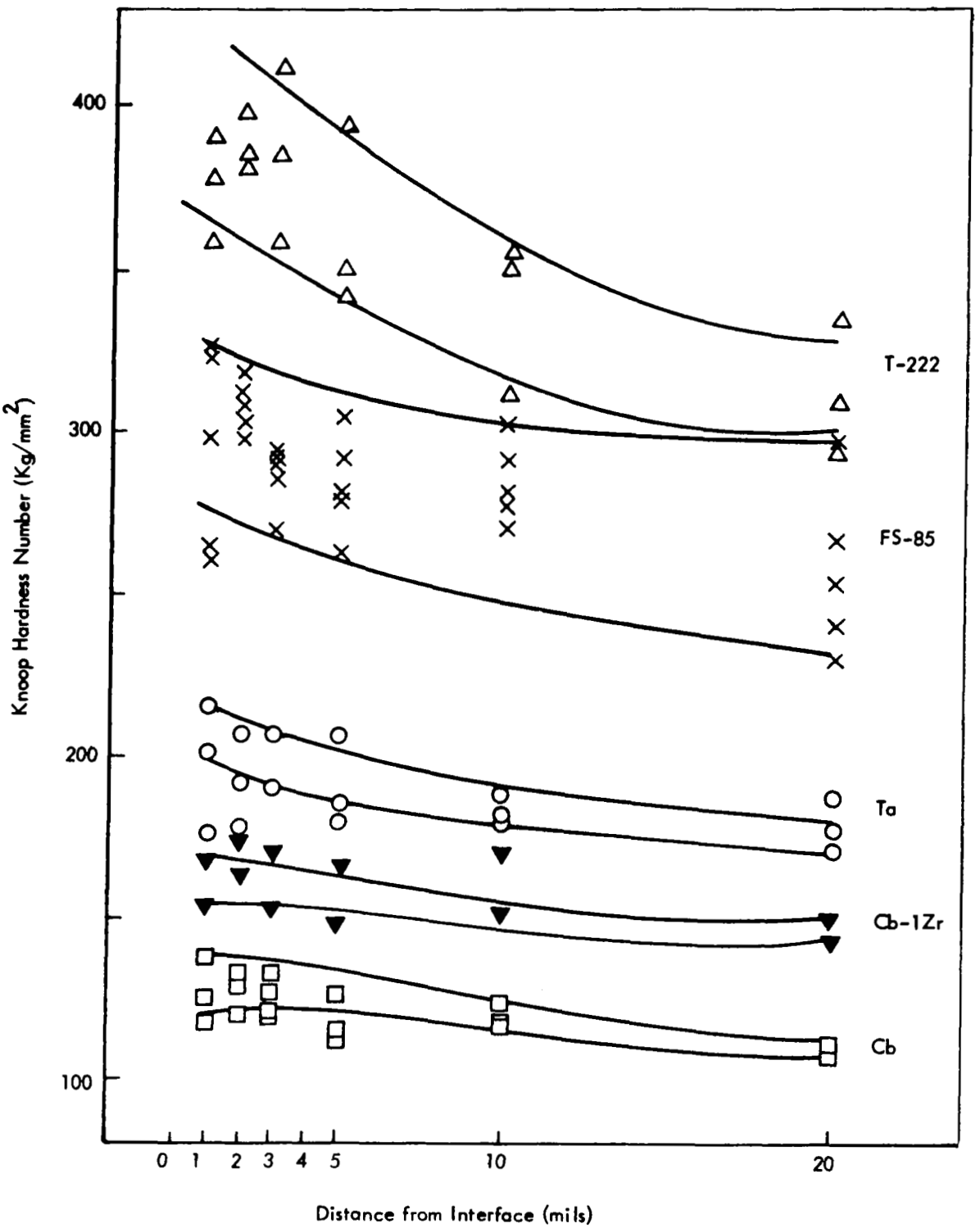

FIGURE 6d - Hardness Traverses of Selected Components of As-Bonded Refractory/ Austenitic Bimetal Composites (d) Refractory Metal Alloys Bonded to Austenitic Materials

metal alloys FS-85 and T-222. Likewise the lowest hardness values occurred when the low strength unalloyed columbium was the refractory metal component. However, it is immediately apparent that the exception is the hardness of the 347 stainless steel, which was lowest when the FS-85 was the refractory metal alloy component. (See Figure 6c) Also the hardness values determined at bonded areas and unbonded areas were similar. Thus there does not appear to be a ready correlation between bond integrity and hardness. As has been discussed previously, the composites which contained the FS-85 as the refractory metal component exhibited the greatest amount of bond defects. It is also evident that the hardness traverse data on the FS-85 (Figure 6d) exhibits a much broader range of values than that of the other refractory alloy components. This again suggests that there may have been lack of process control during the explosive bonding of the FS-85/austenitic bimetal composite. This can only be a speculative conclusion since none of the explosive bonding process parameters or observations were available.

Further evaluation of the bond integrity consisted of observing the behavior during reverse bend testing and cold rolling. Two specimens, 1 inch wide by 4 inches long by 0.09 inches thick, of each of the bimetal composites were subjected to reverse bend testing. One specimen of each composite prior to reverse bend testing was quenched to liquid N_2 temperature and warmed to room temperature, the cycle being repeated five times. Reverse bend testing was performed by clamping the specimen vertically in a vise. The free half of the specimen was bent, by impacting, 90° from the original portion, and then returned to original position and then 90° in the opposite direction. This process was repeated until the composite fractured. Visual inspection of the bend area was made after each 90° bend. Only the FS-85 combinations showed any delamination tendency and then separation of each base material extended approximately 3/16 inch from the point of fracture. Generally the composites fractured in a ductile manner and the fracture or delamination characteristics were not influenced by the prior low temperature thermal cycle. The total number of reversals each composite withstood before fracture was a function of the properties of the

refractory metal portion only. Composites with the high strength FS-85 and T-222 fractured after four to five cycles while the composites made up with low strength Cb withstood at least ten reversals before failure.

Samples of each composite were reduced by rolling at room temperature with the direction of working both logitudinal and transverse to the direction of wave propagation during bonding. All of the samples were ultrasonically and dye penetrant checked to insure that there were no defects in the material prior to reduction. The 0.090 inch thick composites were reduced to 0.015-0.018 inch thick strip by multiple rolling passes. All of the combinations were reduced successfully with no visual defects with the exception of the FS-85/321 combination. The as-rolled sheets were examined by simple hand flexing. The FS-85/321 sheet exhibited audible clicks while the integrally bonded combinations did not.

Thus all of the composites with the exception of those containing FS-85 exhibited excellent bonding between the austenitic and refractory metal components. The defects observed are attributed to the limited amount of material prepared and if each particular combination were fabricated using optimum bonding parameters only a minimum of defects would be expected.

B. SELECTION OF COMPOSITES FOR EVALUATION

Although sixteen bimetal combinations were prepared, only the following nine combinations were examined in detail.

Cb/321
Cb/347
Cb/Inconel 600
Cb-1Zr/347
Cb-1Zr/Inconel 600
FS-85/321
Ta/321
Ta/347
Ta/Inconel 600

The combinations selected represent the iron base and nickel base austenitic materials in combination with unalloyed columbium and tantalum, columbium containing a getter element, (Zr), and a high strength columbium base alloy (FS-85). All of these selected combinations studied can be processed to tubing by conventional techniques with the exception of the combination containing the high strength columbium alloy FS-85. At the start of this program, only the pure refractory metals (Cb, Ta) or a very dilute low strength alloy such as Cb-1Zr could be processed concurrently with stainless steel by conventional tube manufacturing techniques. However it has been demonstrated recently that small diameter bimetal tubing can be fabricated by explosively bonding to size thus allowing the use of a high strength alloy such as FS-85 or T-222 as the refractory metal alloy component.

C. DIFFUSION ANNEALING

The degree of interdiffusion between the austenitic and refractory metal components of each bimetal composite was determined after exposures of 1600 and 2700 hours at 1400, 1500, and 1600°F. All exposures were conducted under ultra high vacuum conditions ($<1 \times 10^{-8}$ torr) in a bakeable, metal sealed system which is shown in Figure 7. The samples, contained within a 1-1/2 inch diameter Vycor glass tube, were heated by radiation from a hot wall furnace. A Pt/Pt-13Rh thermocouple imbedded within the sample load was used to monitor specimen temperature. The temperature was maintained within $\pm 5^{\circ}$F by a proportioning controller. Temperature uniformity over the heated test zone was within $\pm 2^{\circ}$F. Test pressures during exposure typically were less than 1×10^{-8} torr at 1600°F and $<1 \times 10^{-9}$ torr at 1400°F. The specimens for diffusion annealing, 1/4 inch wide x 1 inch long, were prepared by shearing. The edges were belt sanded, etched, and dye penetrant inspected to ensure no delamination at the interface. The specimens were then cleaned, weighed, and wrapped in tantalum foil prior to exposure. The specimens were positioned to offset the differences in coefficient of expansion and thus maintain the specimens flat during the thermal treatments. During each exposure, a deposit was formed on the cooler portion of the glass tube (see Figure 8). This deposit was identified by emission x-ray analysis as predominantly manganese

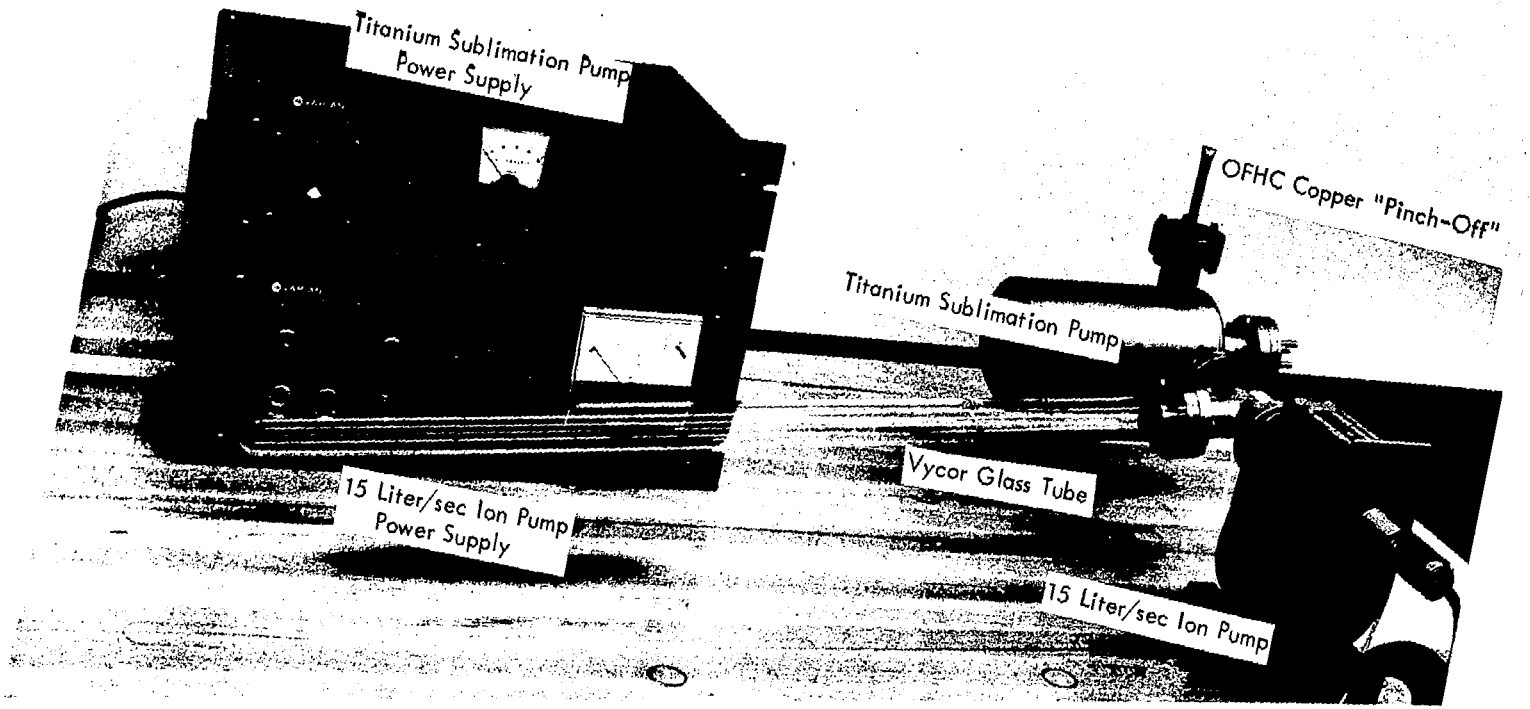

FIGURE 7 - Vacuum System for Diffusion Annealing Study

FIGURE 8 - Vycor Capsule Containing Ta Wrapped Bimetal Specimens After Annealing 1600 Hours at 1500°F. Black Deposit Identified as Mn is Apparent on Upper End of Tube

with a trace of chromium. No inward transfer of silicon from the Vycor tube into the specimens was indicated by emission spectrographic analysis of successive layers of the tantalum foil in which the specimens were wrapped.

After exposure, each specimen was unwrapped, weighed and visually examined for any indications of unbonding. A small number of specimens delaminated during the isothermal anneal. Generally, the specimens lost weight with the highest weight loss (0.06-0.08%) at 1600°F noted for combinations with the high manganese (1.5%) containing 321 and 347 stainless steels. The low manganese containing (<0.5%) Inconel 600 and Hastelloy N combinations lost up to 0.02-0.03% at 1600°F. At 1400°F, the weight loss was from nil up to 0.02%, again depending on the manganese content of the austenitic component. A few samples showed a slight weight gain (0.01%) which could be indicative of a slight oxygen pickup during exposure. Each specimen was mounted and examined metallographically to determine the extent of interdiffusion. Interdiffusion zones formed between the refractory and austenitic components were measured from photomicrographs taken at a magnification of 400X and the data are listed in Table 8. Photomicrographs illustrating the various interdiffusion zones formed are shown in Figure 9. In some instances, the interdiffusion zone was irregular and thus a range of zone thickness was measured. This variation in zone thickness most likely occurred as a result of mechanical mixing of the components during the explosive bonding process. Only the austenitic component of each specimen was etched, because the etch polishing procedure used to delineate the microstructure of the refractory materials severely attacks the austenitic components and the interdiffusion zones.

It is evident from the photomicrographs that the makeup of some of the zones is quite complex. Occasionally they are composed of two or more phases, some of which may have precipitated out during cooling from the diffusion annealing temperature. The composition of the interdiffusion zones which will be discussed later in this section, was studied using an electron beam microprobe. It should be noted that the position of the original refractory/ austenitic metal interface is not known. However, voids, when present, were always within

TABLE 8 - Interdiffusion Zone Thickness[1] Data for Diffusion Annealed Refractory/Austenitic Bimetal Composites

Composition	Zone Thickness (inches x 10^3)					
	1600 Hours At:			2700 Hours At:		
	1400°F	1500°F	1600°F	1400°F	1500°F	1600°F
T-222/321	a	0.20	0.15	a	0.06	0.15
T-222/347	a	0.15	0.30	a	0.12	0.30
Ta/321	a	0.25	0.30	0.04	0.35	0.63
Ta/347	a	0.15	b	0.04	0.25	b
Cb/321	0.17	0.31-0.70	1.20	0.16-0.31	0.55	1.55
Cb/347	0.17	0.30	1.00	0.12-0.23	0.31	1.25
Cb-1Zr/347	a	0.15	1.20	a	0.15	1.33
FS-85/321	a	0.55	0.75	0.08	0.16	1.40
FS-85/347	a	0.30	b	0.08	0.20	b
T-222/Inc. 600	c	0.65	1.30	0.12	0.62	1.33
Cb/Inc. 600	0.60	1.20	1.60	0.86	1.25	1.87
Ta/Inc. 600	0.45	1.00	b	0.70	b	b
FS-85/Inc. 600	0.50	1.35	2.00	0.63	1.4	2.50
Cb-1Zr/Inc. 600	0.50	1.15	1.80	0.78	1.37	2.20
FS-85/Hast. N	0.45	0.75d	1.30	0.55	1.12	2.03

a - None detected

b - Specimen delaminated during exposure

c - Interdiffusion zone present, not well enough defined to measure.

d. Data point excluded from range and average.

(1) Determined Metallographically(400X)

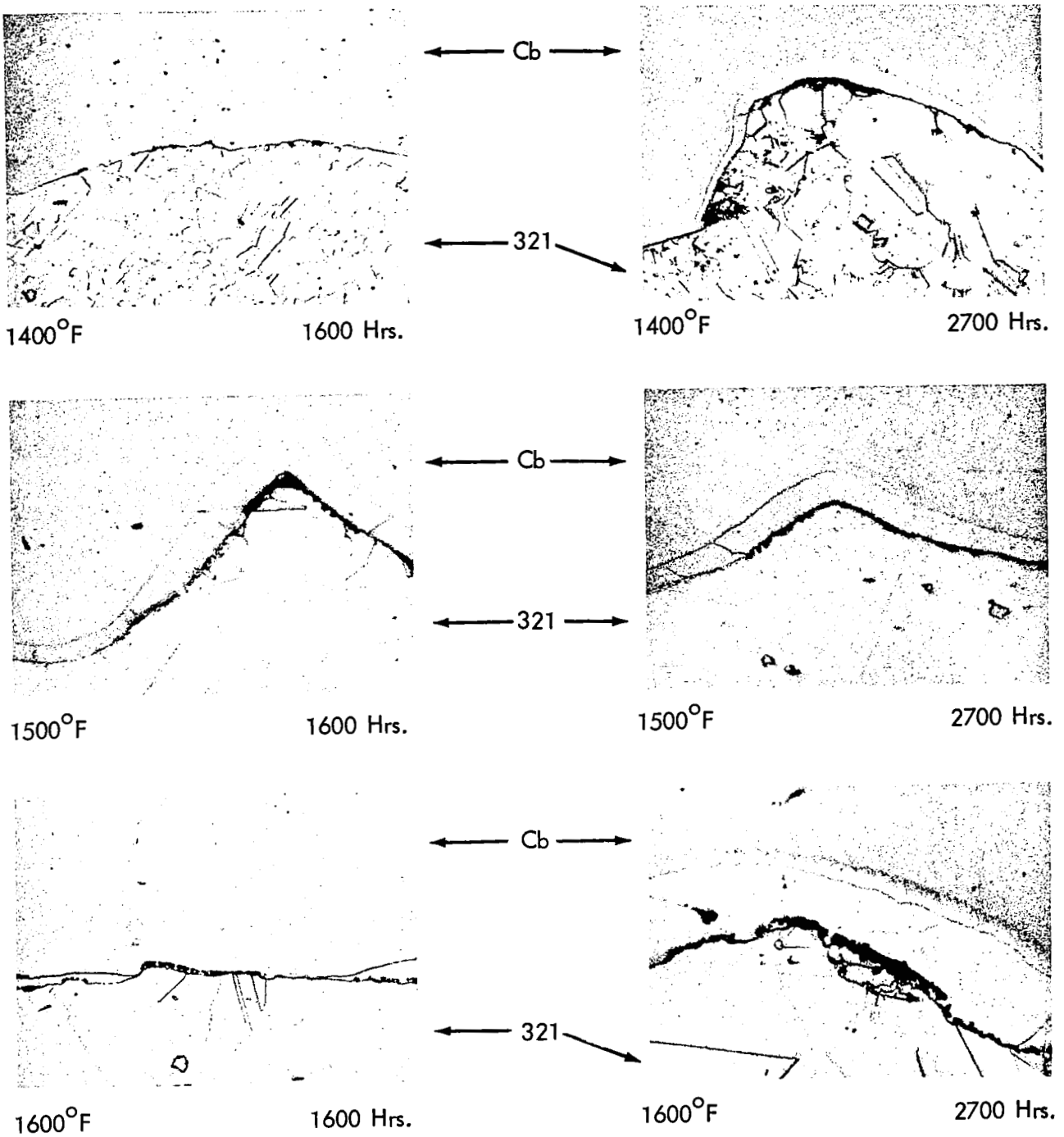

FIGURE 9 - Interdiffusion Zone Between Cb/321 Stainless Steel After Indicated Exposure (Mag. 400X 1" = 2.5 mils)

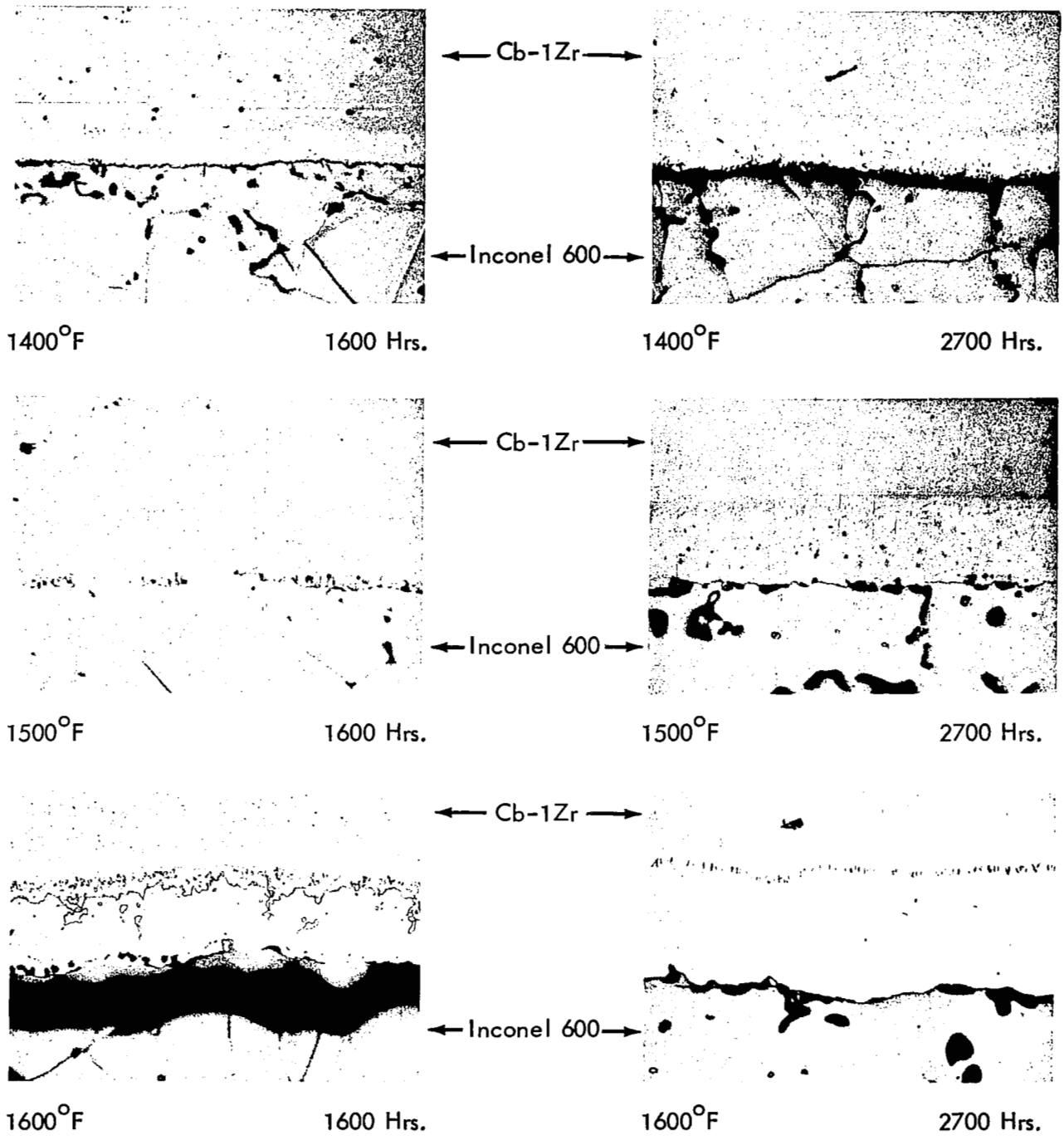

FIGURE 9 (continued) - Interdiffusion Zone Between Cb-1Zr/Inconel 600 After Indicated Exposure (Mag. 400X 1" = 2.5 mils)

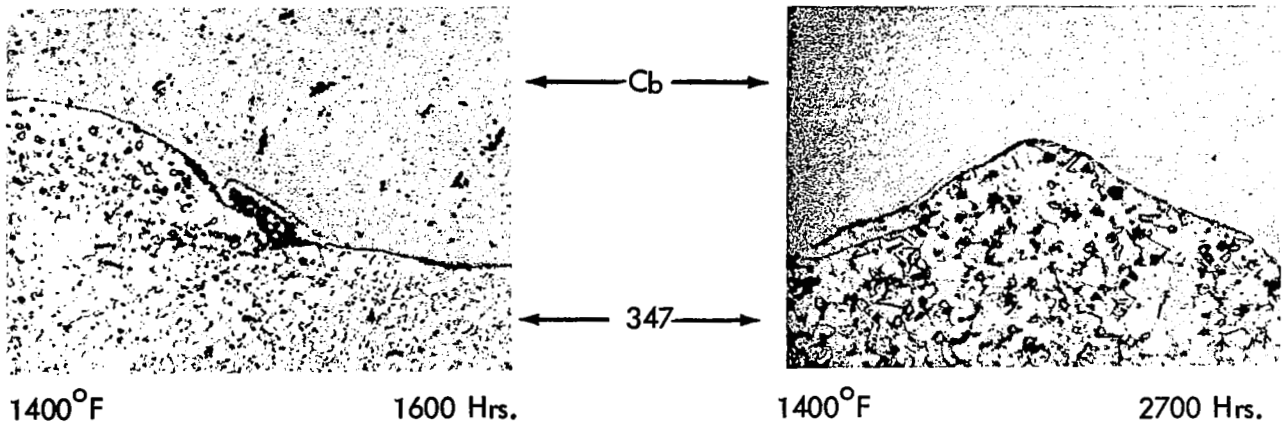

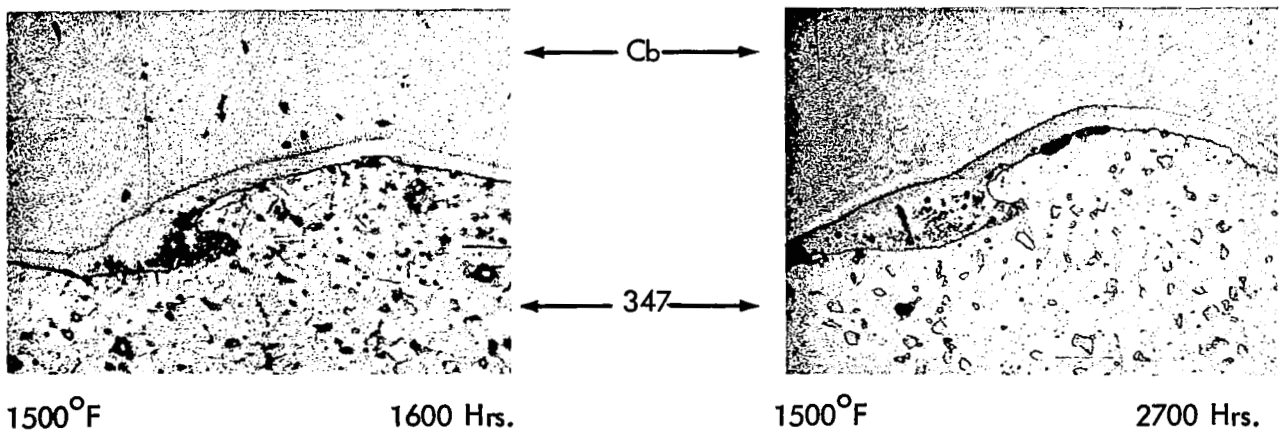

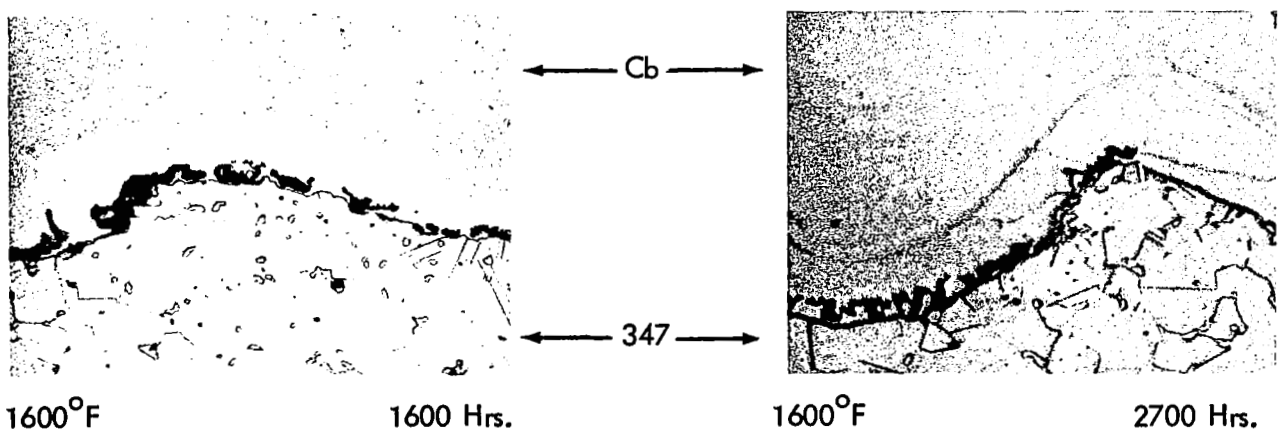

FIGURE 9 (continued) - Interdiffusion Zone Between Cb/347 Stainless Steel After Indicated Exposure (Mag. 400X 1" = 2.5 mils)

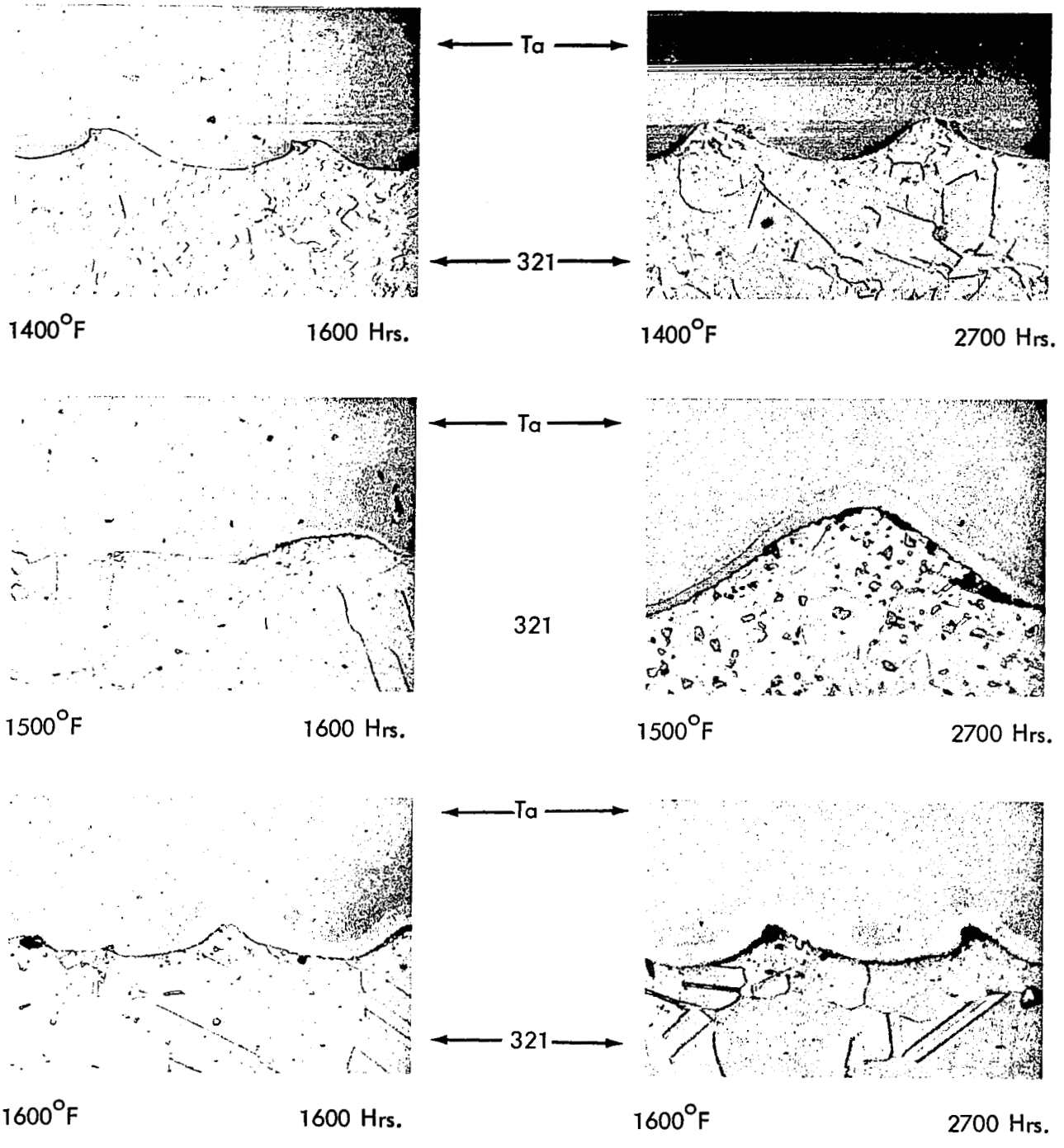

FIGURE 9 (continued) - Interdiffusion Zone Between Ta/321 Stainless Steel After Indicated Exposure (Mag. 400X 1" = 2.5 mils)

the austenitic material. Thus there appears to have been a net diffusion of Ni, Cr, and Fe into the refractory material.

Effect of Isothermal Exposure on Hardness

Microhardness traverses were taken on each of the diffusion annealed bimetal composite specimens using the same procedure as for the as-explosively bonded composites and the data are in Appendix II. Where interdiffusion zones were present, the measurements were taken at the same increments from the zone interfaces as observed metallographically since the location of the original interface could not be precisely ascertained.

The annealing behavior of the refractory metals and austenitic components is summarized in Figure 10 where the bulk hardness* is plotted as a function of annealing time for the various annealing temperatures. It was generally observed that the hardness of the austenitic material was essentially recovered after the 1600 hour exposure at 1400°F and little change was observed after heating for longer times or at higher temperatures. The hardness of the columbium and tantalum was not raised significantly during the explosive bonding process and this increment of hardness increase was recovered in the columbium after 2700 hours at 1400°F and 1600 hours at 1600°F. Since the tantalum was bonded in the as-worked condition, a greater reduction in hardness was observed as the annealing temperature was increased from 1400 to 1600°F.

Rate of Interdiffusion Zone Growth

The rate of interdiffusion zone formation followed the parabolic rate low, with a plot of zone thickness versus the square root of time giving an excellent linear fit of the data (see Figure 11). It is evident from the data plotted in Figure 11 that there are three separate grouping of curves. The lowest rate of interdiffusion at 1600°F was observed to occur between

---

* The bulk hardness value was determined 20 mils from the interface and is assumed to represent changes caused by shock hardening during bonding and subsequent recovery thereof.

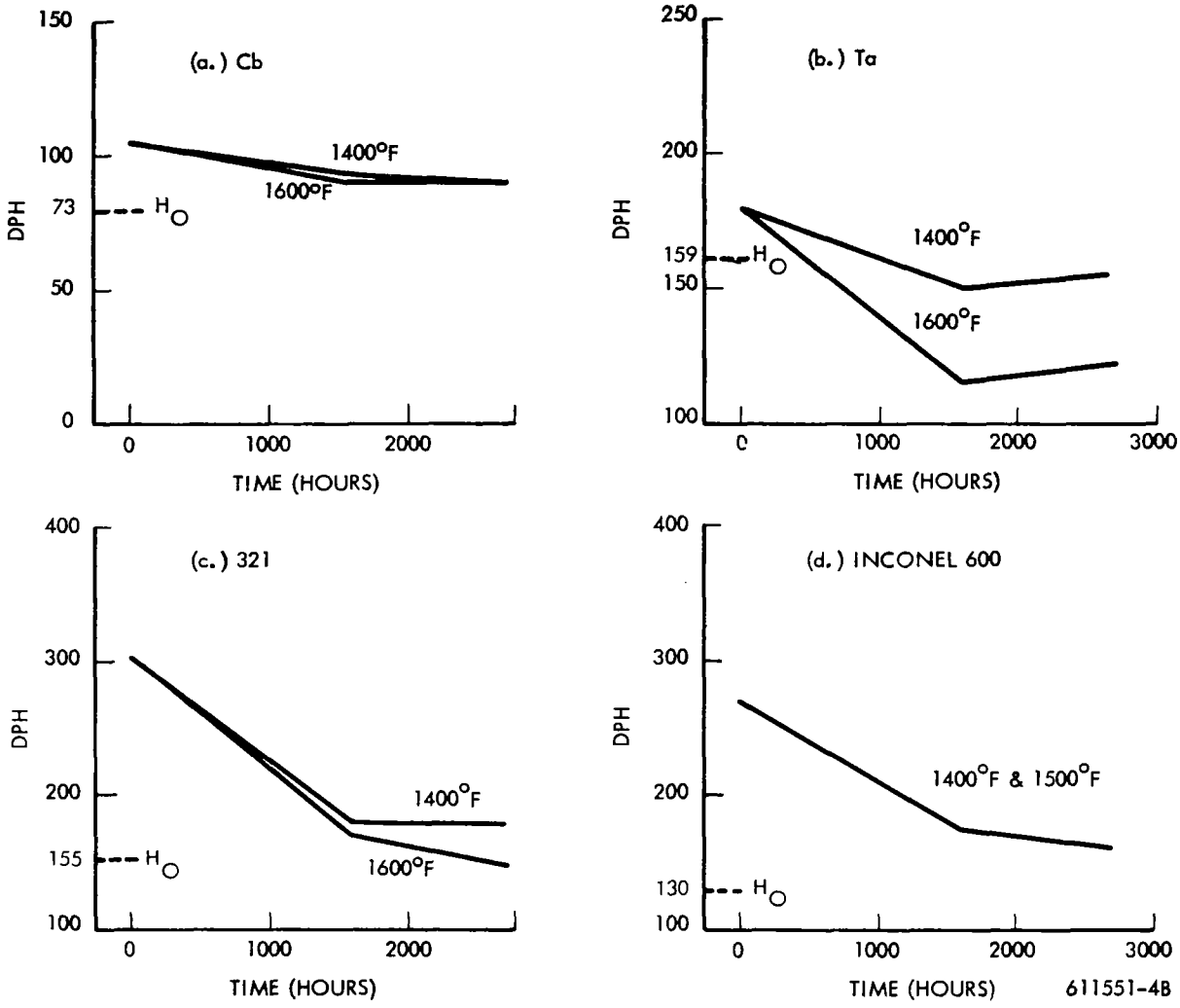

FIGURE 10 - Hardness Change in Refractory and Austenitic Components after Annealing for Specified Time. (H_O is Hardness of Material Prior to Explosive Bonding).

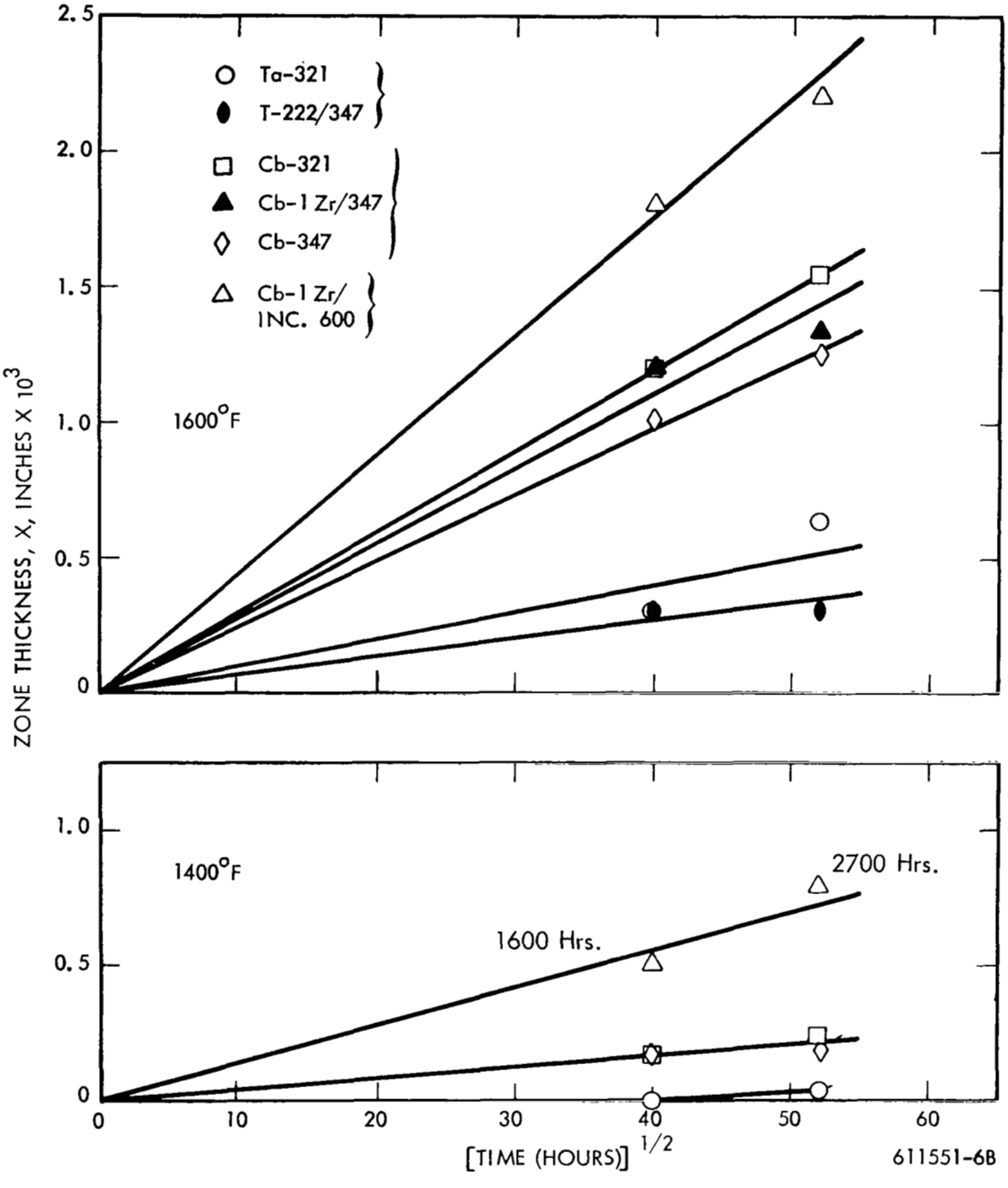

FIGURE 11 - Interdiffusion Zone Thickness as a Function of Time and Temperature for Selected Refractory/Austenitic Bimetal Composites

tantalum or T-222 and type 321 and 347 stainless steel. The average parabolic rate constant ($K = \partial X/\partial t^{1/2}$, in-hr$^{-1/2}$) for interdiffusion zone formation for this group of bimetals was 6.9×10^{-6}, in-hr$^{-1/2}$. The highest rate of interdiffusion zone formation occurred between the nickel base alloys Inconel 600 or Hastelloy N and all the refractory metals with the exception of T-222. The average parabolic rate constant (K) for this group of bimetal combinations at 1600°F was 4.1×10^{-5} inch-hr$^{-1/2}$. The remaining bimetal combinations consisting of columbium and the columbium alloys with 321 and 347 stainless steels plus the T-222/Inconel 600 composite exhibited an intermediate rate of zone growth at 1600°F with $K = 2.6 \times 10^{-5}$ inch-hr$^{-1/2}$

The rate of growth of the interdiffusion zone between the refractory and austenitic components was assumed to obey the Arrhenius rate equation ($K = A \exp(-Q/RT)$ where K is the parabolic rate of zone growth in (in-hr$^{-1/2}$), A is a constant, Q is an activation energy, cal/mole, R is the appropriate gas constant and T is the temperature in °K. The rate constant K for the bimetal couples Cb/321, Ta/321, T-222/347, and Cb/Inconel 600 is plotted as a function of reciprocal temperature in Figure 12. Also on Figure 12 is similar data for Cb-316 reported by Ferry and Page[5] which were determined for shorter times at higher temperatures than studied during this investigation. The rates of zone growth for the Cb-321 and Cb-347 are essentially identical and agree well with the data for Cb-316 indicating the similarity in behavior for these three types of stainless steels.

The rate of interdiffusion between tantalum and the stabilized stainless steels was significantly less than for that exhibited by columbium. This no doubt reflects the difference in melting temperature between Cb and Ta. However, as the annealing temperature was lowered from 1500°F to 1400°F, there is a break in the curve for the Ta/321 indicating a possible change in the rate controlling mechanism. The T-222 alloy exhibited the lowest rate of interdiffusion at all test temperatures with no observable zone formed after 2700 hours at 1400°F. This increased resistance to interdiffusion may be caused by the tungsten and hafnium additions.

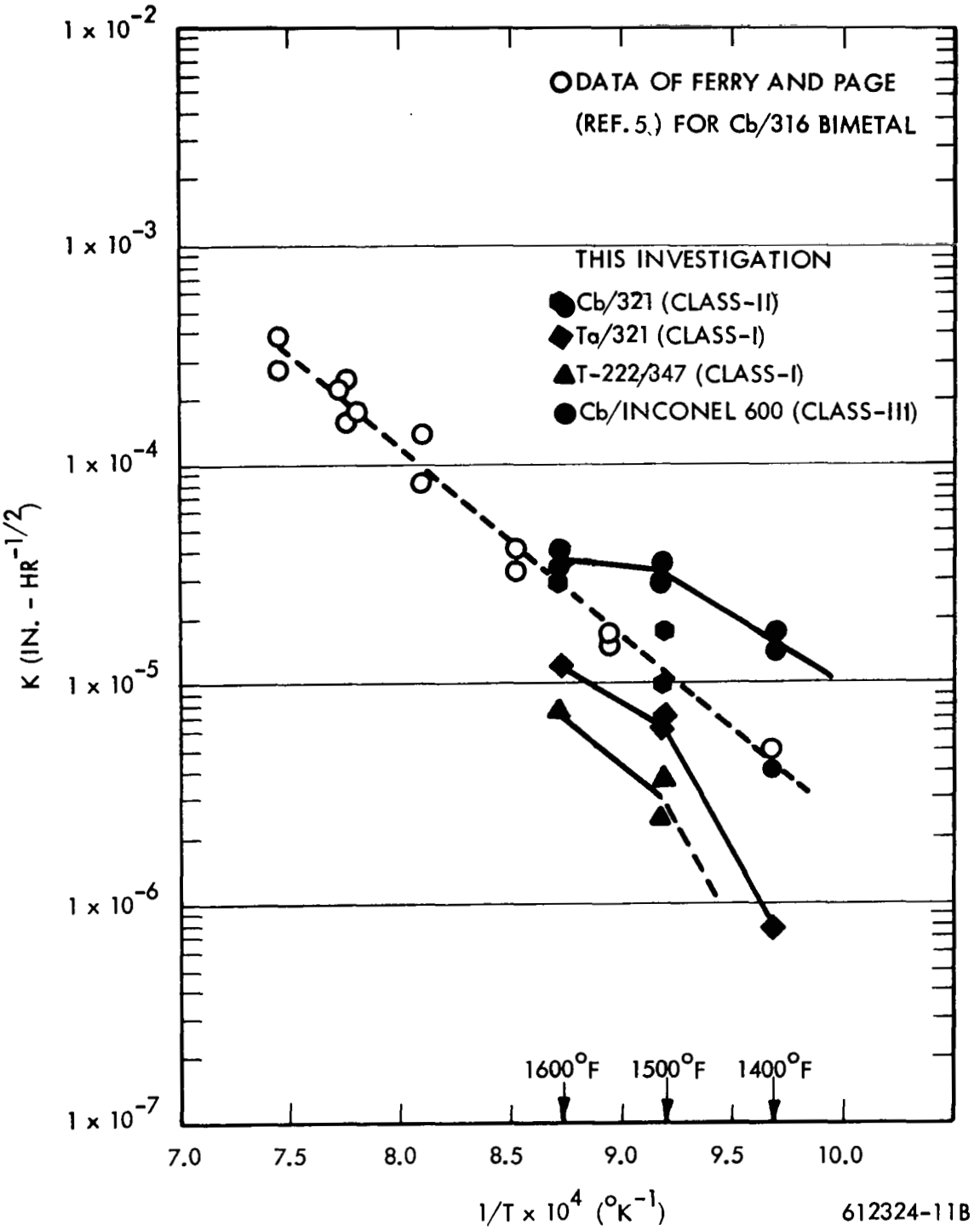

FIGURE 12 - The Parabolic Reaction Rate of Interdiffusion Zone Growth as a Function of Reciprocal Temperature for Selected Refractory/Austenitic Bimetal Composites

Substitution of Inconel 600 or Hastelloy N as the austenitic material resulted in a higher rate of interdiffusion irrespective of the refractory metal component. From compositional considerations, it appears that the nickel level may be exerting the greatest influence in the diffusion kinetics (Inconel 600 and Hastelloy N contain 75% Ni versus 10% Ni for the 321 and 347 stainless steels).

The interdiffusion zones of the nine bimetal specimens listed in Table 9 were examined with an electron beam microprobe at the Advanced Metals Research Corporation, Burlington, Massachusetts.

Three types of data were obtained. (1) Elemental concentration profiles - Obtained from traverses across the interdiffusion zones, made at an angle of 45° to the composite interface, with the concentrations of two elements being recorded simultaneously. These concentrations were subsequently corrected using appropriate calibration data. (2) Individual point analyses - Obtained on areas of interest, not necessarily intersected by the traverses. (3) Scanning display - Whereby the distribution of a specific element in an area of interest was graphically displayed. The brightness of an electron beam in a cathode ray tube scanning in synchronization with the microprobe beam is modulated by a characteristic x-ray line signal received by the x-ray spectrometer. This results in a CRT display where dark areas represent regions of low concentration of the specific element being studied. The technique is qualitative and while not as sensitive as the traversing or point analysis technique, it does provide a graphic representation of the local variation in concentration of a specific element.

The specimens analyzed with the electron beam microprobe are representative of bimetal combinations which exhibited the lowest, intermediate, and highest rates of interdiffusion and will be discussed in that order. It should be pointed out that the compositional changes that will be discussed concern only the substitutional alloying elements. Analysis for the distribution of the interstitial elements carbon, oxygen, and nitrogen was beyond the scope of work. However, the interstitial sink effect would be expected to be operative,

TABLE 9 - Diffusion Annealed Refractory Metal/Austenitic Alloy Composites Examined with the Electron Beam Microprobe

Composition	Annealing Temperature (^{o}F)	Annealing Time (hrs.)	Interdiffusion Zone Thickness (in. x 10^{3})
Ta/321 SS	1500	1600	0.25
Ta/321 SS	1600	1600	0.30
Ta/321 SS	1600	2700	0.63
T-222/347 SS	1600	1600	0.15
T-222/347 SS	1600	2700	0.30
Cb/347 SS	1500	1600	0.30
Cb/321 SS	1500	1600	0.31-0.70
Cb-1Zr/347 SS	1600	1600	1.20
Cb-1Zr/Inc. 600	1500	1600	1.15

particularly in combinations containing refractory metal alloys with reactive metal (Hf or Zr) additions. Analysis of the microhardness data did not permit any specific conclusions concerning the distribution of the interstitial elements, since hardness was being affected by a number of competing processes. These would include recovery and recrystallization in the heavily plastically deformed areas adjacent to the interface.

The intermetallic compounds which are identified in the interdiffusion zones are based on comparison of the average compositions determined from the microprobe results with compounds known to exist in the appropriate binary system. There was no verification of these compounds by x-ray diffraction analysis.

Ta/321 and T-222/347

The interdiffusion behavior of Ta/321 and T-222/347 is typical for the group of bimetal combinations exhibiting the lowest rate of interdiffusion. The concentration profile for the major alloying constituents in the Ta/321 specimen annealed for 2700 hours at 1600°F is shown in Figure 13. The photomicrograph shown in Figure 13a defines the traverse path (RS) used for microprobe analysis. Positions labeled X, Y, and T indicate areas where spot analysis data was obtained. (All spot analysis data is in Appendix 3). As shown in Figure 13a, the interdiffusion zone between tantalum and 321 stainless steel consisted of two distinct bands. Since 321 stainless steel is an iron base alloy, it was assumed that the phase relations within the interdiffusion zone should approximate that exhibited by the Ta-Fe (see Figure 14) binary phase diagram[6]. However, the Ta-Fe binary phase diagram is not very well defined with only the compound $TaFe_2$ positively established. From the concentration profile (Figure 13) and spot analysis data, it was concluded that the zone formed adjacent to the tantalum could be approximated by a compound of the type $Ta_8(Fe,Ni)$. A similar compound Cb_XFe has been proposed to exist in the Cb-Fe system[7]. The concentration profile of nickel in the zone next to the tantalum indicates an uphill gradient which was confirmed by the scanning micrograph shown in Figure 15.

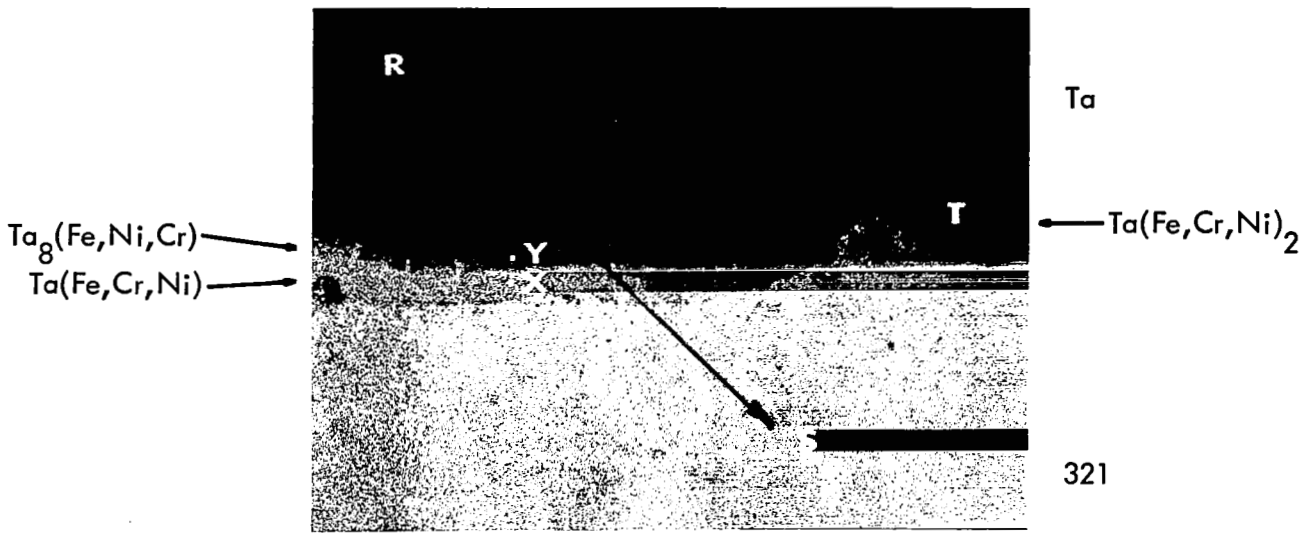

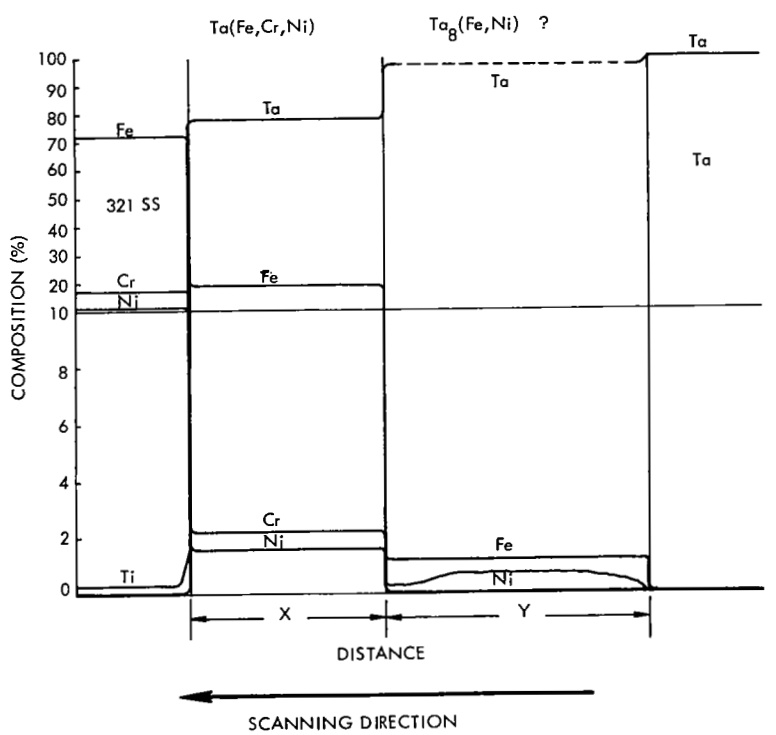

FIGURE 13 - Microstructure and Concentration Profile for Ta/321 Bimetal Annealed for 2700 Hours at 1600°F

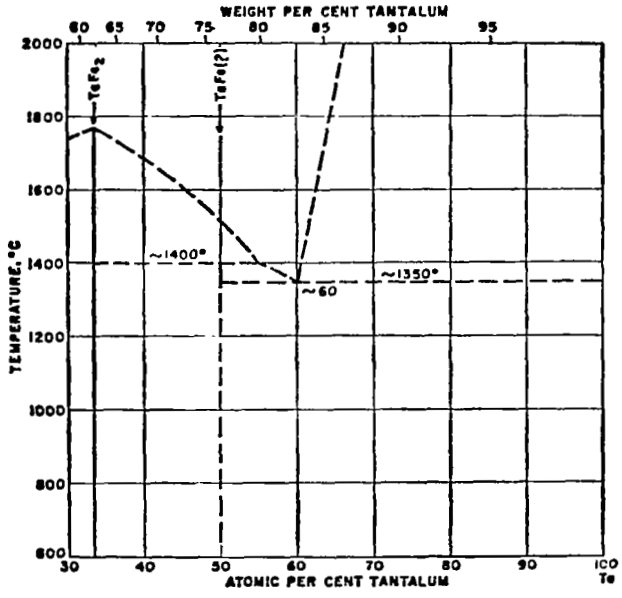

FIGURE 14 - Iron-Tantalum Phase Diagram
(Reference 6, p. 437)

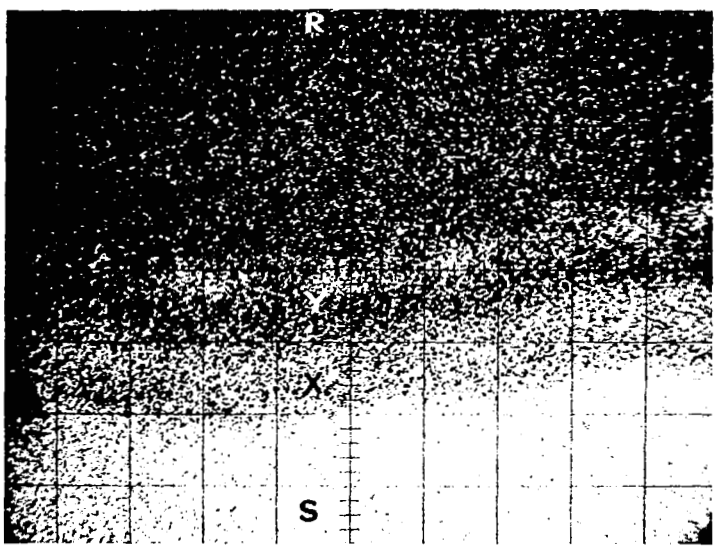

Mag. 540X 1" = 1.85 mils

FIGURE 15 - Electron Beam Scanning Display Illustrating Distribution of Nickel in Ta/321 Composite Specimen Annealed for 2700 Hours at 1600°F (Dark Areas Indicate Low Concentration While the Bright Areas are Indicative of High Concentration)

The composition of the zone formed next to the 321 stainless steel varied somewhat with the annealing time and temperature. However, in the specimen annealed for 2700 hours at 1600°F, an intermetallic compound was definitely indicated. (See Figure 13 and Appendix 3). The composition of this phase was approximately 77.5Ta-18.9Fe-2.2Cr-1.6Ni-0.6Ti, which is in excellent agreement with that of the compound TaFe (76.5Ta-23.5Fe) proposed for the Ta-Fe system (see Figure 14). However, no indication of a $TaFe_2$ compound between the "TaFe" and the 321 stainless steel was detected. Either the $TaFe_2$ type compound was not present or it was too thin to resolve. However, in the localized thick areas of the interface (marked T in Figure 13a,) where mechanical mixing evidently occurred during the explosive bonding process, the $TaFe_2$ type intermetallic compound having Cr and Ni substitution for Fe did exist. The Ta content decreased from 72.0% and the Fe and Cr content increased from 21.9 and 4.5% respectively, with increasing zone thickness (longer times and higher temperatures of annealing) to a composition of 61Ta-30Fe-6.4Cr-2.2Ni for the specimen annealed for 2700 hours at 1600°F. This would suggest that the composition range of the intermetallic compound may be much greater than that indicated in the published Ta-Fe phase diagram.

Judging from both the element traverses and the spot analyses, little or no diffusion occurred past the metallographically observed interdiffusion zones into either base material. Thus, to a first approximation, diffusion in the Ta/321 composite can be explained in terms of the Ta-Fe binary phase diagram.

The interdiffusion between the T-222/347 was significantly less than that exhibited between the Ta/321 or Ta/347 and reflects the effect of the W and/or Hf addition on the diffusion kinetics. The interdiffusion zone between T-222 and 347 appeared homogeneous. (See Figure 16.) The extremely narrow zone (3×10^{-6} inches) made interpretation of the microprobe traverse difficult. However, it appears that the zone is (Ta, W, Hf) $(Fe, Cr, Ni)_2$ with the composition 46Ta-5.7W-1.6Hf-36.5Fe-7.2Cr-3.0Ni.

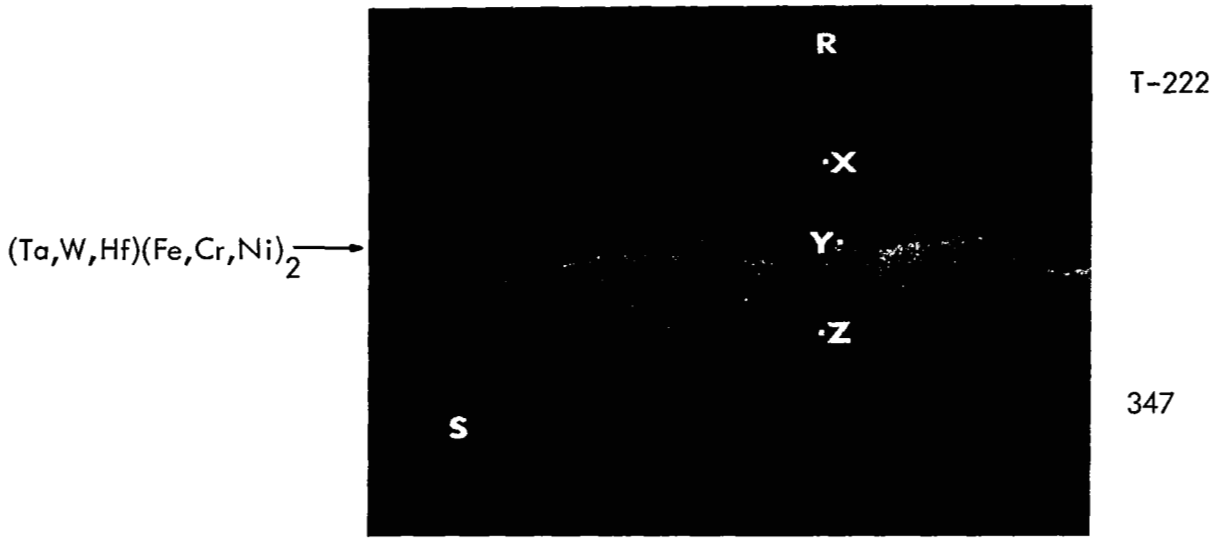

Mag. 540X 1" = 1.85 mils

FIGURE 16 - Microstructures of Interdiffusion Zones Present in T-222/347 Composite Annealed for 2700 Hours at 1600°F

The slow rate of interdiffusion zone growth between T-222 and 347 may be due to the formation of a thin layer of HfC since an indication of hafnium enrichment was observed at the T-222-compound interface. A similar enrichment was also observed for the titanium concentration at the 321 stainless-compound interface in the Ta/321 bimetal couple (see Figure 13b). Titanium, similar to hafnium, is also a strong carbide former. However, more work would have to be done to establish if such a barrier did exist and what factors affect its formation and stability.

Cb/347, Cb/321, and Cb-1Zr/347

Concentration profiles across the interdiffusion zones between Cb/321, Cb/347 and Cb-1Zr/347 are shown in Figures 17, 18 and 19 respectively. Although the addition of zirconium to columbium retarded the rate of interdiffusion at 1400°F, all three combinations displayed similar rates of interdiffusion zone formation at 1600°F. The traverse and spot analyses indicated that the dark layer adjacent to the Cb or Cb-1Zr in each specimen (see Figures 17, 18 and 19) may be the intermetallic compound of the type 89 a/o Cb-11a/o Fe as discussed earlier. This zone had a hardness of 2000 KHN.

The lighter layer in each specimen was a compound having a composition of about 46.5Cb-40.5Fe-7.5Cr-5.0Ni. This composition (i.e., 46.5Cb+53.0Fe,Ni,Cr) corresponds to the $CbFe_2$ type phase. The width of the interdiffusion zone is controlled primarily by the growth of this compound. Its hardness was about 800 KHN.

One additional very thin zone was also observed between the $Cb(Fe,Cr,Ni)_2$ zone and the stainless steel in the Cb/321 specimen. This zone, marked X, was too thin to obtain a spot analysis or to determine its hardness. However, the composite traverse indicated that it was rich in Cr and Ti and depleted in Fe and Ni. The zone may be a Cr-Ti carbide layer. It should be noted, however, that no such zone was observed in the Cb-1Zr/347 or Cb/347 specimens.

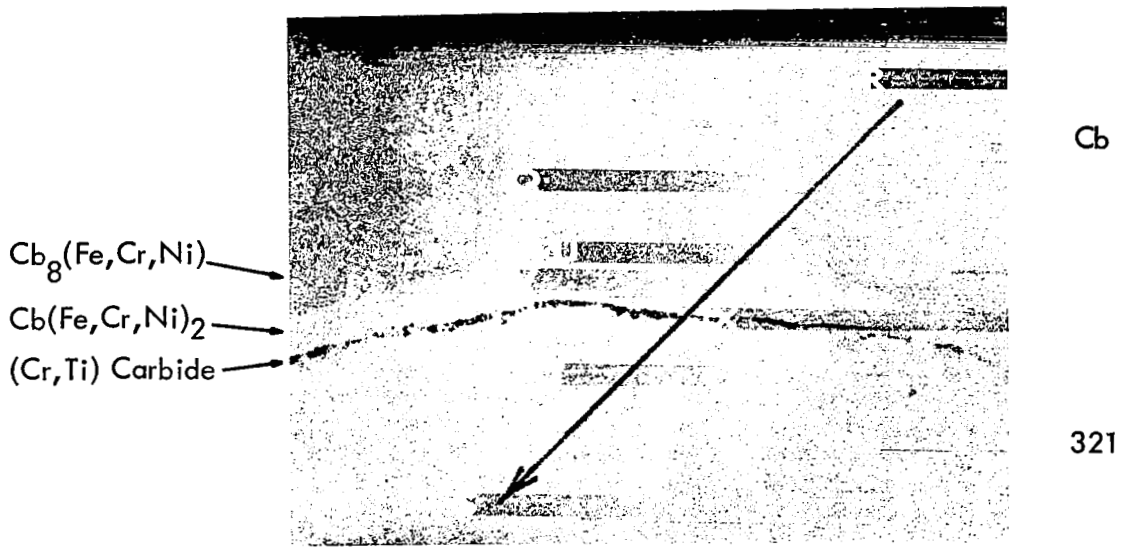

Mag. 540X 1" = 1.85 mils

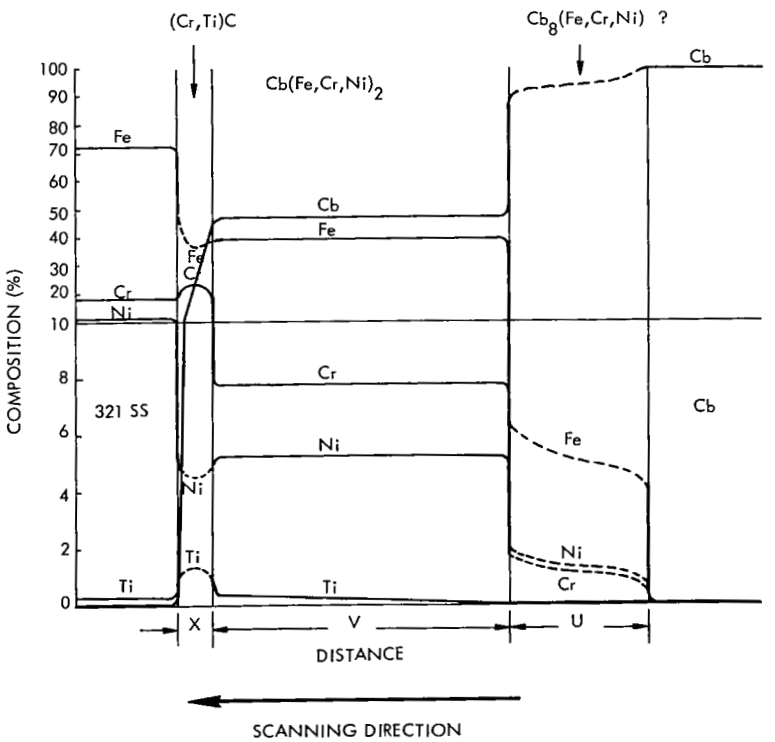

FIGURE 17 - Microstructure and Concentration Profiles for Cb/321 Bimetal Specimen Annealed for 1600 Hours at 1500°F

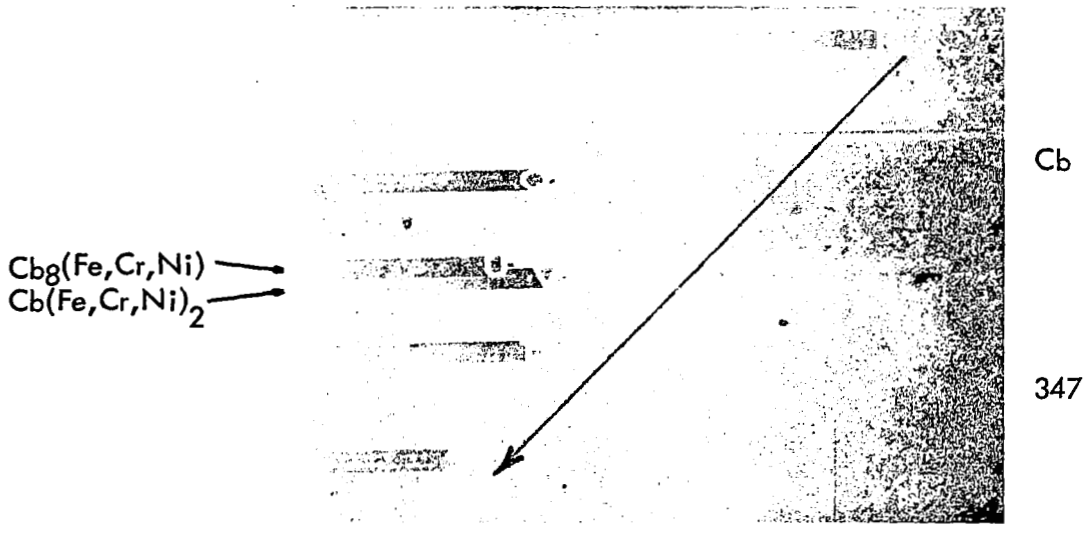

Mag. 540X 1" = 1.85 mils

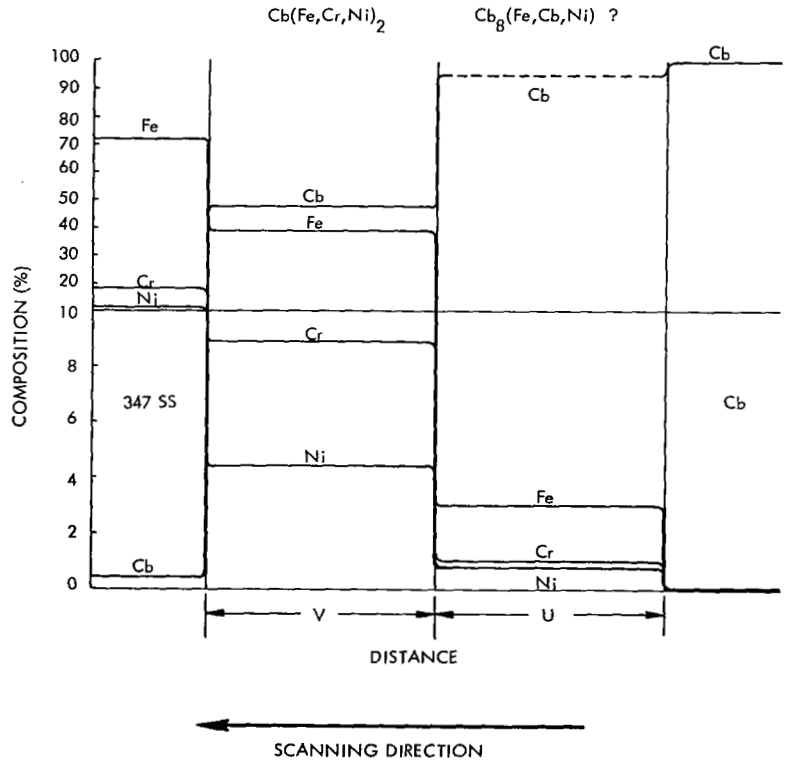

FIGURE 18 - Microstructure and Concentration Profile for Cb/347 Bimetal Specimen Annealed for 1000 Hours at 1500°F

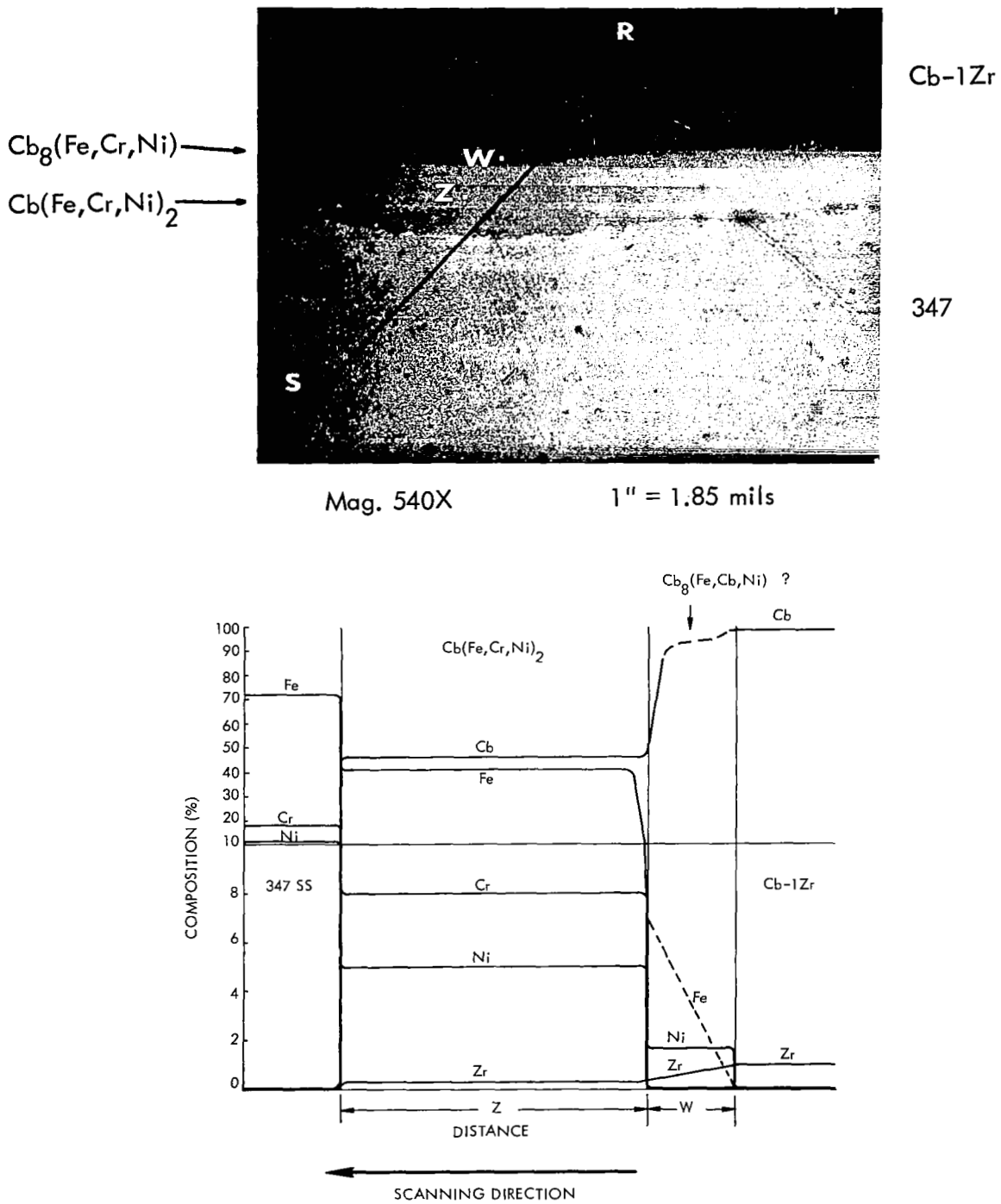

FIGURE 19 - Microstructure and Concentration Profile for Cb-1Zr/347 Bimetal Specimen Annealed for 1600 Hours at 1600°F

The Cb_3Fe_2 and CbFe type intermetallic compounds were not observed in any of the specimens. Either they were too thin to observe or they did not exist because of the presence of the other elements. Otherwise the diffusion in the Cb and Cb-1Zr/321 and 347 stainless steel composites could be described in terms of the Cb-Fe phase diagram, with Cr and Ni atoms substituting for Fe atoms.

Cb-1Zr/Inconel 600

The highest rate of interdiffusion occurred between the refractory metals and the nickel base alloys Inconel 600 and Hastelloy N. The concentration profile for Cb-1Zr/Inconel 600 annealed for 1600 hours at 1500°F is shown in Figure 20. The microstructure of the interdiffusion zone as it appeared under normal and polarized lighting is shown in Figure 21. Three distinct layers were observed to exist within the interdiffusion zone. The center zone is identified as a compound of the $CbNi_3$ type with a composition, averaged from the element traverse and spot analysis data, of 34.4Cb-63.7Ni-0.9Cr-0.3Zr. The hardness of this zone was 1250 KHN. The zones formed adjacent to the Cb-1Zr and Inconel 600 are more complex and are multiphased. For example, in the zone next to the Inconel 600, two separate phases were observed and spot analysis data (see Appendix 3) indicated the composition of one phase to be 59.8Cr-27.2Ni-10.3Cb-3.3Fe with traces of Ti and Zr. The other phase had a composition of 62.3Ni-20.1Cb-10.7Cr-7.1Fe-0.3Zr and 0.14Ti. The phase diagram on the columbium rich side of the Cb-Ni binary has not been defined. However, the average composition of this zone is 40Cb-50Ni-5Cr-5Fe which would correspond to a $CbNi_2$ compound, although as of yet a compound of this type has not been reported in the Cb-Ni binary. As noted earlier, all compounds are identified from microprobe data and are probably accurate representations in homogeneous zones of sufficient width to obtain reproducible microprobe traces. However, in multiphase areas, compositional information alone is not sufficient to identify the phase relationships and supplementary x-ray diffraction studies would be required for more positive conclusions. The perturbation of the concentration profiles in the zones next to the Cb-1Zr and Inconel 600 were again confirmed by scanning micrographs. It does appear that nickel has a much higher rate of diffusion in the refractory metal alloys than does iron.

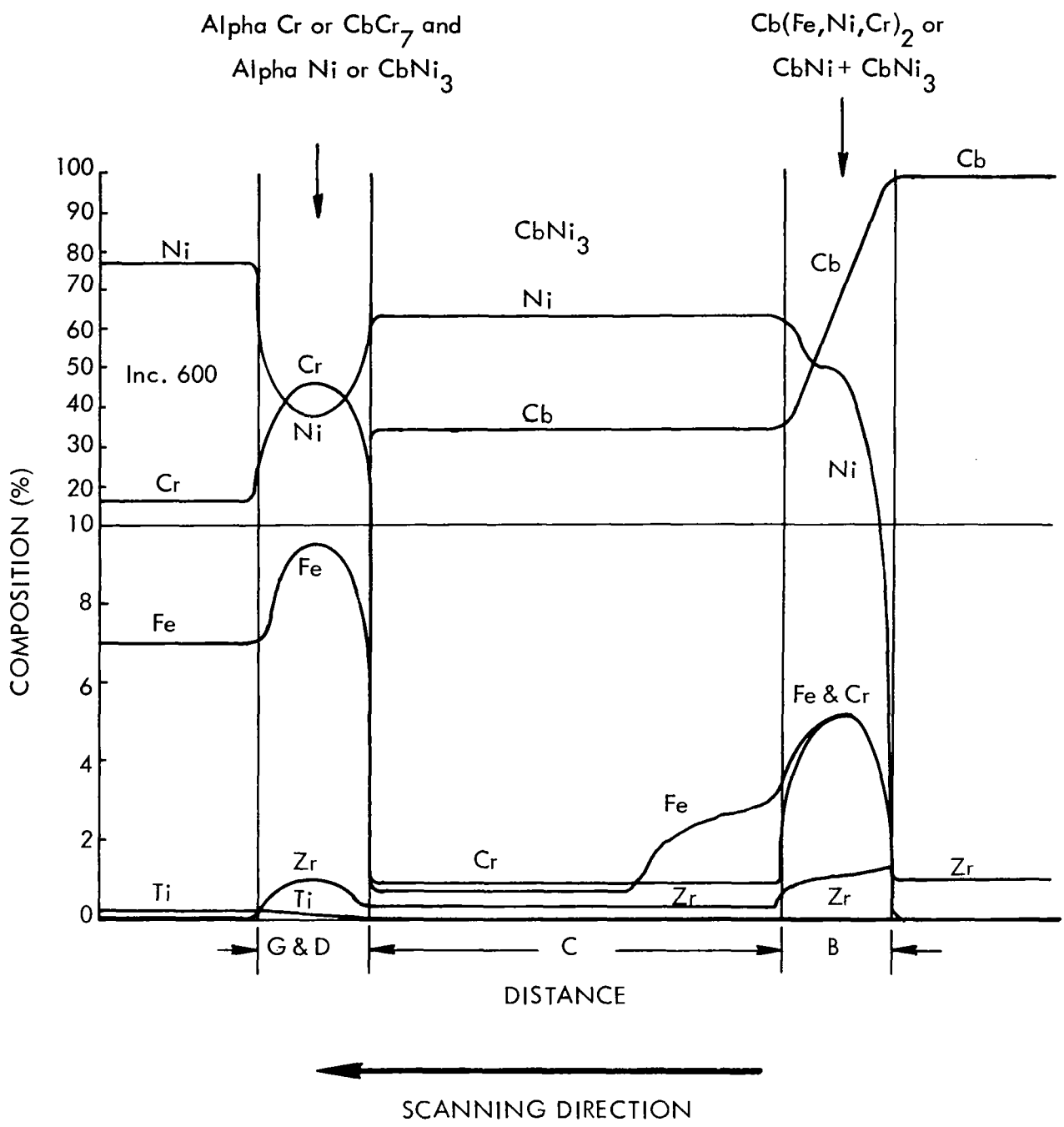

FIGURE 20 - Concentration Profile for Cb-1Zr/Inconel Bimetal Specimen Annealed for 1600 Hours at 1500°F

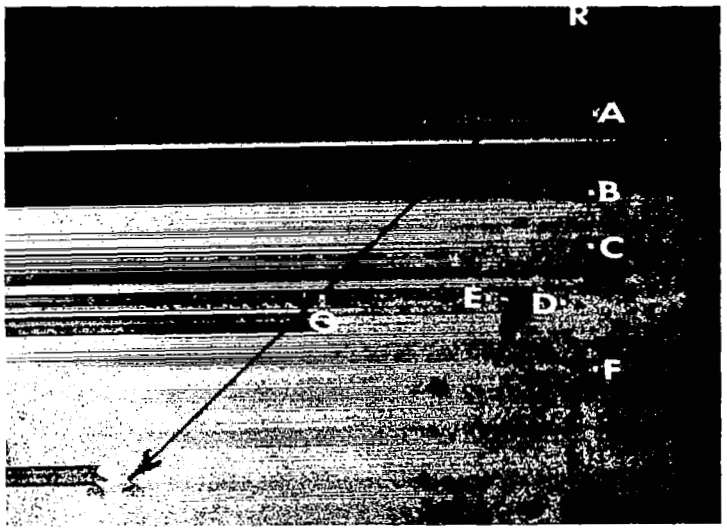

Cb-1Zr

Inc. 600

(a) Normal Light

$CbNi + CbNi_3$ or $Cb(Fe,Ni,Cr)_2$

$CbNi_3$

aNi or $CbNi_3$

Cb-1Zr

Inc. 600

(b) Polarized Light

FIGURE 21 - Microstructure of Interdiffusion Zones Present in Cb-1Zr/ Inconel 600 Composite Specimen Annealed for 1600 Hours at 1500°F (Mag. 540X 1" = 1.85 mils)

D. BOND INTEGRITY

Strip samples of each of the nine selected combinations were thermally cycled between 600°F and 1350°F to determine the endurance of the interface bond. Specimens were cycled in the as-bonded conditioned and after exposing for 1600 hours at 1500°F. Thermal cycling was conducted on 1 inch wide x 8 inch long x 0.09 inch thick bimetal strips in the apparatus shown schematically in Figure 22 and pictured in Figure 23. The thermal cycle, which was repeated 20 times, consisted of heating to 1350°F±25°F within 5 minutes, holding for 10 minutes and cooling to 600°F within 30 seconds. Traces from typical time-temperature cycles are shown in Figure 24.

Three specimens were positioned symmetrically in the induction coil and held securely in a molybdenum restraining fixture to prevent bending during heating and cooling. The specimens were heated by radiation from a stainless steel susceptor coupled to a RF induction coil using 450 KHz at a power level of 10 KW. Heating was accomplished at 10^{-5} torr. Cooling was accomplished by a stream of helium gas directed at the refractory side. The helium gas contained less than 10 ppm total active impurities. Cooling to 600°F required approximately 35 seconds. Details of the specimen and restraining fixture are illustrated in Figure 25.

Temperature at the austenitic/refractory metal interface was monitored using 0.005 inch diameter Pt/Pt-13%Rh thermocouples, which were spot welded to the center of each specimen. The symmetry of heating was very good with less than 10°F difference from specimen to specimen. The temperature distribution from top to bottom of the 8 inch long specime was maintained within ± 15°F.

Duplicate specimens of each of the nine selected composites in the as-bonded condition were thermally cycled. Prior to test, each strip was ultrasonically and dye penetrant inspected to ensure that they were free of any defects. After thermal cycling, the specimens again were ultrasonically and dye penetrant inspected and the results are listed in Table 10. No unbonded areas were detected in the thermally cycled strips nor were any

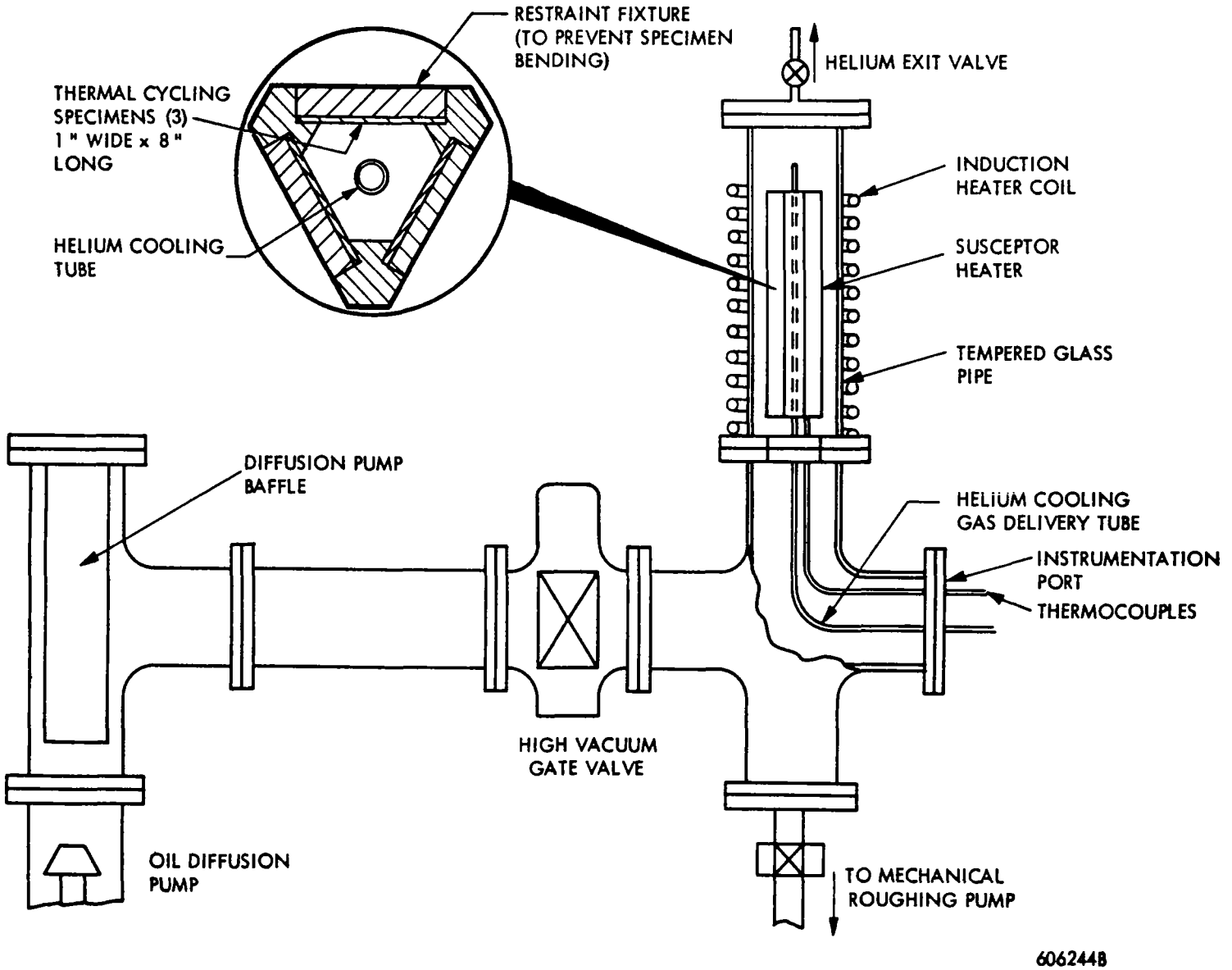

FIGURE 22 - Schematic of Thermal Cycling Apparatus

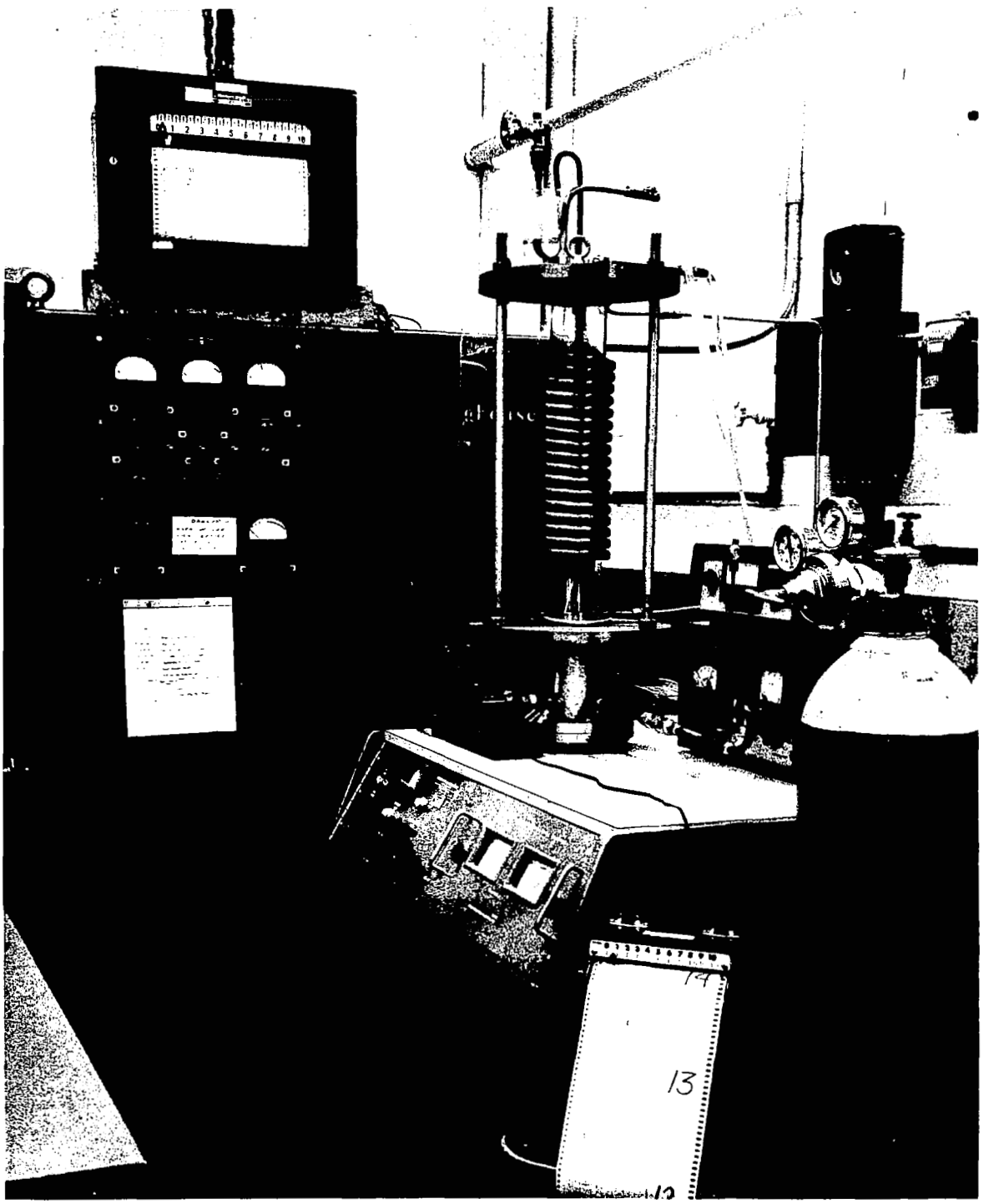

FIGURE 23 - Thermal Cycling Test Rig

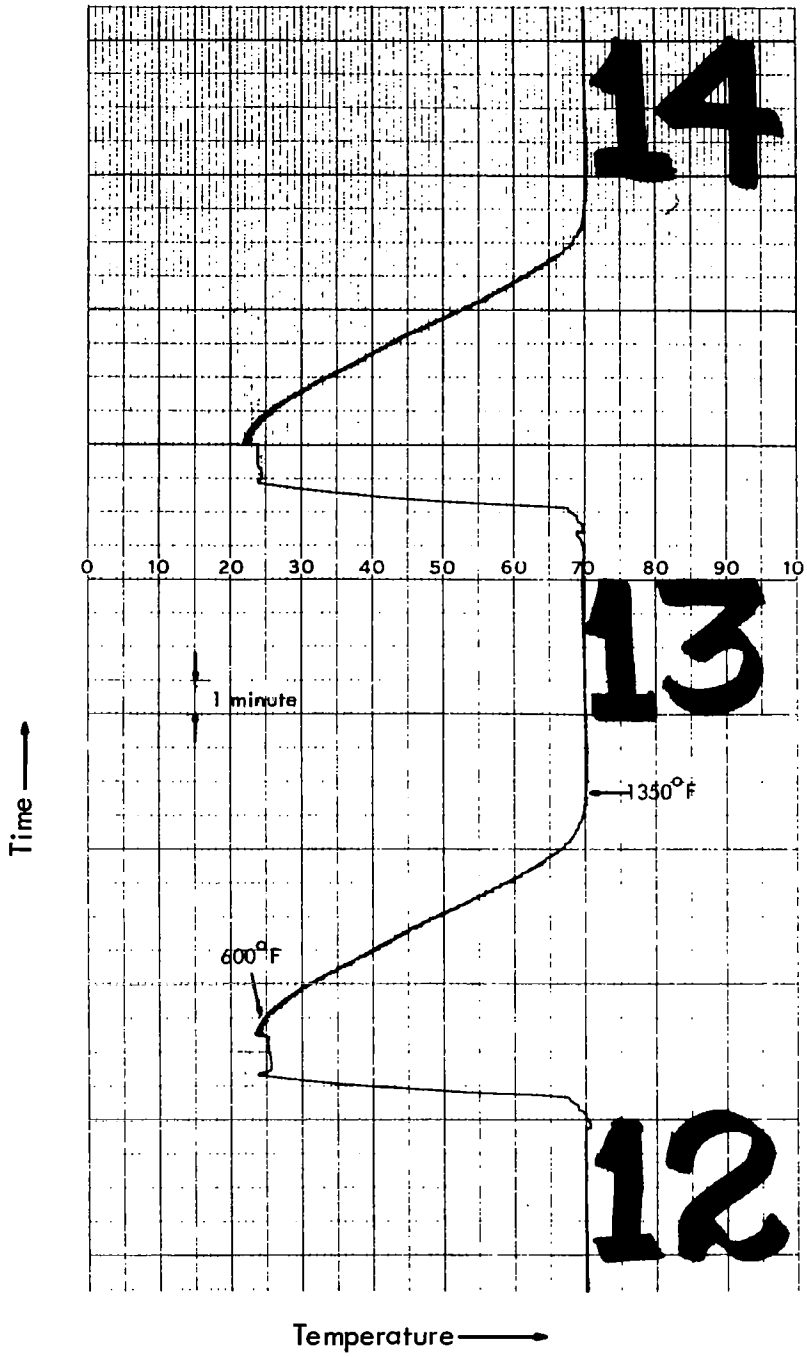

FIGURE 24 - Typical Time-Temperature Printout for Thermally Cycled Specimens

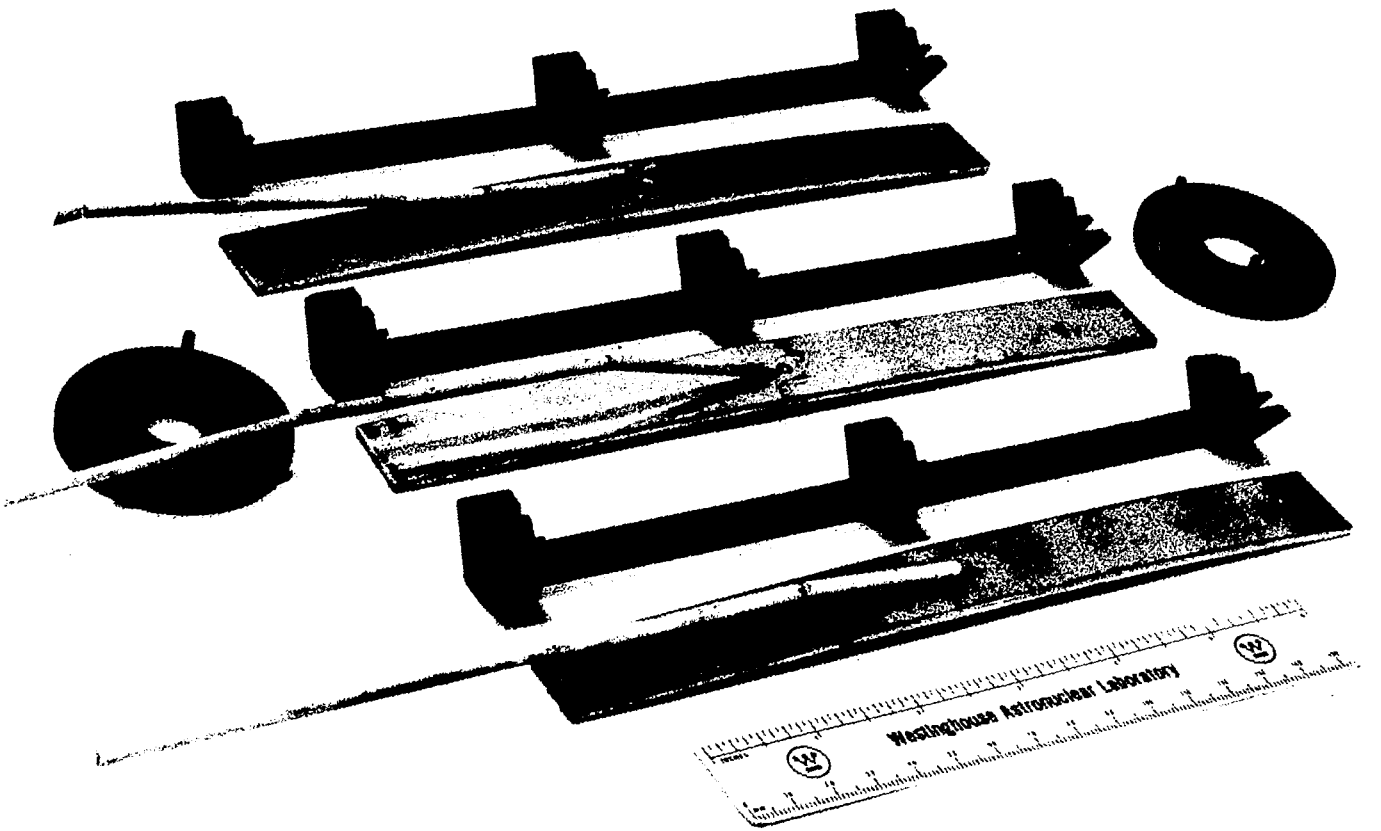

FIGURE 25 - Thermal Cycle Specimens and Restraint Fixture Prior to Assembly

TABLE 10 - Summary of Visual and Dye Penetrant Inspection Results of Thermally Cycled Refractory/Austenitic Bimetal Composite Specimens

Composition	Dye Penetrant Indications
Cb/321	1/4" Defect (1 end)
Cb/321	None
Cb/Inc. 600	None
Cb/Inc. 600	None
Cb-1Zr/347	1/8" Defect (2" from end)
Cb-1Zr/347	1/8" Defects (2" from end - both sides)
Cb/347	1/2" Defect (1 end)
Cb/347	1/8" Defect (1 end)
FS-85/321	None
FS-85/321	1/8" Defect (1-1/2" from end)
Ta/Inc. 600	None
Ta/Inc. 600	None
Ta/347	1/4" Defect (both ends)
Ta/347	None
Ta/321	None
Ta/321	1/8" Defect (1 end)
Cb-1Zr/Inc. 600	None
Cb-1Zr/Inc. 600	1/8" Defect (1 end)

defects observed visually unaided. Minor dye penetrant indications were observed on the edges of some of the specimens. It was concluded that all of the combinations withstood the thermal cycling test without degradation of the integrity of the bond interface.

After being released from the restraining fixtures, the specimens bowed with the refractory component the convex side of the sample. The amount of bow was measured and the data are recorded in Table 11.

The amount of bow appeared to be dependent upon the strength of the refractory metal component. The composites exhibiting the greatest amount of bow had the high strength FS-85 as the refractory alloy component. During heat-up, the greater expansion coefficients of the austenitic materials (i.e., about 10×10^{-6} -in/in$^{\circ}$F versus about 4×10^{-6} -in/in$^{\circ}$F for the refractory materials) tended to bow the specimens with the austenitic material to the outside. The austenitic and refractory components plastically deformed in compression and tension respectively during the time the specimens were at temperature, with the respective amounts of deformation being proportional to the temperature, relative strengths at temperature (corrected for area), and the amount of imposed restraint. The amount of plastic deformation in each member occurring during holding at 1350°F would be proportional to the strength of the refractory metal component. During cooldown the greater rate of contraction of the austenitic material reversed the stress tending to bow the specimens in the direction observed.

Each bimetal combination was roll straightened and re-inspected. No additional indications were detected after roll straightening, by either dye penetrant or ultrasonic inspection.

Thirteen 1 inch x 8 inch strips were exposed for 1600 hours at 1500°F under ultra-high vacuum conditions and then thermally cycled. The samples were stacked and wired to prevent bending during the isothermal exposure. After thermal exposure, however, the specimens bowed when unwrapped with the refractory metal again the convex side of the

TABLE 11 - Comparison of Amount of Bow[(b)] of As-Bonded and As-Thermally Cycled Bimetal Composites

Composition	Bow (in inches)	
	Thermally Exposed[(a)]	As-Thermally Cycled
Cb/347	0.23	0.09
Cb/347		0.10
Cb/321		0.13
Cb/321		0.12
Cb/Inc. 600		0.12
Cb/Inc. 600		0.13
Cb-1Zr/Inc. 600		0.25
Cb-1Zr/Inc. 600		0.23
Cb-1Zr/347	0.42	0.25
Cb-1Zr/347		0.25
Ta/347	0.55	0.33
Ta/347		0.34
Ta/Inc. 600		0.34
Ta/Inc. 600		0.34
Ta/321		0.37
Ta/321		0.38
FS-85/321	0.67	0.57
FS-85/321		0.57

(a) 1600 Hours at 1500°F

(b) Dimension A defines the bow

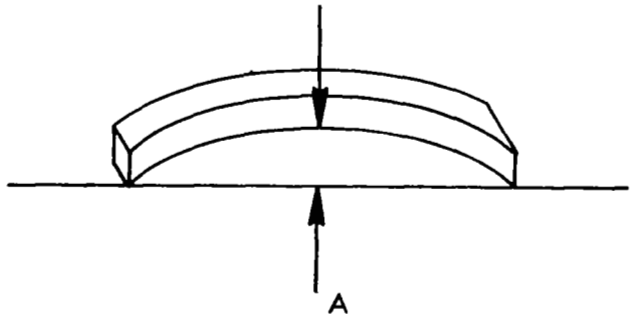

bow. The amount of bow appeared to be somewhat greater than exhibited by the thermally cycled specimens. This probably reflects the additional 150°F higher temperature from which the specimens cooled (1500°F for thermal exposure versus 1350°F for thermal cycling).

Each specimen was dye penetrant and ultrasonically inspected and the results are summarized in Table 12. The location and size of the unbonded areas is illustrated in Figure 26 for Cb/Inconel 600 and Ta/Inconel 600. None of the strips with the exception of the Ta/Inconel 600 and Cb/Inconel 600 suffered degradation of the bond as a result of the exposure. The interdiffusion zone between Ta/Inconel 600 and Cb/Inconel 600 after 1600 hours at 1500°F is approximately 0.0012 inch. Thus this thick brittle intermetallic layer would be susceptible to fracture during cooling from temperature or at a temperature where the residual stress exceeds the fracture stress of this brittle layer. The bowed strips were flattened by roll straightening with a 0.003-0.005 inch reduction in thickness of the composite. The same defect indications were observed both prior to and after flattening.

The isothermally exposed strips were then thermally cycled in the same manner as the as-bonded specimens. Again upon release from the restraint fixture, the specimens were bowed and the degree of bow for the sound composites was essentially the same as exhibited by the as-bonded specimens. This behavior is indicative of the high integrity of the interdiffusion zone which was able to transmit the residual stress.

Ultrasonic and dye penetrant inspection results on the thermally cycled thermally exposed strips are summarized in Table 13. The bimetal combinations which had interdiffusion zone growth of less than 5×10^{-4} inch withstood the thermal cycling without degradation. When the interdiffusion zone exceeded 5×10^{-4} inch, there was evidence of degradation of the interface during the thermal cyclic testing (see Figure 27). The Cb/Inconel 600 strip which had a 1.2×10^{-3} inch interdiffusion zone had unbonded severely during the isothermal exposure. The subsequent thermal cycling did not further propagate the defects.

TABLE 12 - Final Inspection Results for Isothermally Exposed (1600 Hours at 1500°F) Refractory/Austenitic Bimetal Composite Specimens

Composition	Inspection Indications	
	Dye Penetrant	Ultrasonic(Pulse Echo)
1" x 8" Strips		
Ta/321	None	None
Ta/321	None	None
Ta/347	None	None
Ta/347	None	None
Cb/321	Light indications near ends.	1/16 inch square area
Cb/321	None	1/16 inch square area
Cb/347	None	None
Cb/347	None	None
Cb-1Zr/347	None	1/4 inch square area
Cb-1Zr/347	None	None
FS-85/321	None	None
FS-85/321	None	None
Ta/Inconel 600	Heavy indications around most of specimen.	See Figure 26
Ta/Inconel 600	Heavy indications around most of specimen.	See Figure 26
Cb/Inconel 600	None	None
Cb/Inconel 600	Heavy indications on both ends and light indications on remainder of specimen.	See Figure 26

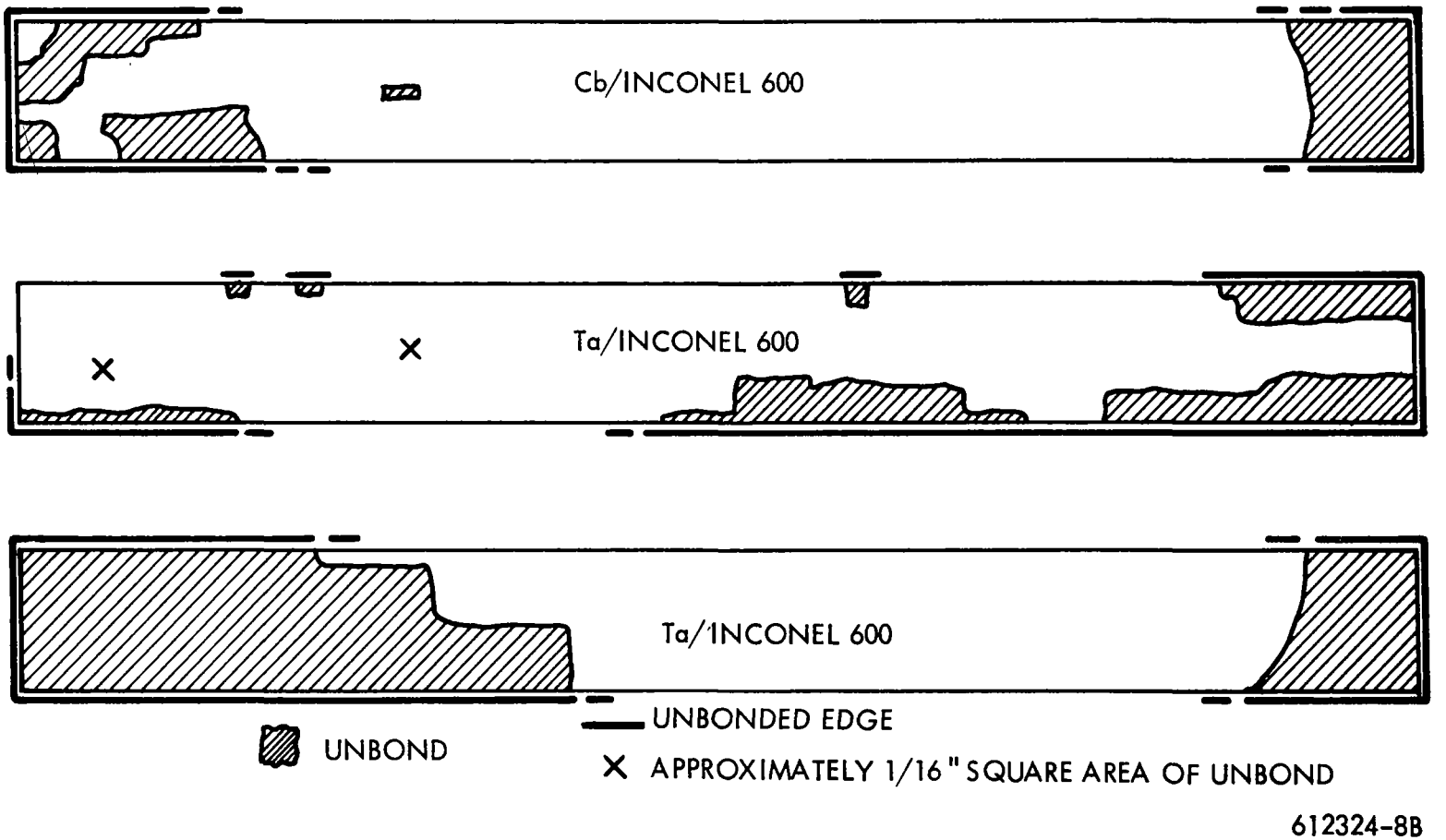

FIGURE 26 - Final Inspection Results of Thermally Exposed (1600 Hrs/1500°F) Bimetal Specimens

TABLE 13 - Summary of Dye Penetrant and Ultrasonic Inspection Results of Thermally Exposed[a] and Thermally Cycled Refractory/Austenitic Bimetal Composite Strips

Composite Composition	Zone Thickness (inches x 10^3)	Inspection Indications	
		Dye Penetrant	Ultrasonic (Pulse Echo)
Ta/321	0.25	None	None
Ta/321		None	None
Ta/347	0.15	None	None
Ta/347		None	None
Cb/321	0.31-0.7	Light indications around much of specimen.	See Figure 27
Cb/321			See Figure 27
Cb/347	0.3	None	None
Cb/347		Minor indications around most of specimen.	None
Cb-1Zr/347	0.15	Light indications along one edge and one end.	None
Cb-1Zr/347	0.15	1/2" long light indication near one end.	None
FS-85/321	0.55	Minor scattered indications.	See Figure 27
FS-85/321		Specimen delaminated at one end.	See Figure 27
Cb/Inc. 600	1.2	Same as after thermal exposure	Same as after thermal exposure (See Figures 26 and 27

a) 1600 hours at 1500°F

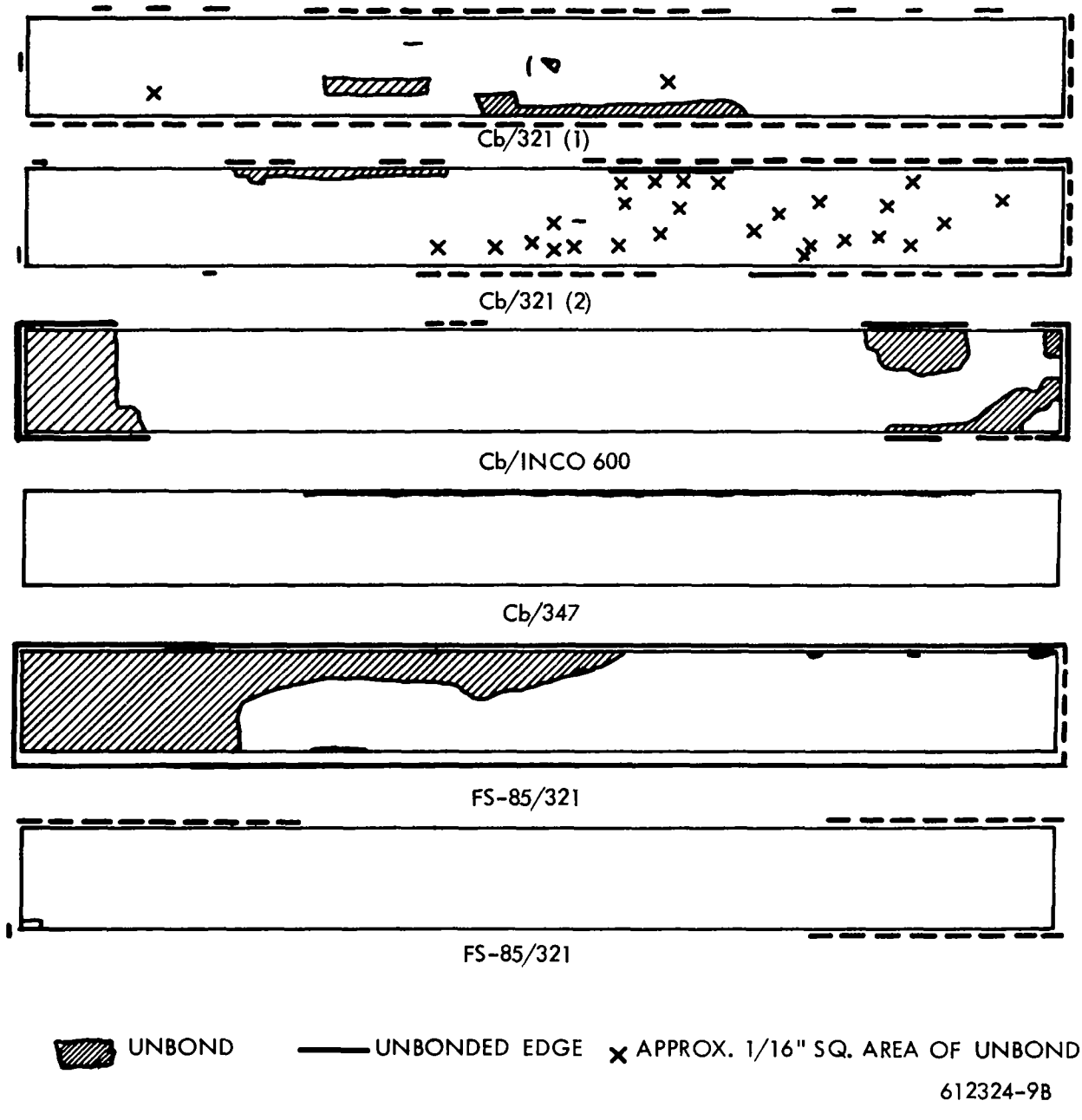

FIGURE 27 - Ultrasonic Inspection Results of Thermally Exposed (1600 Hours at 1500°F) and Thermally Cycled Bimetal Composite Strips

Several specimens were examined metallographically. Small cracks were observed to exist along the entire length of the interdiffusion zone approximately perpendicular to the zone interface in the Ta/321 specimen (Figure 28a). However, they did not extend into the base materials. While there were no ultrasonic indications of bond defects in either of the Ta/321 strips, such defects would not be expected to be detected because of their direction. The cracks most probably occurred during the thermal cycling since they were not observed in the diffusion annealed specimens. Figure 28b shows the type of interface bond degradation that occurred in the checked area of the Cb/321 specimen, number 2, as illustrated in Figure 27. Figure 28c illustrates that indeed no bond degradation had occurred in the center part of the Cb/Inconel 600 specimen (in agreement with ultrasonic inspection results). Thus, with the exception of the fine cracks in the Ta/321 composite, ultrasonic inspection for interface bond integrity is seen to correlate well with metallographic observations.

E. MECHANICAL PROPERTIES

1. Tensile Properties. Room temperature tensile properties were determined on sheet specimens with a 0.250 inch reduced section x 0.09 inch thick with a 1.00 inch long gage length. Testing was done on the pin loaded specimens using a Wiedemann, Mark G, 60,000 lb. capacity universal testing machine. Duplicate specimens were tested at a constant cross-head motion of 0.05 in/min. Prior to test, the specimens were lightly etched to delineate the refractory/austenitic interface and the behavior of each specimen during testing was recorded by motion picture at 32 frames/second. Bimetal specimens were tested in the following conditions:

a. as-bonded
b. as-bonded plus 1600 hours at 1500°F
c. as-bonded plus thermally cycled from 1350 to 600° for 20 cycles

The tensile data that were obtained were tabulated in Table 14. Unless otherwise noted, both components fractured simultaneously with less than 1/8 inch delamination of the interface at the fracture.

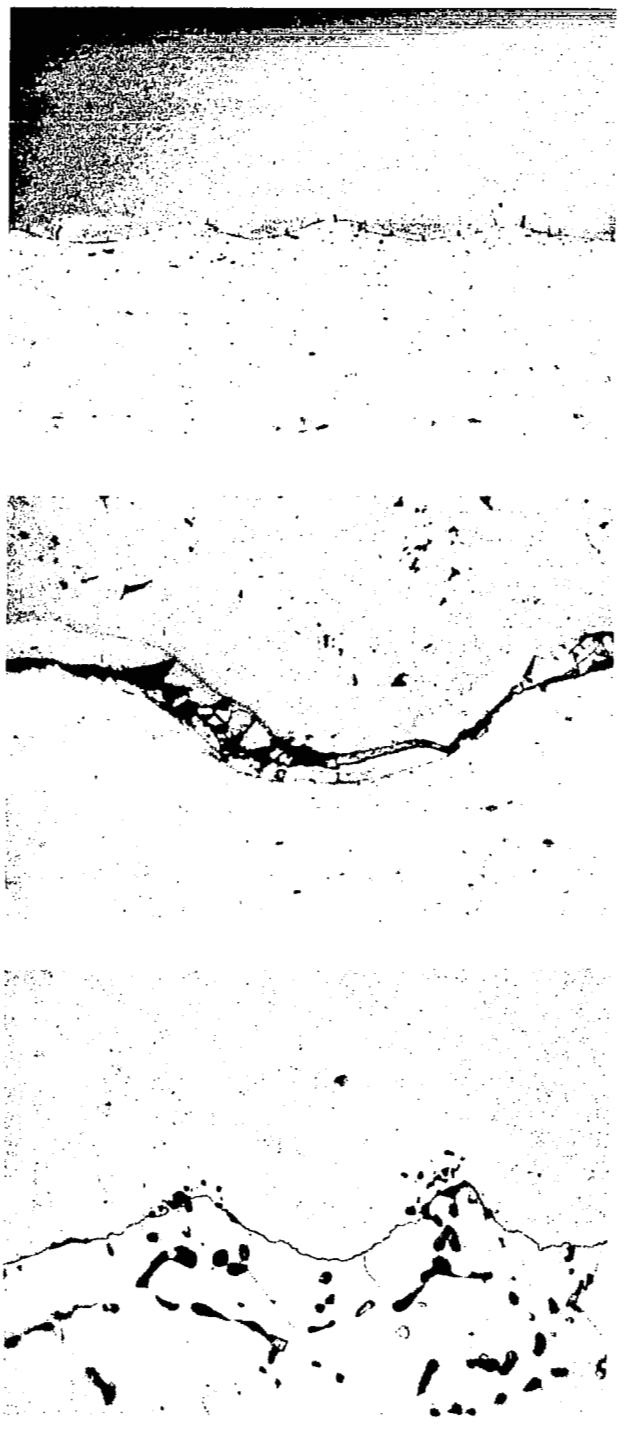

a) Ta/321

b) Cb/321 (Defective Interface Area)

c) Cb/Inc. 600 (Sound Interface Area)

FIGURE 28 - Micrographs of Interface Bonds in Selected Thermally Exposed (1600 Hrs/1500°F) and Thermally Cycled Bimetal Composite Strips (Mag. 400X 1" = 2.5 mils)

TABLE 14 - Room Temperature Tensile Properties[a] of Refractory/Austenitic Bimetal Composites

Composition	Condition[b]	0.2% Offset Yield Strength (psi)	Ultimate Tensile Strength (psi)	% Elongation			% Reduction in Area		
				Refractory	Austenitic	Total	Refractory	Austenitic	Total
Ta/321	A	92,000	96,600	--	--	20	62	57	57
		90,100	94,800	--	--	31	59	55	58
	B	43,700	77,300	59	62	--	83	63	--
		44,500	76,400	65	66	--	81	65	--
	C	64,800	89,600	43	42	--	65	66	--
Ta/347	A	86,900	94,400	--	--	27	67	57	59
		85,100	92,500	--	--	31	48	60	56
	B	33,200	77,100	34	34	--	50	53	--
		48,500	81,700	52	53	--	82	81	--
	C	68,900	91,100	33	31	--	100	60	--
T-222/321	A	87,200	99,500	--	--	38	57	47	55
		88,800	98,200	--	--	34	49	56	55
Ta/Inconel 600	A	90,300	94,000	--	--	21	64	69	68
		89,300	93,700	--	--	21	67	53	58
	B	18,500	52,200	12	50	(c,d)	82	51	--
		36,800	73,900	50	52	--	100	57	--
Cb/321	A	74,900	82,000	--	--	41	77	56	66
		74,100	80,600	--	--	43	56	59	61
	B	24,800	56,500	25	48	(d)	75	59	--
		27,500	62,000	47	75	(d)	77	66	--
	C	53,800	76,200	54	54	--	77	60	--
Cb/347	A	78,300	85,800	--	--	35	50	55	--
		80,200	88,000	--	--	32	67	65	--
	B	26,800	67,200	37	35	(e)	58	50	--
		29,700	70,200	64	60	(e)	86	53	--
	C	62,200	82,700	42	41	--	69	57	--

TABLE 14 (continued) - Room Temperature Tensile Properties[a] of Refractory/Austenitic Bimetal Composites

Composition	Condition[b]	0.2% Offset Yield Strength (psi)	Ultimate Tensile Strength (psi)	% Elongation			% Reduction in Area		
				Refractory	Austenitic	Total	Refractory	Austenitic	Total
Cb/Inconel 600	A	75,100	81,000	--	--	24	81	59	68
		73,200	80,900	--	--	30	81	56	69
	C	26,500	65,500	52	52	--	66	54	--
		24,100	62,100	42	57	--	75	58	--
Cb-1Zr/321	B	33,400	68,300	23	64	(d)	100	60	--
		31,100	62,800	16	64	(c,d)	53	60	--
Cb-1Zr/347	A	86,200	92,100	--	--	24	51	65	62
		85,700	92,100	--	--	29	42	52	51
	B	25,600	73,800	35	35	--	74	50	--
		35,800	77,000	49	49	--	87	51	--
	C	61,800	88,900	44	41	(f)	88	58	--
		63,400	86,200	21	24	(f)	59	45	--
Cb-1Zr/Inconel 600	A	82,800	90,900	--	--	22	61	55	59
		81,800	90,700	--	--	22	60	56	59
	B	28,900	69,800	48	48	--	78	54	--
FS-85/321	A	98,600	102,100	--	--	26	48	57	57
		97,500	101,400	--	--	28	40	56	52
	B	52,400	84,600	54	55	--	66	66	--
		49,900	83,100	54	56	--	72	63	--

(a) *Tested at a constant cross-head motion of 0.05 inch/minute.*

(b) A - As-explosively bonded condition
B - A plus 1600 hours at 1500°F
C - A plus 20 cycles between 1350°F to 600°F

(c) Specimen delaminated prior to testing.

(d) *Specimen delaminated during test, refractory metal component fractured first.*

(e) Same as (d) except austenitic component fractured first.

(f) Specimen delaminated at fracture.

The tensile properties of the as-explosively bonded composites are characterized by a yield strength of approximately 80,000 psi and an ultimate strength of about 90,000 to 95,000 psi. There was little difference in strength between the various combinations. Both components of the as-bonded specimens fractured simultaneously and there was no evidence of delamination. This typical behavior is illustrated in Figure 29 which shows a Cb/Inconel 600 bimetal specimen at the time of fracture and one film frame after fracture.

The tensile values obtained on the bimetal composites are significantly higher than the values reported for the starting materials used in the fabrication of the composite. (See Tables 3 and 5.)

As discussed earlier, there has been a strength increase in both components as a result of the explosive bonding. A measure of this strength was evaluated by machining away either component from a Cb/347 composite and testing them in tension. The tensile properties which are tabulated in Table 15 reflect the strength increase due to the explosive bonding process and explain the properties exhibited by the as-explosively bonded material.

The tensile strength values of thermally cycled specimens were only slightly lower than the as-bonded composites while the yield strength values were lowered by about 25%, thus reflecting the recovery occurring during the 5 hours accumulated at 1350°F during thermal cycle testing.

Tensile properties of as-explosively bonded specimens, exposed for 1600 hours at 1500°F, were also determined. After exposure the specimens were bowed as discussed previously and were roll straightened by giving the specimens a 0.003 to 0.005 inch reduction. Identical defect indications prior to and after roll straightening were observed by both dye penetrant and ultrasonic inspection. A summary of the inspection results on the thermally exposed bimetal tensile samples is in Table 16. As illustrated in Figure 30, the Cb-1Zr/321, Cb/Inconel 600, and Ta/Inconel 600 debonded severely as a result of the thermal exposure.

(a) At Fracture

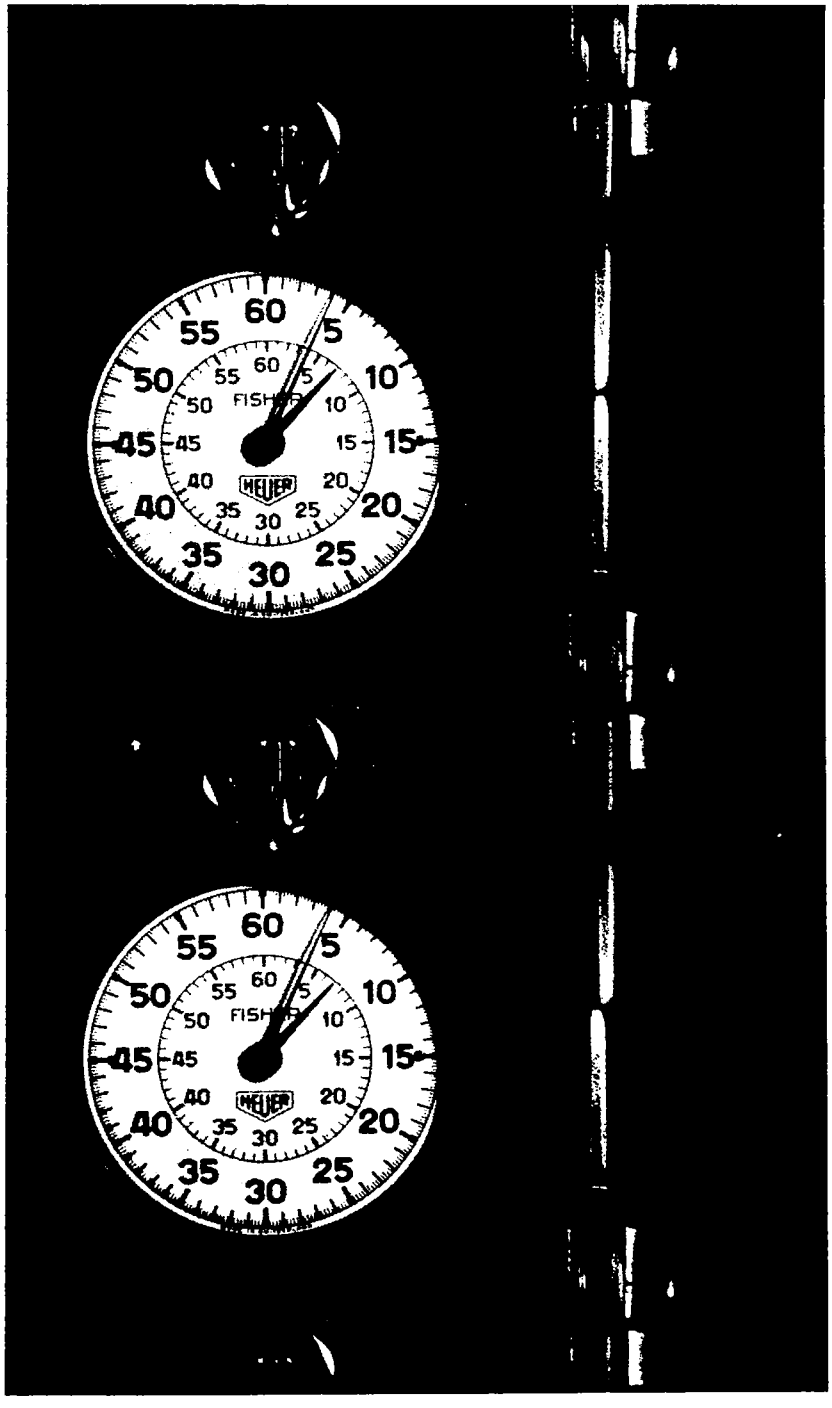

(b) 1 Frame After Fracture

FIGURE 29 - Failure of As-Bonded Cb/Inconel 600 Composite During Tensile Testing (Photographed at 32 Frames Per Second)

TABLE 15 - Effect of Explosive Bonding[(a)] on the Room Temperature Properties of Columbium and Type 347 Stainless Steel

Material	0.2% Offset Yield Strength (psi	Ultimate Tensile Strength (psi)	Elongation (%)	Hardness DPH
As-Explosively Bonded Cb	30,100 (+17,000)	33,200 (+8,300)	14 (-31)	100 (+27)
As-Explosively Bonded Type 347	86,800 (+44,900)	102,800 (+16,600)	42 (-4)	201 (+48)

(a) Values in parentheses represent change in property as result of explosive bonding process.

TABLE 16 - Summary of Dye Penetrant and Ultrasonic Inspection Results of Isothermally Exposed (1600 Hours at 1500°F) Refractory/ Austenitic Bimetal Composite Specimens

Composition	Inspection Indications	
	Dye Penetrant	Ultrasonic(Pulse Echo)
Tensile Specimens		
Ta/321	None	None
Ta/347	None	None
Ta/347	None	None
Cb/321	None	None
Cb/321	Light indications on whole specimen.	None
Cb/347	None	None
Cb/347	None	None
Cb-1Zr/321	None	See Figure 30
Cb-1Zr/321	Gauge length completely separated.	See Figure 30
Cb-1Zr/347	None	None
Cb-1Zr/347	None	None
FS-85/321	None	None
Ta/Inconel 600	Heavy indications on one end and light indications on remainder of specimen.	See Figure 30
Cb/Inconel 600	Heavy indications on one end and along gauge length.	See Figure 30

As expected, the tensile properties of the thermally exposed material were significantly lower and the elongation values higher than the as-bonded material. As indicated earlier by hardness data, the austenitic components have completely recovered the annealed strength properties while the refractory metal components have recovered to a lesser degree. However, in the case of the pure columbium it has probably been almost entirely recovered. Using the rule of mixtures, calculation of the tensile strength of a Cb/347 composite, using the annealed properties of the starting materials, gave a value of 65,600 psi. The average tensile strength measured on the thermally exposed Cb/347 composite was 68,600 psi, which is good agreement.

The behavior of each thermally exposed specimen during tensile testing was recorded photographically. Those specimens which exhibited significant bond defects prior to testing usually delaminated very early in testing and failure of the components did not occur simultaneously. The majority of the specimens which showed no evidence of unbonding by the inspection techniques used failed in a manner similar to that of the as-bonded composites. However, some of the composite which showed no evidence of bond degradation as a result of the thermal exposure delaminated during testing and failure of one component preceded the other. Shown in Figure 31 is the failure of a Cb/347 specimen which delaminated during testing. Fracture of the austenitic component occurred before that of the refractory metal.

Selected thermally exposed tensile specimens were metallographically examined. Photomicrographs, illustrating the fracture characteristics and bond integrity of Ta/321 and Cb/347 composite specimens, are illustrated in Figures 32 and 33. Failure of each component of each composite studied occurred primarily by shear, regardless of the types of fracture previously discussed. There was little or no tendency for the interface delamination at the fracture to propagate away from the point of fracture as shown by the photomicrographs of the interface bonds (Figures 32b and 33b) which were taken about 3/16 inch from the fracture surfaces. The photomicrographs also illustrate the occurrence of cracks perpendicular to the existing zones similar to those observed in the thermally exposed and thermally cycled Ta/321 strips (see Figure 28a). These cracks were observed in all of the specimens studied. Apparently

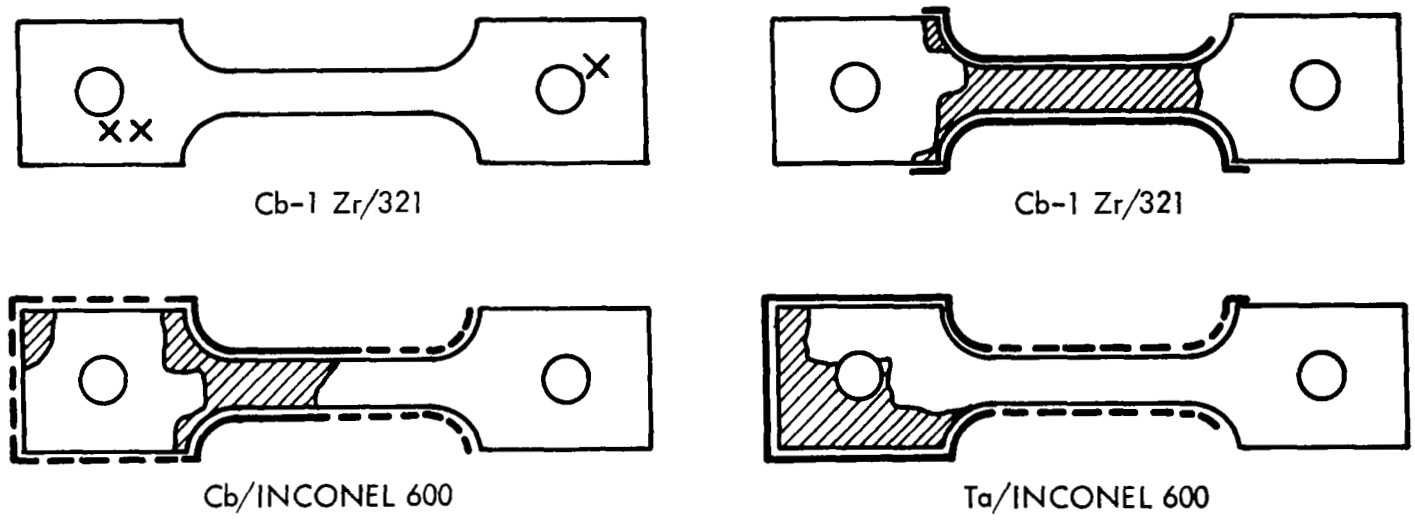

FIGURE 30 - Debonded Areas in Bimetal Tensile Specimens after 1600 Hours at 1500°F

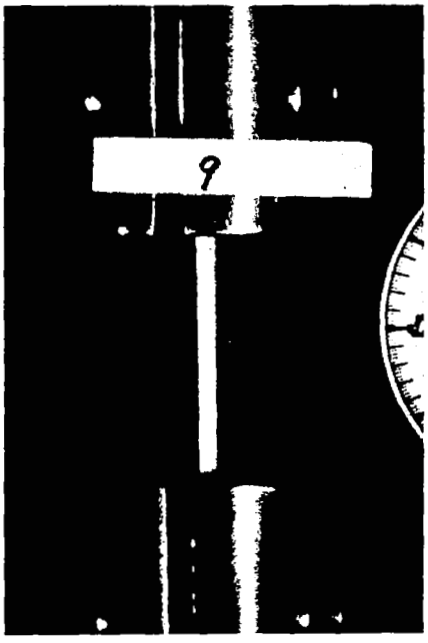

(a) Time 0 Strain 0%

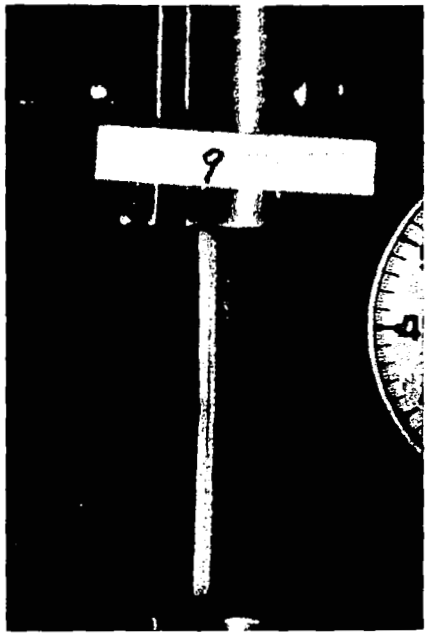

(b) Time 12 mins. 54.4 secs.
Strain ~65%

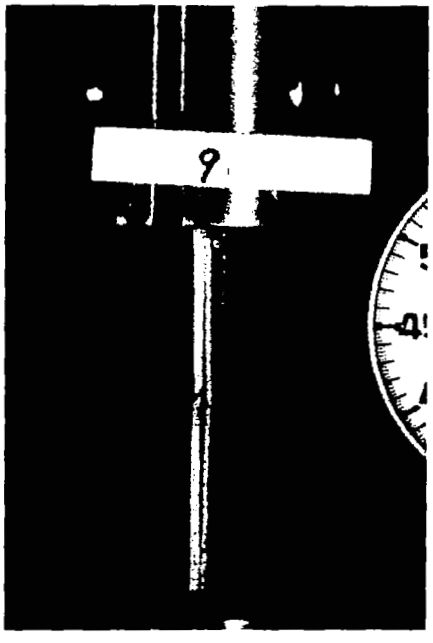

(c) Time 12 mins. 54.4 secs.
Strain~65%

FIGURE 31 - Room Temperature Tensile Failure of Thermally Exposed (1600 Hrs./ 1500°F) Cb/347 Composite (Photographed at 32 Frames Per Second)

Ta

a) Mag. 75X (1" = 13.3 mils)

321

Ta

b) Mag. 400X (1" = 2.5 mils)

321

FIGURE 32 - Photomicrographs of Fractured Thermally Exposed (1600 Hrs./1500°F) Ta/321 Composite Tensile Specimen

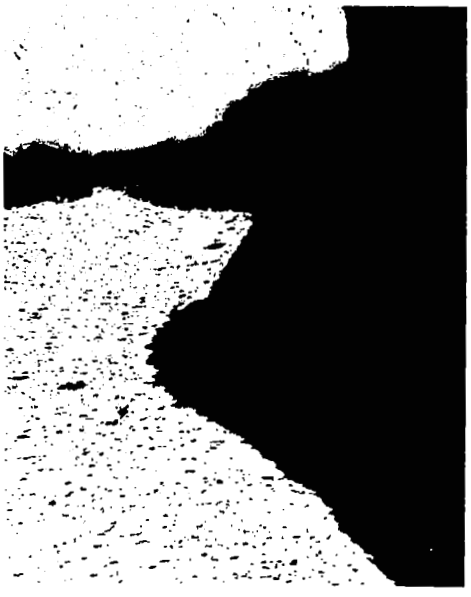

Cb

a) Mag. 75X (1" = 13.3 mils)

347

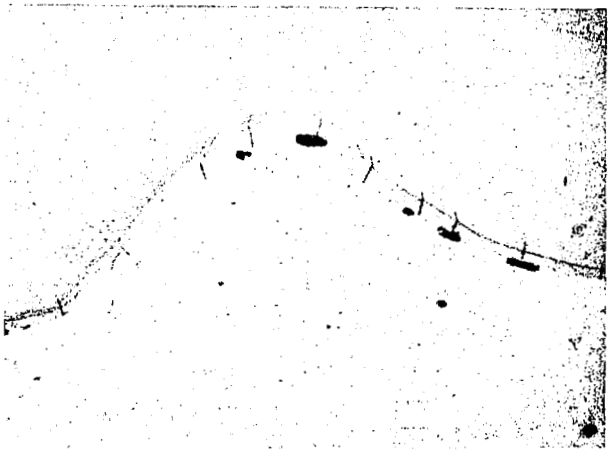

Cb

b) Mag. 400X (1" = 2.5 mils)

347

FIGURE 33 - Photomicrographs of Fractured Thermally Exposed (1600 Hrs./1500°F) Cb/347 Composite Tensile Specimen

they occurred during tensile testing as similar cracks were not observed in the diffusion annealed specimens. It should be noted that the extent of interdiffusion zone formation and the hardness levels were in excellent agreement with those measured for the diffusion annealed specimens.

2. Creep-Rupture Behavior Properties. Creep-rupture properties were determined on a number of the explosively bonded composites in the as-bonded condition and a limited amount of testing was done on bimetal combinations which had been previously thermally cycled between 600 and 1350°F. Also tested were samples of columbium and tantalum taken from the starting material used to produce the bimetal composites as well as specimens of as-explosively bonded Cb and 321 which had the other component removed by machining prior to testing.

Creep rupture testing was done in sputter ion pumped, internally loaded, ultra high vacuum units that have been described by Buckman and Hetherington.[8] The system consists of a 14 inch diameter bell jar, a feedthrough spool, and weight chamber which is pumped by a 500 liter/sec internally baked sputter ion pump. Roughing is accomplished by using molecular sieve cryogenic sorption pumps. Heating of the test specimen, 0.250 inch wide by 1 inch gage length, was accomplished by radiation from a resistance heated split tantalum corrugated element. Power was provided to the hot zone by a 7.5 kva low voltage, high current power supply that employs a magnetic amplifier driven saturable reactor in series with the primary winding of a step-down transformer. Temperature was controlled by means of a thermal watt converter. This device measures the true ac power delivered to the hot zone and provides a dc millivolt signal to a controller which maintains the power input to the heating element at a constant value. At 1350°F, the temperature uniformity over the gage length was within 10°F and the system pressure was below 5×10^{-9} torr.

The weight for stressing the test specimen was contained internally within the weight chamber and was applied by retracting a support platform, activated by means of a screw jack

connected to the bellows assembly. Distortion of the specimens during heating to test temperature necessitated application of the load prior to the start of heat-up. Thus it was not possible to determine the "no load" gage length at the test temperature. This procedure prevented determining the initial portion of the creep curve. Creep strain was determined optically by direct measurement of the separation of fiducial scratches applied to the extremes of the uniform gage section of the test specimen. Readings were made with a vertical scale and a 100 part drum equipped with a 10 part vernier. The instrument can be read to 0.00005 inch. Strain data were recorded manually.

The creep-rupture results obtained are tabulated in Table 17. Creep-rupture data on austenitic-refractory metal composites is essentially non-existent; thus there is no similar data reported in the literature to use for comparison.

Cb-321 - Cb-347

As described previously, the full load was applied to the test specimen at room temperature and then the specimen was heated to 1350°F at a rate sufficient to maintain the pressure in the test chamber at less than 5×10^{-7} torr. This was normally accomplished in less than five hours. Pressure during testing was below 5×10^{-8} torr within two hours after the testing temperature was reached and below 5×10^{-9} torr within eight hours after the test temperature was reached. The necessity to apply the full load prior to heat-up did not permit determination of the primary portion of the creep curve. However, the creep curves obtained can be described as consisting of an initially linear creep rate followed by a transition into tertiary creep with subsequent rupture. Creep-rupture data for the Cb/347 and Cb/321 bimetal composites tested in the as-received condition are plotted in Figure 34. These data indicate that the Cb/321 combination has superior creep properties to the Cb/347 composite.

TABLE 17 - Creep-Rupture Properties for Austenitic/Refractory Bimetal Composites

Combination	Condition[a]	Stress (psi)	Time to Rupture (hours)	Time to 1% Strain (hours)	Rupture Ductility		Secondary Creep Rate (%/hr.)	Transition to Third Stage (hours)	Transition Strain (%)
					(% Elong)	(% R.A.)			
Cb/347	A	8,000	1,180	195	23.9	18.8	0.005	350	2.0
	A	10,000	197	66	15.6	21.8	0.0087	30	0.3
	A	12,000	132	52	11.1	7.5	0.017	27	0.8
	A	14,100	95	22	10.8	8.2	0.032	10	0.5
	B	12,800	46	25	7.5	(b)	0.021	12	0.4
Cb/321	A	8,000	994	496	15.5	18.4	0.0013	325	0.5
	A	10,000	657[c]	312	(c)	(c)	0.0028	280	0.8
	A	10,000	420	200	11.2	9.3	0.0033	130	0.5
	B	10,000	566	192	11.9	21.4	0.0033	105	0.4
	A	12,000	338	158	9.6	5.7	0.0041	51	0.2
Cb-1Zr/347	A	11,000	1,007[d]	(d)	0.18	0.4	0.0	---	---
Ta/347	A	20,000	1,269	182	12.8	18.1	0.004	700	3.0
	A	18,000	905	105	14.5	32.4	0.007	420	3.1
	B	18,000	805	94	13.8	28.6	0.009	550	5.2
Ta/321	A	14,000	1,110[d]	870	1.15[d]	0.88[d]	0.001	---	---
	A	20,000	1,180	915	8.2	13.3	0.001	900	0.95
	B	20,160	585	132	9.6	11.9	0.0057	200	1.4
Ta	C	14,000	1,015[d]	---	0.22	---	0.00017	---	---
Cb	C	14,000	(e)	---	56.9	50	---	---	---
Cb	A[f]	14,000	(e)	---	13.2	32.1	---	---	---
321	A[f]	14,000	126	32	8.1	10.0	0.025	23	0.8

NOTES FOR TABLE 17

a) A - tested in as-explosively bonded condition

B - tested after thermally cycling as-bonded material 20 times between 600°F and 1350°F

C - starting material used for explosive bonding

b) Specimen fractured through defect in gage length

c) Specimen overheated after 657 hours of testing due to faulty controller

d) Test Terminated - Specimen did not rupture

e) Specimen broke on loading

f) Other component removed by machining

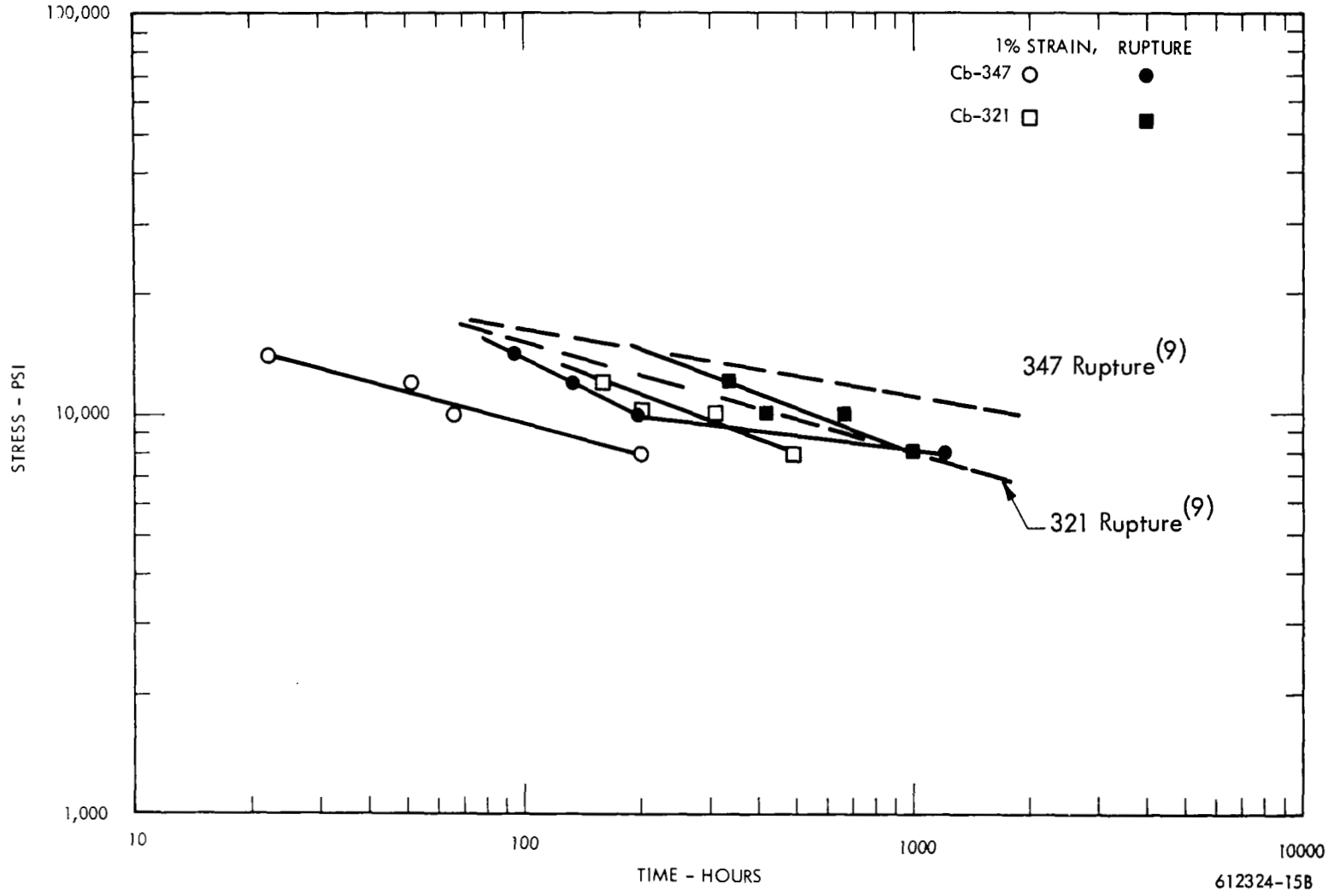

FIGURE 34 - 1350°F Creep Rupture Properties of Cb-347 and Cb/321 Tested in the As-Explosively Bonded Condition

Generally, the average rupture strength of 347 stainless steel is reported to be higher than that of 321 stainless steel, the difference being greater at the longer rupture times.[9] For example, the average 100 and 1000 rupture strength of annealed type 347 at 1350°F is 16,000 psi and 11,000 psi respectively while that for type 321 is 15,000 and 8,000 psi. However, the range of 1350°F rupture strength values reported for type 347 for 1000 hour rupture life is 6,500 psi to 16,080 psi. These represent values obtained on both sheet material and bar stock. Thus the higher creep rupture strength of the Cb/321 combination is not considered an anomalous result from the limited amount of data that was obtained. Also, the variations between the bimetal composites, because of possible variabilities in the explosive bonding process, could result in metallurgical differences which could not be evaluated. It is well-known that creep-rupture behavior is significantly affected by metallurgical condition[10]. Material which had been previously thermally cycled between 600°F and 1350°F when creep rupture tested did not appear to behave any differently from as-received material.

Ta-321, and Ta-347, the composites which had tantalum as the refractory metal component were significantly stronger than the composites which had columbium as the refractory metal component. This was not surprising since the tantalum starting material was in the cold worked condition while the columbium starting material was completely recrystallized prior to explosive bonding. At 1350°F, the stress for 1 hour rupture life of the annealed columbium is approximately 12,000 to 13,000 psi while that for the cold worked tantalum is estimated to be approximately 47,000 psi[11]. Thus a direct comparison of the rupture properties between the Cb and Ta composites is not meaningful.

As with the columbium, the Ta/321 combination had better creep-rupture properties than the Ta/347 combination, the superiority being evident in the lower secondary creep rate and time to elongate 1%. The Ta/347 combination appeared to behave anomalously

in that when tested at a stress of 18,000 psi, the rupture life was less than when tested at 20,000 psi. The reduction in strength was not only evidenced in the rupture life but also in the secondary creep rate and transition time to tertiary creep. This behavior has been observed previously for columbium alloys tested at this temperature range [12,13]. The explanation however has not been advanced to explain this phenomenon.

Thermal cycling of the Ta/347 combination before testing did not appear to effect subsequent creep-rupture behavior. However, the Ta/321 which was thermal cycled before testing did have its creep-rupture life significantly shortened. Since there was only a limited amount of material, the testing which could be accomplished within the scope of this investigation was more screening in nature rather than a definitive characterization study.

Effect of Explosion Bonding on Creep Rupture Properties

To determine what effect the explosive bonding process had on the creep rupture properties of the starting materials, samples were taken from (1) the pure columbium and tantalum starting sheet and (2) the Cb/321 and Ta/321 bonded composites by machining away either the refractory metal or austenitic portion. All of the samples were then tested at 1350°F and 14,000 psi. These data are listed in Table 17.

Both the annealed and the as-explosively bonded columbium specimen ruptured at 1350°F upon application of the load. The as-explosively bonded 321 specimen rupture life was 126 hours. This value agrees reasonably well with the average 15,000 psi, 100 hour rupture strength reported for annealed 321 at 1350°F[9].

Since extrapolation of the 1350°F rupture data for the Cb-321 composite indicate the 14,000 psi rupture time would be approximately 100 hours, it is apparent that at this

stress level, the austenitic component is exerting the greater influence on the strength. As discussed earlier, the shock loading during explosive bonding does result in strengthening. However, there were not enough test data to allow any conclusion on the effects of the shock loading on the rupture strength except that there did not appear to be any of significance. The explosive bonding did, however result in a significant reduction in rupture ductility for the columbium (i.e., 57% for as-annealed to 13% for as-bonded).

While the strength of the austenitic material was controlling for the Cb/321 composites, the reverse was observed for the Ta/austenitic composite where the high strength tantalum component controlled the properties. The tantalum starting material when tested at 1350°F and 14,000 psi exhibited a creep rate of 0.00017%/hr. and after 1000 hours of test had elongated only 0.22%. At 20,000 psi, the 1350°F rupture life of annealed austenitic (18-8) stainless steel is on the order of 10 hours. However, the Ta/321 bimetal when loaded to 20,000 psi at 1350°F did not rupture until 1,180 hours.

Metallographic Examination of Test Specimens

Metallographic examination of the tested specimens revealed several interesting microstructural features which gave some insight into the fracture behavior of the bimetal composition. The rupture ductilities of the bimetal composites were characteristically low, generally below 15%. This may be a result of the effect of the explosive shock loading on rupture ductility as discussed previously. However, also contributing to the low ductility is the mode of fracture. Examples of the fracture characteristics of the bimetal composites tested in the as-bonded condition and after being thermally cycled are shown in Figures 35 through 39. The fractures can all be characterized by:

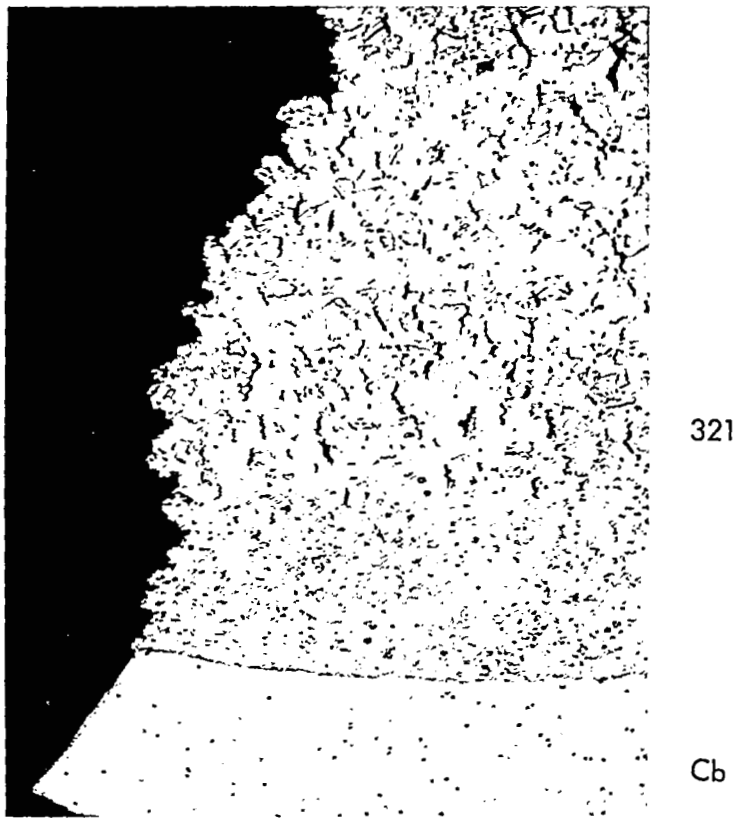

FIGURE 35 - Photomicrograph of As-Bonded Cb/321 Composite Tested at 1350°F and 12,000 psi. Rupture Elongation 9.6%

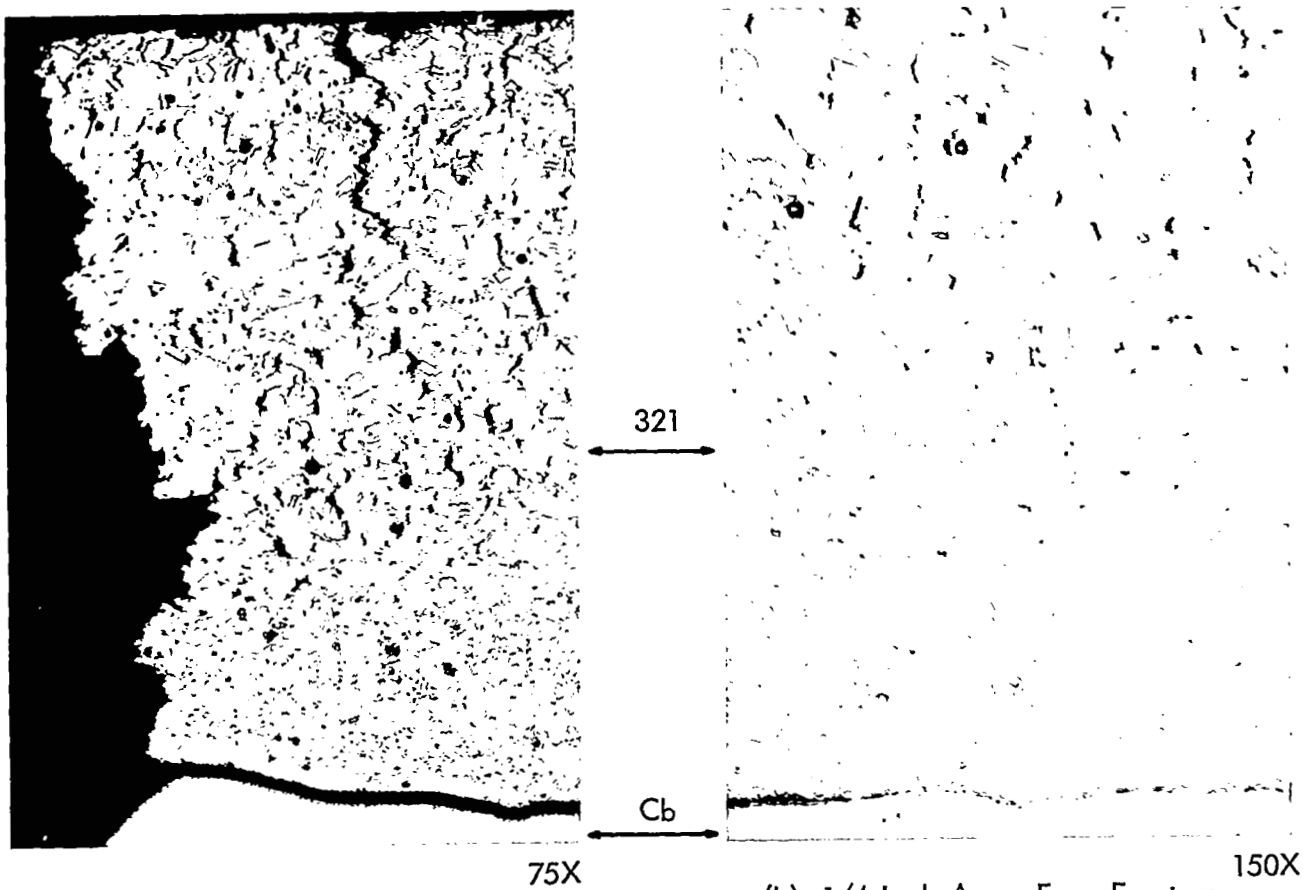

(a) Fracture

(b) 1/4 Inch Away From Fracture

FIGURE 36 - Photomicrographs of Cb/321 Tested at 1350°F, 10,000 psi. Specimen was Thermally Cycled Prior to Test. Rupture Elongation 11.9%

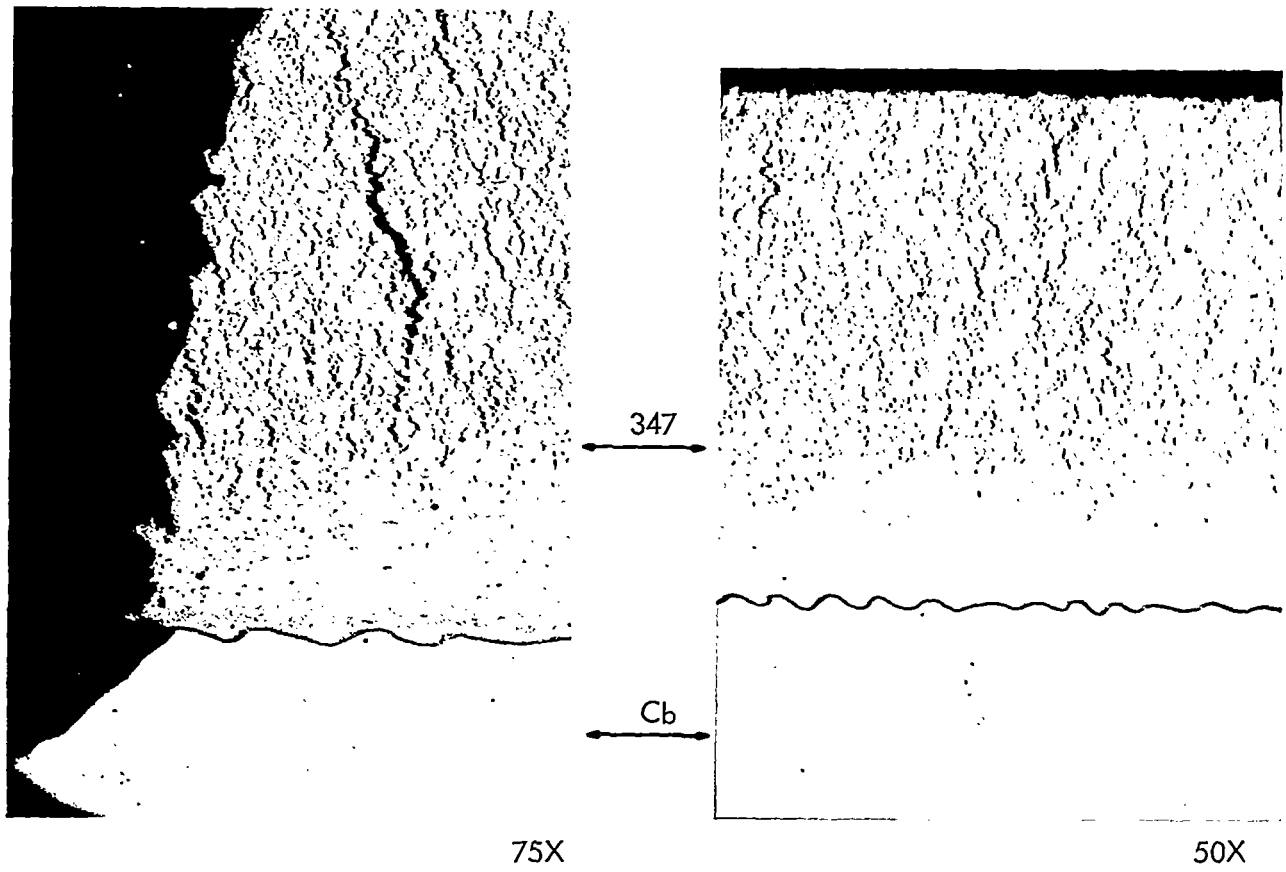

(a) Fracture

(b) 1/4 Inch Away From Fracture

FIGURE 37 - Photomicrograph of Cb/347 Tested at 1350°F and 12,000 psi Rupture Elongation 11.1%

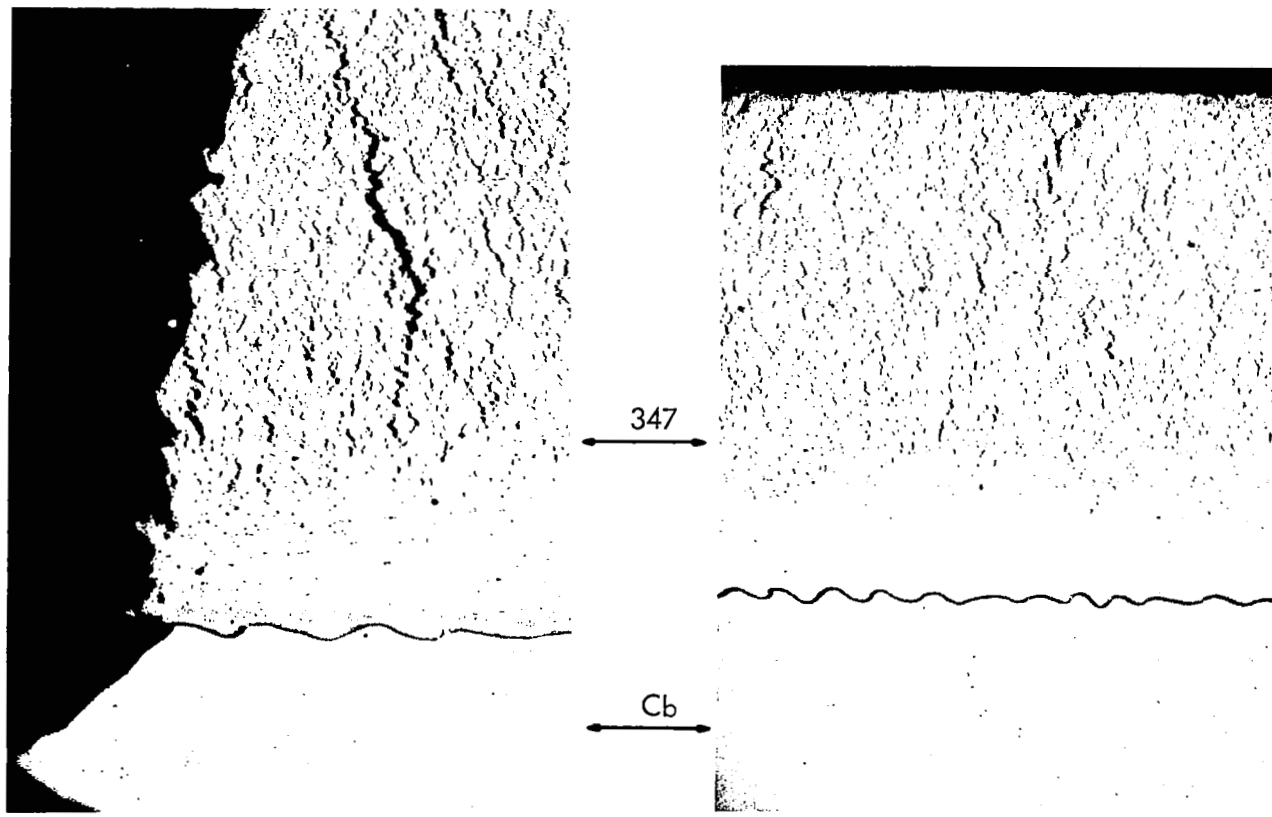

(a) Fracture

(b) 1/4 Inch Away From Fracture

FIGURE 37 - Photomicrograph of Cb/347 Tested at 1350°F and 12,000 psi
Rupture Elongation 11.1%

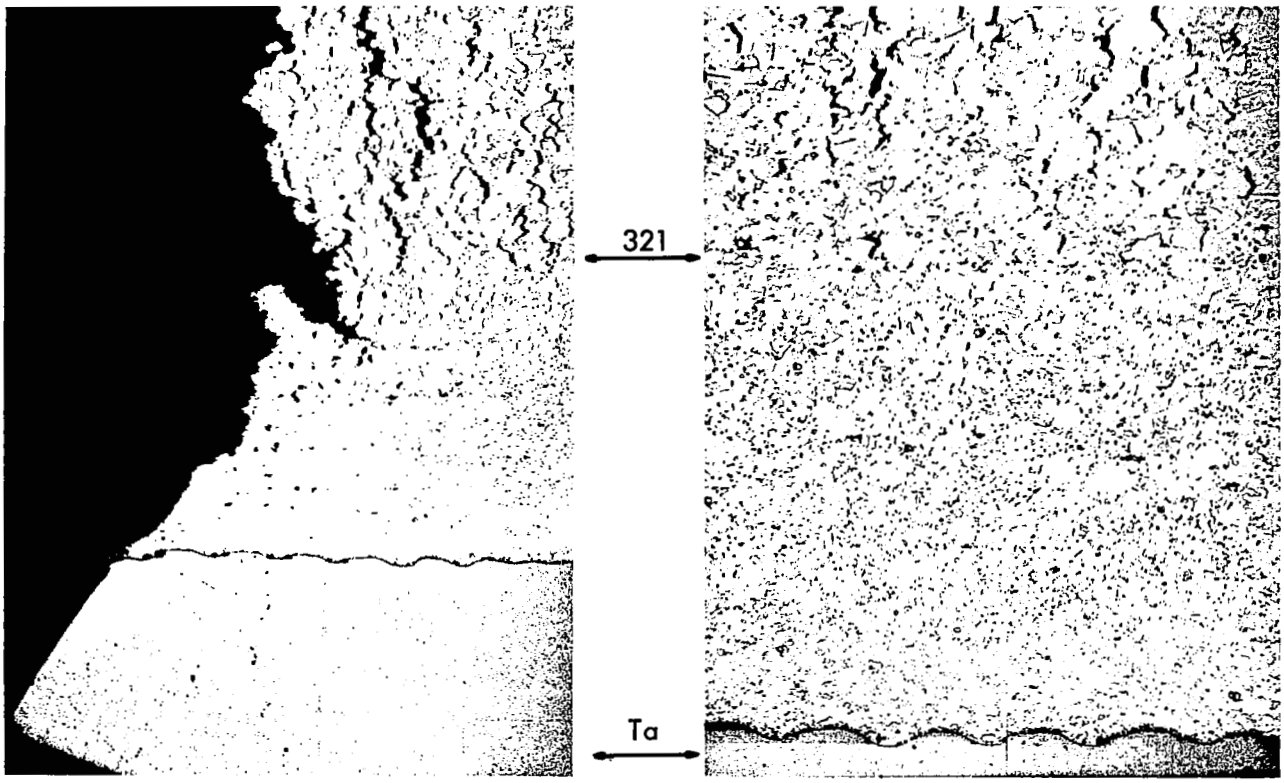

75X

(a) Fracture

150X

(b) 1/4 Inch Away From Fracture

FIGURE 38 - Photomicrograph of Ta/321 Tested at 1350°F and 20,000 psi Rupture Elongation 8.2%

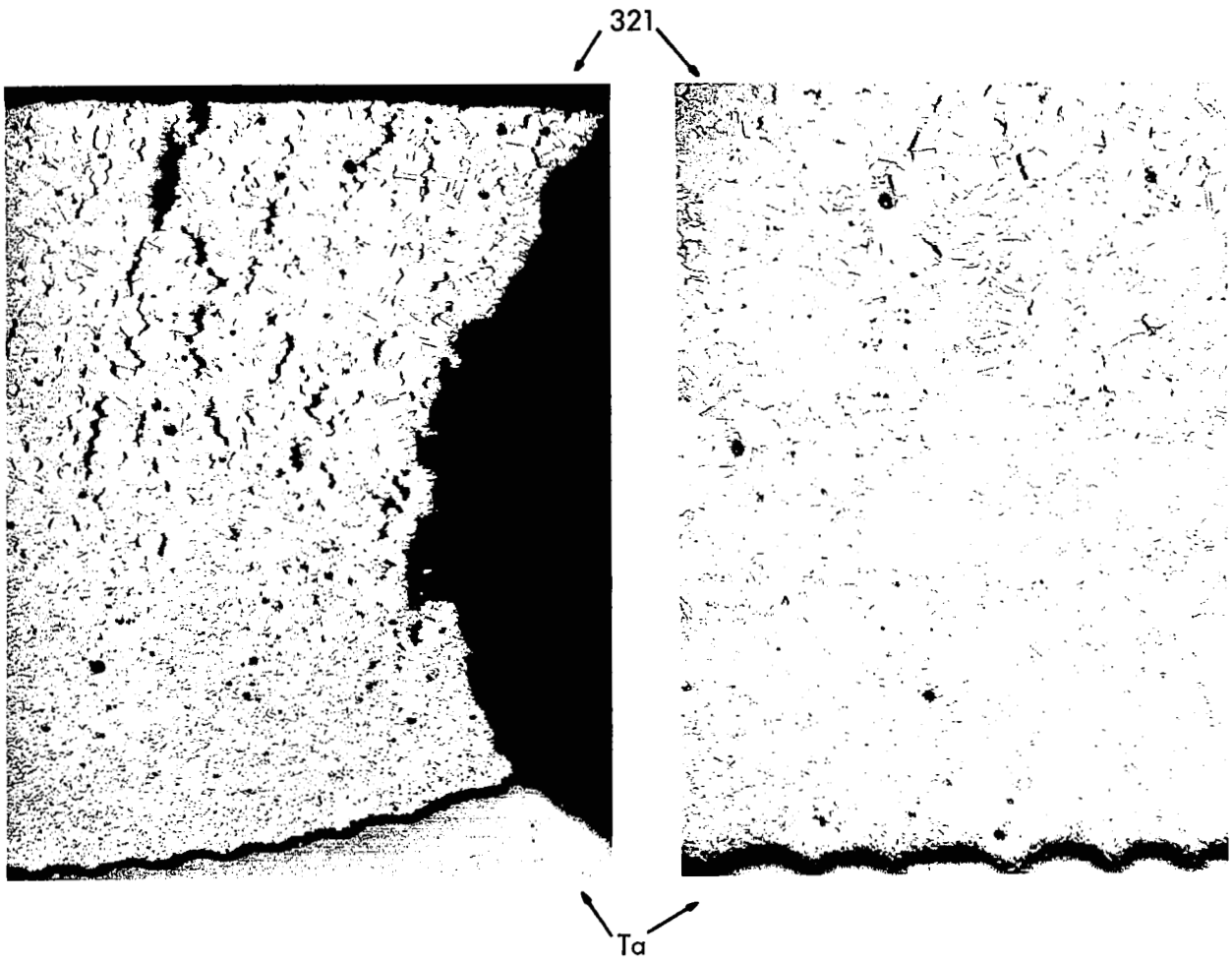

(a) Fracture 75X

(b) 1/4 inch away from fracture 150X

FIGURE 39 - Photomicrograph of Ta/321, Thermally Cycled, Then Tested at 1350°F and 20,160 psi, Rupture Elongation 9.6%

(1) a highly ductile failure in the refractory metal component with essentially 100% reduction in area for the refractory metal,

(2) intergranular fracture in the austenitic component with little reduction in area, except for a 0.015 inch zone adjacent to the refractory metal interface where no intergranular failure occurred.

Also evident from examination of the fracture is the lack of delamination at the interface indicative of the excellent bond between the two components.

III. CONCLUSIONS AND RECOMMENDATIONS

From the results of this investigation, it was concluded that in spite of the thermal coefficient mismatch between the austenitic and refractory metals, explosively bonded refractory/austenitic bimetals could withstand repeated cyclic thermal exposure without failure at the interface provided the interdiffusion zone thickness was less than 5×10^{-4} inch. Thus assuming 20,000 hour service life, the limiting temperature for formation of an interdiffusi· zone of 5×10^{-4} inch for the various refractory/austenitic bimetal combinations would be:

Ta, T-222/321 or 347	1500°F
Cb, Cb-1Zr/321 or 347	1400°F
Cb, Cb-1Zr/Inconel 600	1250°F

From the standpoint of ease of fabricability, rate of interdiffusion, resistance to cyclic thermal exposure, and elevated temperature creep properties, the optimum refractory/austenitic bimetal combination evaluated was the combination which had unalloyed tantalum as the refractory metal component and type 321 stainless steel as the austenitic component.

Further suggested areas of investigation should include more detailed investigation of interdiffusion behavior between tantalum and austenitic stainless steels and the possible use of a diffusion barrier to increase the operating temperature limits.

V. REFERENCES

1. H. O. Slone, "SNAP-8 Development Status", Space Power Systems Advanced Technology Conference, Lewis Research Center, Cleveland, Ohio, August 23-24, 1966, NASA-SP-131.

2. G. R. Cowan and A. H. Holtzman, "Flow Configurations in Colliding Plates", Journal of Applied Physics 34 (4) 928-929 (1963).

3. A. H. Holtzman and G. R. Cowan, "Bonding of Metals with Explosives", Welding Research Council Bulletin 104, April, 1965.

4. G. E. Dieter, "Hardening Effect Produced with Shock Waves", 1960 Seminar, Strengthening Mechanisms in Solids, ASM.

5. P. B. Ferry and J. P. Page, "Metallurgical Study of Niobium/Type 316 Stainless Steel Duplex Tubing", NAA-SR-11191, January 5, 1966.

6. R. P. Elliot, "Constitution of Binary Alloys , First Supplement", McGraw-Hill Book Company, 1965.

7. Ibid. page 254.

8. R. W. Buckman, Jr. and J. S. Hetherington, "Apparatus for Determining Creep Deformation Under Conditions of Ultra-High Vacuum", Rev. of Sc. Instr., 37, No. 8 (Aug. 1966).

9. W. Simmons and H. Cross, "The Elevated Temperature Properties of Stainless Steel" ASTM-STP-124.

10. F. Garafolo, "Fundamentals of Creep and Creep Rupture in Metals", MacMillan Series in Materials Science, 1965.

11. R. W. Fountain and C. R. McKinsey, "Physical and Mechanical Properties of Columbium and Tantalum and their Alloys," pages 198-303, Columbium and Tantalum - Edited by F. T. Sisco and E. Epremian, 1963.

12. R. W. Buckman, Jr. and G. G. Lessmann, "Effects of Welding on the Mechanical Properties of B-33", WANL-TME-376, May 31, 1963, Westinghouse Astronuclear Laboratory.

13. J. A. DeMastry, F. R. Shober, and R. F. Dickerson, "High Temperature Niobium Bar Alloys for Sodium Cooled Reactors", Report No. BMI-1513, April 14, 1961, Battelle Memorial Institute, Columbus, Ohio.

APPENDIX I

METALLOGRAPHIC PREPARATION OF REFRACTORY/AUSTENITIC BIMETAL COMPOSITES

The method for metallographically preparing specimens of refractory/austenitic bimetal composites is as follows:

Mechanical Polishing: All of the bimetal composite specimens, regardless of their compositions, are polished in the same manner. Initially the specimens are mounted in bakelite and ground on 120 through 600 grit silicon carbide papers. The scratches from the last paper are then removed by polishing with 30, 15, and 6 micron diamond abrasives for short times on Metcloth, using a few drops of lapping oil as a lubricant. The mechanical polishing is then continued on a Microcloth charged with a thick, hot slurry of Linde B alumina abrasive and water.* This process, used for 6 minutes with heavy pressure and for 1 minute with light pressure polishes down below the scratches on the austenitic materials, while leaving only slight scratchi on the refractory materials. To complete the polish on the refractory materials, the specimens are finally polished for 1 hour in a Syntron using a very thin slurry of Linde B and water.

Etching: Etching of the different austenitic materials of the composite specimens must be done with different etchants, which are listed below. Two etches are listed for Inconel 600 as its etching characteristics appear to be sensitive to differences in its thermal history. However, the first etch generally gives the best results and should be tried initially.

321 and 347 Stainless

Etchant - Glyceregia (30 ml HCl, 50 ml glycerine, and 15 mil HNO_3)

Procedure - Swab specimen for approximately 1-1/2 minutes. Etch no more than 3 specimens before renewing etchant.

---

*An appreciable quantity of Linde B is mixed in 250 ml of water and the mixture is heated to boiling just prior to being applied to the Microcloth.

Hastelloy N

Etchant - Nital (7 ml HNO_3 and 93 ml water)
Procedure - Electrolytically etch specimen for 5 to 10 seconds at 6 volts.

Inconel 600 - Procedure 1

Etchant - Glyceregia (30 ml HCl, 50 ml glycerine, and 15 ml HNO_3)
Procedure - Swab specimen for approximately 1-1/2 minutes

Procedure 2

Etchant - 10 grams of oxalic acid in 90 ml of water
Procedure - Electrolytically etch specimen for 4 to 6 seconds at 6 volts.

Etching procedures are not given for the refractory components of the bimetal composites. The etchants, both chemical and electrolytic, contain hydrofluoric acid and severely over etch the austenitic components and much of the interdiffusion zones and therefore the refractory metal component was not etched.

APPENDIX II

Interdiffusion Zone Thickness and Knoop Hardness Traverse Data for Diffusion Annealed Refractory/Austenitic Bimetal Composites

Class and Composition	Condition	Inter-Diffusion Zone Thickness (mils)	Knoop Hardness Distance from Interface (mils)											
			Refractory Material						Austenitic Material					
			20	10	5	3	2	1	1	2	3	5	10	20
Class I														
T-222/321	As Bonded	---	310	351	351	385	381	390	468	447	387	409	324	274
	1400°F/1600 Hrs.	a	332	322	330	340	382	424	245	242	226	215	209	204
	1500°F/1600 Hrs.	0.20	374	385	407	417	430	438	235	227	234	221	227	206
	1600°F/1600 Hrs.	0.15	332	374	361	417	420	367	189	201	195	163	174	173
	1400°F/2700 Hrs.	a	289	313	342	348	361	381	241	236	230	254	212	233
	1500°F/2700 Hrs.	0.06	310	339	358	434	430	458	224	221	227	247	202	202
	1600°F/2700 Hrs.	0.15	345	368	390	409	443	468	201	194	178	152	135	153
T-222/347	As Bonded	---	335	355	394	413	385	378	488	417	447	458	355	303
	1400°F/1600 Hrs.	a	319	349	324	346	377	349	203	212	218	196	189	182
	1500°F/1600 Hrs.	0.15	368	307	425	400	475	434	184	219	204	215	212	190
	1600°F/1600 Hrs.	0.30	322	371	407	435	451	451	156	171	166	161	169	163
	1400°F/2700 Hrs.	a	326	335	351	342	351	345	259	219	205	209	176	219
	1500°F/2700 Hrs.	0.12	332	336	401	371	378	394	166	194	188	184	182	194
	1600°F/2700 Hrs.	0.30	315	378	425	413	409	374	129	159	151	164	150	150
Ta/321	As Bonded	---	171	189	207	207	207	201	473	473	443	405	368	326
	1400°F/1600 Hrs.	a	154	163	171	184	180	186	188	186	196	178	168	160
	1500°F/1600 Hrs.	0.25	186	173	176	180	191	185	173	174	186	178	177	176
	1600°F/1600 Hrs.	0.30	128	164	165	167	173	163	167	181	173	156	143	140
	1400°F/2700 Hrs.	0.04	155	167	166	176	172	175	187	185	186	185	175	167
	1500°F/2700 Hrs.	0.35	111	130	146	171	186	216	177	200	196	191	194	173
	1600°F/2700 Hrs.	0.63	162	162	168	157	168	143	155	182	145	127	138	134
Ta/347	As Bonded	---												
	1400°F/1600 Hrs.	a	168	171	160	165	181	169	212	209	218	190	216	181
	1500°F/1600 Hrs.	0.15	170	183	206	192	200	189	186	217	221	207	202	205
	1600°F/1600 Hrs.	b												
	1400°F/2700 Hrs.	0.04	167	157	164	172	177	179	217	212	217	205	213	197
	1500°F/2700 Hrs.	0.25	163	168	169	168	169	183	174	196	196	196	197	249
	1600°F/2700 Hrs.	b												
Class II														
Cb/321	As Bonded	---	108	125	116	128	133	138	421	398	381	409	305	293
	1400°F/1600 Hrs.	0.17	83	96	97	106	111	108	171	171	174	166	165	161
	1500°F/1600 Hrs.	0.31-0.70	65	98	107	120	107	106	135	164	169	156	164	150
	1600°F/1600 Hrs.	1.20	90	110	109	116	136	92	145	153	155	151	151	125
	1400°F/2700 Hrs.	0.16-0.31	80	93	92	96	98	96	177	167	180	173	191	165
	1500°F/2700 Hrs.	0.55	76	93	102	112	96	87	154	145	144	140	144	148
	1600°F/2700 Hrs.	1.55	81	88	106	104	105	98	119	133	133	132	144	131

Interdiffusion Zone Thickness and Knoop Hardness Traverse Data for Diffusion Annealed Refractory/Austenitic Bimetal Composites

Class and Composition	Condition	Inter-Diffusion Zone Thickness (mils)	Knoop Hardness Distance from Interface (mils)											
			Refractory Material						Austenitic Material					
			20	10	5	3	2	1	1	2	3	5	10	20
Cb/347	As Bonded	---	107	119	127	121	120	118	434	458	430	394	336	315
	1400°F/1600 Hrs.	0.17	77	87	88	103	105	110	225	222	229	207	195	180
	1500°F/1600 Hrs.	0.30	97	107	114	107	112	117	191	206	205	224	217	224
	1600°F/1600 Hrs.	1.00	80	89	109	118	124	113	159	162	169	150	166	150
	1400°F/2700 Hrs.	0.12-0.23	87	95	113	112	115	113	201	204	206	210	196	186
	1500°F/2700 Hrs.	0.31	81	102	108	93	94	95	179	186	183	189	182	161
	1600°F/2700 Hrs.	1.25	83	96	110	96	96	106	139	151	156	135	135	144
Cb-1Zr/347	As Bonded	---	150	171	167	171	174	168	463	409	409	425	364	313
	1400°F/1600 Hrs.	a	123	126	153	167	171	175	219	222	229	208	196	189
	1500°F/1600 Hrs.	0.15	133	149	169	200	202	219	195	214	222	215	191	194
	1600°F/1600 Hrs.	1.20	102	126	156	190	203	211	145	191	184	188	176	166
	1400°F/2700 Hrs.	a	125	126	153	167	169	180	219	217	219	205	217	177
	1500°F/2700 Hrs.	0.15	155	169	163	185	182	147	162	158	153	162	172	153
	1600°F/2700 Hrs.	1.33	123	132	162	183	201	198	209	197	140	149	164	177
FS-85/321	As Bonded	---	267	303	282	285	218	265	430	405	390	390	303	318
	1400°F/1600 Hrs.	a	232	238	266	295	292	301	178	191	192	175	165	161
	1500°F/1600 Hrs.	0.55	240	247	294	347	353	344	156	176	200	171	166	179
	1600°F/1600 Hrs.	0.75	222	336	295	354	356	341	117	136	158	147	132	147
	1400°F/2700 Hrs.	0.08	236	229	259	274	278	267	177	178	180	166	162	153
	1500°F/2700 Hrs.	0.16	238	247	271	282	330	313	147	182	169	165	146	157
	1600°F/2700 Hrs.	1.40	231	230	318	338	348	368	145	174	147	159	112	139
FS-85/347	As Bonded	---	298	293	305	271	308	326	413	390	329	329	271	271
	1400°F/1600 Hrs.	a	256	257	286	300	316	295	228	233	233	215	199	197
	1500°F/1600 Hrs.	0.30	262	264	272	385	388	329	196	204	205	214	198	195
	1600°F/1600 Hrs.	b												
	1400°F/2700 Hrs.	0.08	236	241	278	282	285	276	189	205	212	182	189	173
	1500°F/2700 Hrs.	0.20	224	234	293	326	361	355	202	214	207	200	209	157
	1600°F/2700 Hrs.	b												
T-222/Inc. 600	As Bonded	---	295	313	374	358	398	358	430	409	374	342	321	278
	1400°F/1600 Hrs.	c	295	334	361	344	353	382	178	185	180	169	152	197
	1500°F/1600 Hrs.	0.65	309	338	341	403	421	388	188	190	177	169	169	186
	1600°F/1600 Hrs.	1.30	312	330	361	374	394	394	134	161	167	166	180	179
	1400°F/2700 Hrs.	0.12	305	336	336	361	390	364	192	186	174	155	175	188
	1500°F/2700 Hrs.	0.62	315	329	387	417	394	417	161	173	167	179	174	169
	1600°F/2700 Hrs.	1.33	305	335	326	378	355	378	140	143	157	157	164	176

Interdiffusion Zone Thickness and Knoop Hardness Traverse Data for Diffusion Annealed Refractory/Austenitic Bimetal Composites

Composition	Condition	Inter-Diffusion Zone Thickness (mils)	Knoop Hardness Distance from Interface (mils)											
			Refractory Material						Austenitic Material					
			20	10	5	3	2	1	1	2	3	5	10	20
Class III														
Cb/Inc. 600	As Bonded	---	112	118	112	119	129	126	374	300	295	313	295	236
	1400°F/1600 Hrs.	0.60	93	83	98	105	108	109	154	176	207	165	151	161
	1500°F/1600 Hrs.	1.20	92	98	111	109	97	91	164	158	159	208	200	165
	1600°F/1600 Hrs.	1.60	73	86	102	98	101	92	159	189	201	178	161	156
	1400°F/2700 Hrs.	0.86	78	81	94	82	77	76	111	136	144	153	149	145
	1500°F/2700 Hrs.	1.25	94	97	96	110	98	85	152	162	172	167	150	195
	1600°F/2700 Hrs.	1.87	75	83	100	100	80	81	168	124	166	154	151	167
Ta/Inc. 600	As Bonded	---	188	183	180	191	193	216	378	351	358	351	318	247
	1400°F/1600 Hrs.	0.45	175	165	170	167	178	179	157	186	180	160	174	170
	1500°F/1600 Hrs.	1.00	197	182	189	191	171	185	128	189	197	166	175	200
	1600°F/1600 Hrs.	b												
	1400°F/2700 Hrs.	0.70	130	143	128	153	160	153	164	171	155	152	132	139
	1500°F/2700 Hrs.	b												
	1600°F/2700 Hrs.	b												
FS-85/Inc. 600	As Bonded	---	278	336	269	289	310	298	413	409	451	355	358	267
	1400°F/1600 Hrs.	0.50	256	238	268	271	282	282	172	191	192	165	171	161
	1500°F/1600 Hrs.	1.35	250	258	270	301	294	353	183	169	174	175	176	170
	1600°F/1600 Hrs.	2.00	227	221	245	295	286	275	174	160	162	166	188	180
	1400°F/2700 Hrs.	0.63	231	241	247	269	265	267	145	192	184	179	169	153
	1500°F/2700 Hrs.	1.48	238	234	243	243	254	269	165	162	177	194	150	123
	1600°F/2700 Hrs.	2.50	225	236	225	225	236	225	176	170	178	176	161	157
Cb-1Zr/Inc. 600	As Bonded	---	142	152	148	153	164	154	398	390	381	364	295	292
	1400°F/1600 Hrs.	0.50	127	135	153	156	165	157	149	164	171	159	152	165
	1500°F/1600 Hrs.	1.15	138	153	162	168	173	149	206	217	175	178	170	175
	1600°F/1600 Hrs.	1.80	101	111	107	133	119	112	138	166	169	170	154	170
	1400°F/2700 Hrs.	0.78	137	123	161	155	158	158	144	157	164	185	157	168
	1500°F/2700 Hrs.	1.37	109	123	140	150	154	114	153	146	141	163	163	149
	1600°F/2700 Hrs.	2.20	114	112	133	93	114	120	171	146	148	178	155	158
FS-85/Hast. N	As Bonded	---	241	271	280	293	313	323	451	390	390	390	326	287
	1400°F/1600 Hrs.	0.45	236	256	246	282	280	308	178	176	195	178	173	195
	1500°F/1600 Hrs.	0.50	262	266	258	278	285	292	212	214	190	201	197	202
	1600°F/1600 Hrs.	1.30	207	219	258	292	302	322	127	158	175	169	153	189
	1400°F/2700 Hrs.	0.55	245	254	278	278	274	305	141	184	133	161	174	186
	1500°F/2700 Hrs.	1.12	230	222	249	263	285	300	174	175	187	163	163	137
	1600°F/2700 Hrs.	2.03	193	225	221	212	186	237	140	145	172	151	162	144

NOTES: (a) None detected
(b) Delaminated during exposure

APPENDIX III

Spot Analyses (Electron Beam Microprobe) of Diffusion Zones Present in Diffusion Annealed Refractory/Austenitic Stainless Steel Composite Specimens

Specimen Identification	Interdiffusion Zone Thickness (mils)	Composition (weight percent)					Comments
		Ta	Fe	Cr	Ni	Ti	
Ta/321							
Area Y (Figure 13a)							
1600 Hrs/1500°F	0.25	96.5	2.9	0.5	0.4	0.01	Appears to be a 90 a/o 10 a/o (Fe+Ni) compound similar to that observed in Cb-Fe system (described in FN_2)
1600 Hrs/1600°F	0.30	96.5	2.9	0.5	1.0	0.02	
2700 Hrs/1600°F	0.63	97.7	1.2	0.1	0.7	0.1	
Area X (Figure 13a)							
1600 Hrs/1500°F	0.25	84.0	13.3	2.2	0.5	0.01	Ta (Fe,Cr,Ni)
1600 Hrs/1600°F	0.30	84.5	13.1	1.5	0.3	0.02	
2700 Hrs/1600°F	0.63	77.5	18.9	2.2	1.6	0.6	
Area T (Figure 13a)							
1600 Hrs/1500°F	0.25	72.0	21.9	4.5	1.8	0.01	Ta $(Fe,Cr,Ni)_2$
1600 Hrs/1600°F	0.30	64.5	28.3	4.8	2.3	0.07	
2700 Hrs/1600°F	0.63	61.0	30.0	6.4	2.2	0.03	

APPENDIX III (Continued)

Spot Analyses (Electron Beam Microprobe) of Diffusion Zones Present in Diffusion Annealed Refractory/Austenitic Stainless Steel Composite Specimens

Specimen Identification	Interdiffusion Zone Thickness (mils)	Composition (weight percent)						Comments
		Ta	Fe	Cr	Ni	W	Hf	
T-222/347								
Area Y (Figure 16)								
1600 Hrs/1600°F	0.30	62.3	23.3	6.5	2.0	4.5	1.4	FN_1
2700 Hrs/1600°F	0.30	63.1	22.0	5.1	2.4	5.8	1.6	
		Cb	Fe	Cr	Ni	Zr	Ti	
Cb/321								
Area U (Figure 17a)								
1600 Hrs/1500°F	0.31-0.70	91.8	5.6	1.3	1.4	--	0.03	Slight indication of constant composition on traverses (FN_2)
Area V (Figure 17a)								
1600 Hrs/1500°F		46.8	39.6	7.8	5.3	--	0.3	$Cb(Fe,Cr,Ni)_2$
Area X (Figure 17a)								
1600 Hrs/1500°F		Too thin for spot analysis						FN_3
Cb/347								
Area U (Figure 18a)								
1600 Hrs/1500°F	0.30	95.2	3.0	1.0	0.8	--	--	No indication of constant composition on traverses (FN_2)
Area V (Figure 18a)								
1600 Hrs/1500°F	47.5	47.5	39.2	8.9	4.4	--	--	$Cb(Fe,Cr,Ni)_2$

APPENDIX III (Continued)

Spot Analyses (Electron Beam Microprobe) of Diffusion Zones Present in Diffusion Annealed Refractory/Austenitic Stainless Steel Composite Specimens

Specimen Identification	Interdiffusion Zone Thickness (mils)	Composition (weight percent)						Comments
		Cb	Fe	Cr	Ni	Zr	Ti	
Cb-1Zr/347								
Area W (Figure 19a)								
1600 Hrs/1600°F	1.20	93.5	3.5	0.1	1.7	0.8		Very slight indication of constant composition on traverses (FN_2)
Area Z (Figure 19a)								
1600 Hrs/1600°F		46.0	41.1	7.5	5.0	0.3		$Cb(Fe,Cr,Ni)_2$
Cb-1Zr/Inconel 600								
Area B (Figure 21)	1.15	42.0	3.2	3.3	50.5	0.5	0.05	Very slight indication of constant composition on traverses (FN_4)
Area C (Figure 21)								
1600 Hrs/1500°F		34.4	0.7	0.9	63.7	0.3	0.06	$CbNi_3$ type compound
Phase D in Area E (Figure 21)		10.3	3.3	59.8	27.2	0.1	0.14	(αCr or $CbCr_7$) ?
Area E (Figure 21)								
1600 Hrs/1500°F		20.1	7.1	10.7	62.3	0.3	0.14	(αNi or $CbNi_3$) ?

FN_1 - Slight indication of constant composition on traverses indicated compound composition of 46.1Ta-36.4Fe-7.2Cr-3.0Ni-5.7W-1.6Hf

FN_2 - Appears to be 89 a/o Cb-11 a/o (Fe+Ni+Cr) compound

FN_3 - From traverses, composition was 34.3Cb-36.3Fe-23.5Cr-4.5Ni-1.3Ti

FN_4 - Layer has approximate composition of $Cb(Fe,Ni,Cr)_2$, but may be a mixture of CbNi and $CbNi_3$ type compounds